Veðurstofa Íslands

Meteorological droughts and wet spells in Iceland: an analysis based on daily downscaled CMIP6 projections and historical changes

Andréa-Giorgio R. Massad
Tarek Zaqout
Halldór Björnsson

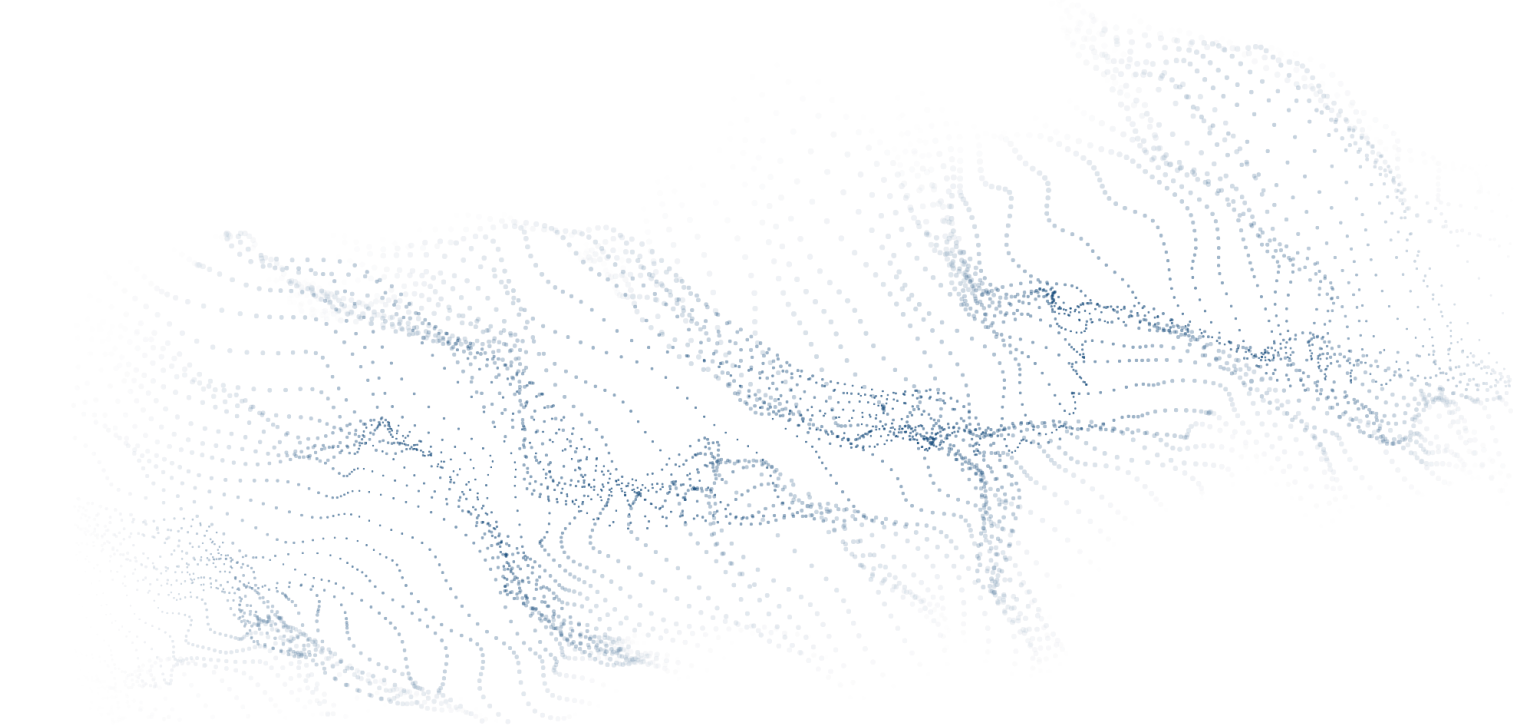

Skýrsla
VÍ 2025-010

Bústaðavegi 7-9 | IS-105 Reykjavík | Iceland | Tel +354 522 6000 | vedur@vedur.is

Veðurstofa Íslands

Meteorological drougths and wet spells in Iceland: an analysis based on daily downscaled CMIP6 projections and historical changes

Höfundar	Andréa-Giorgio R. Massad, Tarek Zaqout, Halldór Björnsson
Unnið fyrir	Orkurannsóknasjóð Landsvirkjunar
Verkefnisstjóri	Tinna Þórarinsdóttir
Yfirfarið af	Guðrún Nína Petersen
Samþykkt af	Tinna Þórarinsdóttir, deildarstjóri loftlag, veður, vatn, jöklar og haf

Veðurstofa Íslands / Icelandic Meteorological Office

Númer	VÍ 2025-010
ISSN	1670-8261
Dagsetning	Nóvember 2025
Dreifing	Opin
Fjöldi síðna	36 + viðaukar
Upplag	Rafræn útgáfa
Verknúmer	4314-0-0001
Málsnúmer	2024-0318
DOI númer	10.33112/YYFI1459

Bústaðavegi 7-9 | IS-105 Reykjavík | Iceland | Tel +354 522 6000 | vedur@vedur.is

Abstract

In this research, the annual maximum number of consecutive dry days (CDD) and consecutive wet days (CWD) are used to analyse temporal and spatial changes in periods of meteorological droughts and wet spells. CDD and CWD are first calculated based on daily precipitation data from twelve automatic weather stations located all around Iceland and compared to simulations from the Copernicus Arctic Regional Reanalysis (known as the CARRA dataset). Results show that while CDD values are smaller in the CARRA dataset than in the observations, and CWD values are larger, both datasets are in accordance with the general pattern of precipitation in Iceland. Early results indicate that longer periods of CDD seemed more frequent during the earlier years covered by the instruments, and the opposite for CWD. CDD and CWD are also extracted for the ensemble of models used in the NEX-GDDP-CMIP6 dataset interpolated to a 2.5-km grid, and two emissions scenarios. Results show small changes for the selected stations and hydropower catchments, ranging from -1 to 2 days when comparing median ensemble values at the end of the century (2090–2100) with the historical period (1986–2015) for both climate scenarios.

Key words: *CDD, CWD, drougths, wet spells, CMIP6 projections*

Ágrip

Í þessari rannsókn eru hámarksfjöldi samfelldra þurra daga (CDD, Consecutive Dry Days) og votra daga (CWD, Consecutive Wet Days) notuð til að greina breytingar í tíma- og rúmi á veðurfarslegum þurrk- og votviðratímabilum. CDD og CWD eru fyrst reiknuð út frá daggildum úrkomu frá 12 sjálfvirkum veðurstöðvum víðs vegar um Ísland og borin saman við líkanagögn úr Copernicus Arctic Regional Reanalysis (CARRA-endurgreiningunni). Niðurstöðurnar sýna að þótt CDD-gildi séu lægri í CARRA-gögnum en í athugunum og CWD-gildi hærri, samrýmast bæði gagnasöfnin almennu mynstri úrkomu á Íslandi. Niðurstöður benda til þess að lengri CDD-tímabil hafi verið algengari á fyrstu árum mælitímabilsins, og hið gagnstæða eigi við um CWD. Einnig eru CDD og CWD unnin fyrir safn loftslagslíkanagagna úr NEX-GDDP-CMIP6 gagnasafninu, reiknað niður í 2,5 km reikninet og fyrir tvær losunarsviðsmyndir. Niðurstöðurnar sýna litlar breytingar fyrir stöðvarnar og vatnasvið vatnsaflsvirkjana, á bilinu –1 til 2 dagar fyrir báðar losunarsviðsmyndirnar þegar borin eru saman miðgildi líkanasafnsins í lok aldarinnar (2090–2100) miðað við sögulegt tímabili (1986–2015).

Lykilorð: *CDD, CWD, þurra daga, votra daga, CMIP6 gagnasafninu*

Table of contents

1 Introduction

In recent years, several studies have been conducted to calculate precipitation extremes in Iceland. In 2020, a study by Massad *et al*. (2020) reassessed precipitation return levels, resulting in a new national map of 24-hour precipitation thresholds for a 5-year event, in agreement with the general precipitation pattern in Iceland documented in Björnsson *et al*. (2018) and Crochet *et al.* (2007). As Arctic and subarctic regions warm rapidly, precipitation extremes are expected to broadly increase in the coming decades (Bintanja, 2018) and recently, two studies partially funded by Orkurannsóknasjóður Landsvirkjunar examined changes in extreme precipitation towards the end of the century. Using the Coupled Model Intercomparison Project Phase 5 and 6 they estimated future precipitation return levels for Iceland, with a focus on the eleven hydropower catchments operated by Landsvirkjun (Massad *et al*. 2022; 2024). Both studies showed a gradual increase in precipitation extremes for the end of the century, with values from the CMIP6 dataset based on daily annual maximum precipitation amounts (RX1D) increasing up to 25% in 2100, depending on the part of the country, the percentile of the ensemble of models used, and the emission scenario considered. While the focus of these studies was on extreme precipitation amounts, they did not take into consideration the temporality of precipitation, and the behaviour of extended dry and wet periods. Few research have centred around droughts in Iceland (Gylfadóttir, 2016; Sienz *et al.,* 2007), and changes related to the ongoing warming of Arctic regions have yet to be analysed.

Recently, the NASA Exchange Global Daily Downscale Projections (NEX-GDDP-CMIP6) dataset based on the global climate model (GCM) output from the Climate Model Intercomparison Project Phase 6 became available. The NEX-GDDP-CMIP6 dataset was created by statistically downscaling GCM output to a higher resolution of 0.25° using a daily variant of the monthly bias correction/spatial disaggregation (BCSD) method described in Wood *et al.* (2002, 2004). The NEX-GDDP-CMIP6 dataset, therefore, enhances the understanding of climate change impacts over regional-to-local scales (Thrasher *et al*., 2022), notably for studies at catchment-scale. Moreover, an ongoing study at IMO has focused on bias correcting and downscaling the NEX-GDDP-CMIP6 projections, using the CARRA reanalysis dataset as a reference dataset, and producing bias-adjusted climate projections at 2.5-km resolution for Iceland. From this downscaled precipitation dataset, two extreme climate indicators are available: the maximum number of consecutive dry days (CDD) and the maximum number of consecutive wet days (CWD). These indicators will be used here to analyse changes in periods of meteorological droughts and wet spells.

This study aims to answer the following questions:

1. Are there signs of change in the temporality of CDD and CWD in the control stations selected for this study, both in the measurements and from simulated data?
2. How are those two extreme climate indicators expected to be affected by the ongoing warming of Arctic regions?

To answer the first question, daily precipitation data from twelve control stations is used in order to create annual maximum series of CDD and CWD based on both measurements

and simulations from the Copernicus Arctic Regional Reanalysis (CARRA dataset, see DMI (2020)). Then, historical changes in those two indicators are analysed for the control stations. Finally, downscaled climate projections down to a resolution of 2.5 km are studied for the twelve control stations, and climate projections shown in maps and tables for the eleven hydropower catchments operated by Landsvirkjun, as well as for the whole country. This is done for two emissions scenarios: SSP2-4.5 and SSP5-8.5, and two future periods: middle (2046–2055) and end (2091–2100) of the century.

2 Study area

In this study, the focus is on a selection of meteorological stations recording precipitation, as well as hydropower catchments operated by Landsvirkjun. This selection can be seen in Figure 1.

As of today, IMO has a network of more than 70 automatic stations, widespread around the country and measuring precipitation down to 10 minutes. Here, twelve stations were hand-picked as control stations. Those stations were first selected in Massad *et al.* (2020) due to their location in narrow fjords or close to complex orography (Eskifjörður and Neskaupstaður in the east; Flateyri, Ísafjörður and Súðavík in the north-west), their exposure to frequent flash-flooding events (Siglufjörður and Ólafsfjörður in the north, Seyðisfjörður in the east), their accumulated annual rainfall (Kvísker and Laufbali in the south-west) or the quality of their recording (Reykjavík and Höfn í Hornafirði).

In addition to those stations, eleven hydropower catchments operated by Landsvirkjun were selected for this study. Those catchments vary in size and elevation, and have been used in several studies carried at IMO in the past years (Massad *et al.* 2022 and 2024). In Figure 1, the discrepancy between the actual catchments outlines (shown in black) and the 2.5-km grid (shaded area) used on the map can be seen, as the grid and the catchment boundaries do not match exactly. For more details about the physical characteristics of individual catchments, see Table 2 in Massad *et al.* 2022.

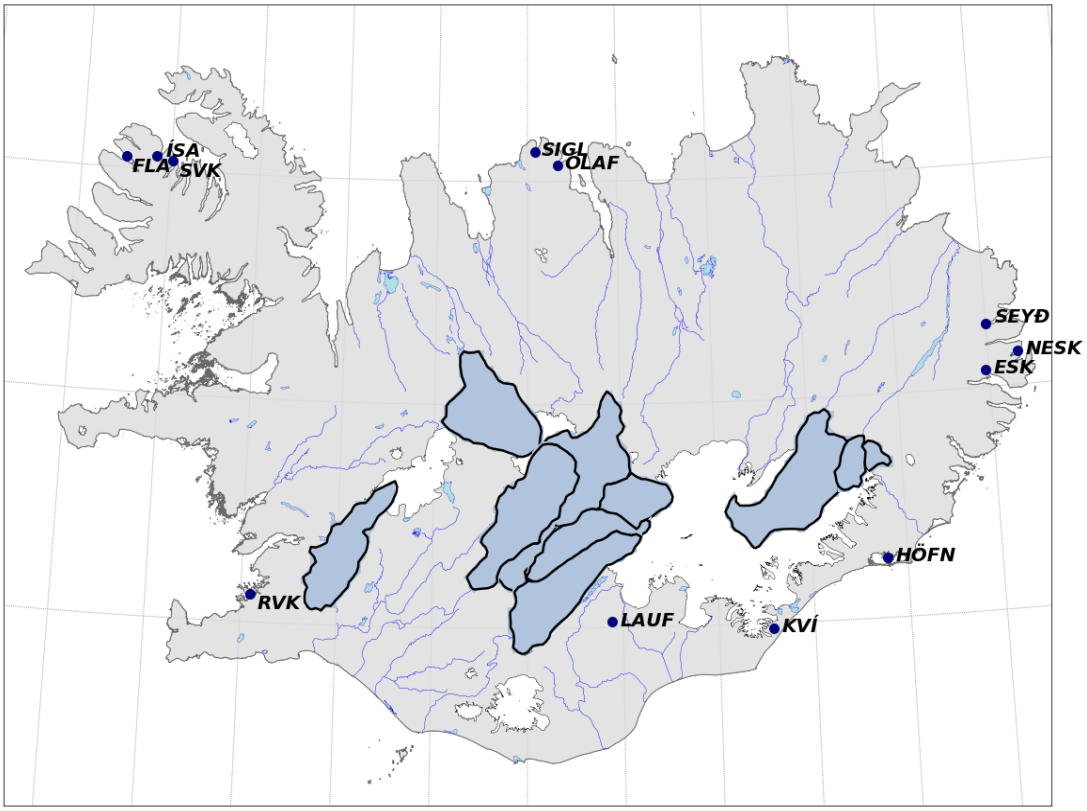

Figure 1 — Location of the twelve control stations (blue dots) and eleven hydropower catchments (grey-shaded areas) used in this study. Black lines show the catchment boundaries, and shaded areas within catchments represent the 2.5-km grid.

3 Data

3.1 Measurements

Table 1 lists the twelve control stations along with the date of their first recording of precipitation, and total number of missing daily values. While most of the stations have been recording precipitation automatically before 2000, some of them were set up more recently. This is the case for Höfn í Hornafirði, as well as Kvísker and Laufbali. For those last two stations, even though they have a rather large number of missing dates in their timeseries, their selection here is justified by their location in the wettest part of the country, with accumulated annual rainfall reaching a national maximum in their area.

While all those stations are still recording today, only data until the end of 2022 were retrieved, in order to match the length of the reanalysis available at IMO and presented in the next paragraph.

Table 1 — List of the control stations along with the date of their first recording, and the number of missing daily values between their first day of recording and 2022-12-31.

Station	First day of recording	Missing values (days)	Station	First day of recording	Missing values (days)
Eskifjörður	1998-10-24	112	**Neskaupstaður**	1997-10-27	2
Flateyri	1997-10-21	63	**Ólafsfjörður**	1997-10-30	383
Höfn	2008-01-01	172	**Reykjavík**	1997-01-01	3
Ísafjörður	1998-09-25	17	**Seyðisfjörður**	1995-11-10	152
Kvísker	2009-01-01	502	**Siglufjörður**	1995-11-09	1,078
Laufbali	2004-06-01	1054	**Súðavík**	1999-09-29	65

3.2 The CARRA dataset: Copernicus Arctic Regional Reanalysis

In this study, the Copernicus Arctic Regional Reanalysis (CARRA) dataset is used, providing precipitation data with a horizontal resolution of 2.5-km with a 3-hour timestep. This reanalysis was developed and produced by the Copernicus Climate Change Service (C3S) with the goal to provide arctic regions with climate monitoring products and climate services (DMI, 2020).

Similarly to the Icelandic Reanalysis (known as the ICRA dataset; see Nawri *et al.* 2017), used for previous studies at IMO, the CARRA dataset was created with the non-hydrostatic HARMONIE–AROME model, with a horizontal resolution of 2.5 km (Bengtsson *et al.*, 2017). The reanalysis covers the period from September 1990 to present, although when this study was started, only data until the end of 2022 were available at IMO. The CARRA dataset is available over two domains, but only the western domain covering Iceland and Greenland, termed CARRA-West, was used. Data were then cropped for a smaller domain around Iceland.

Timeseries for the twelve control stations were extracted by taking the weighted average over the four nearest grid-points surrounding the station location. Daily precipitation were calculated from the initial 3-hour timeseries by summing precipitation from midnight to midnight.

3.3 Downscaled CMIP6 projections

The Coupled Model Intercomparison Project (CMIP) is a large framework that collects the outputs from global coupled ocean-atmosphere general circulation models (GCMs) to project future climatic changes due to anthropogenic activity.

For this project, results from the sixth phase of the project are used, commonly referred to as CMIP6 (see Eyring *et al.* (2016) for details) and featured in the IPCC Sixth Assessment Report (2021). This time, the climate projections are based on a set of Shared Socioeconomic Pathway (SSP; see Figure 2). These SSPs describe various narratives of global societal developments for the end of the century, into which are derived the Representative Carbon Pathways (RCP) used in the fifth phase of the project (CMIP5). In CMIP6, five SSPs named SSP1 to SSP5 are considered, with the more sustainable scenario being SSP1, and the worst, SSP5, the fossil-fuel driven development scenario or the "worst case scenario" (see Figure 2, from O'Neill *et al.,* 2017).

Climate models are then run for a specific SSP, coupled with various radiative forcings. In this analysis, the results from two scenarios are used:

- *SSP2-4.5*. "Middle of the road" pathway in terms of future greenhouse gas emissions, with an additional forcing of 4.5 W m^{-2}. In this scenario, climate protection measures are also being taken.
- *SSP5-8.5*. Represents the upper boundary range of scenarios, with a radiative forcing of 8.5 W m^{-2} by the end of the century. It represents an update of the RCP8.5 scenarios from the CMIP5 but now combined with socioeconomic considerations.

The global mean temperature changes for those two scenarios as well as for SSP1-2.6 are shown in Figure 2. According to the Copernicus Climate Change service, temperature projections under SSP1-2.6, SSP2-4.5, and SSP5-8.5 suggest an increase that ranges between under 2°C (SSP1-2.6) to over 5°C (SSP5-8.5) for the period 2071–2100 when compared to the historical period 1985–2014.

The CMIP6 projections provide a global dataset that include a large range of variables. Depending on the variable, a different number of GCMs is available, both for a historical period spanning from 1850 to 2014, and for a projection period that runs until the end of the century. In 2022, the NASA Earth Exchange Global Daily Downscaled Projections (known as the NEX-GDDP-CMIP6 dataset; see Thrasher *et al.* 2022) was made available, downscaling temperature and precipitation data from the CMIP6 with a horizontal resolution interpolated to 0.25°.

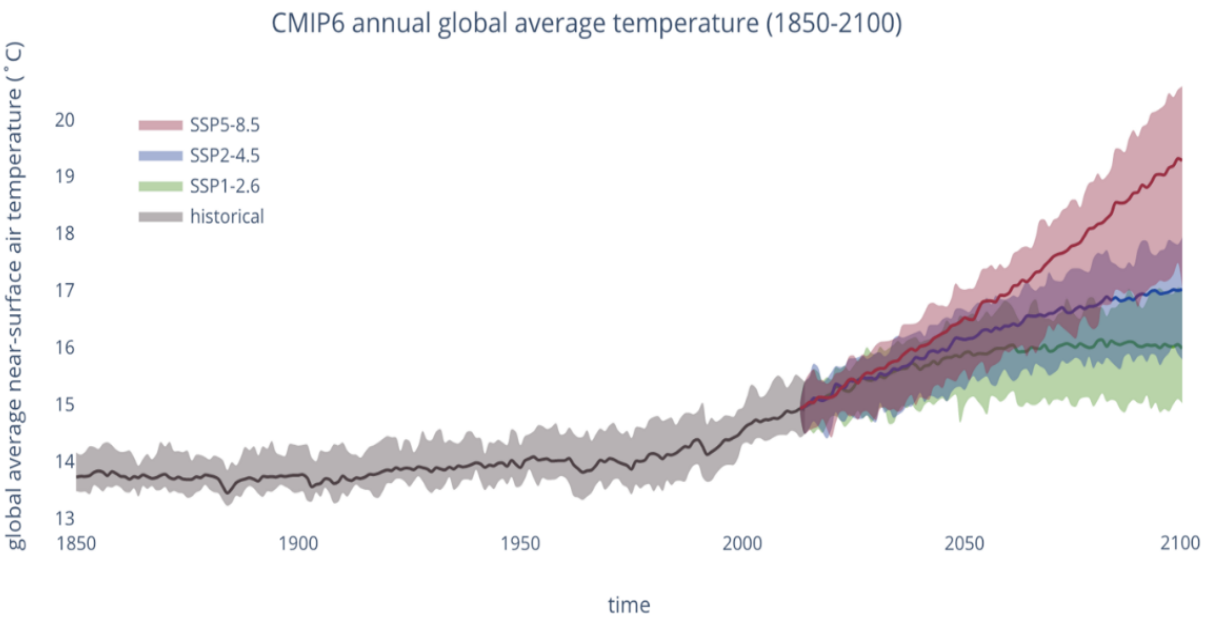

Figure 2 — Global mean temperature between 1850 and 2100 for selected CMIP6 models. The grey shaded area shows the range of historical simulations while the coloured areas show potential future temperature change based on different greenhouse gas emission scenarios (from Copernicus Climate Change Service, ECMWF).

An ongoing project at IMO has further downscaled the NEX-GDDP-CMIP6 down to 5 km, using the CARRA dataset to bias-correct the data. A preprocessing step was carried out before the bias adjustment was performed. Both the NEX-GDDP-CMIP6 dataset (25-km resolution) and the CARRA dataset (2.5-km resolution) were re-gridded to a common 5-km resolution using bilinear interpolation. The bias-adjusted climate data at 5-km resolution include a total of 13 models for both the historical (1950–2014) and future periods (2015–2100) for the two emissions scenarios used in this study (SSP2-4.5, and SSP5-8.5). Further details can be found in Zaqout *et al.* (2024).

Table 2 — List of NEX-GDDP CMIP6 models used for precipitation projections.The variant describes the run (r), initialisation (i), parameterisation (p), and forcing (f) versions used for the simulation.

Model name	Variant	Model name	Variant
ACCESS-CM2	r1i1p1f1	INM-CM5-0	r1i1p1f1
BCC-CSM2-MR	r1i1p1f1	MIROC-ES2L	r1i1p1f2
CMCC-ESM2	r1i1p1f1	MIROC6	r1i1p1f1
CNRM-ESM2-1	r1i1p1f2	MPI-ESM1-2-HR	r1i1p1f1
FGOALS-g3	r3i1p1f1	MPI-ESM1-2-LR	r1i1p1f1
GFDL-ESM4	r1i1p1f1	MRI-ESM2-0	r1i1p1f1

4 Calculation of annual maximum series of consecutive dry days (CDD) and consecutive wet days (CWD)

In the previous section, precipitation timeseries based on observations and the CARRA reanalysis were discussed, as well as the downscaled precipitation projections down to 5-km for two climate scenarios covering the whole country.

In this study, the focus is not directly on precipitation, but on periods of meteorological droughts and wet spells. A method to measure and analyse those periods is to use two extreme climate indicators known as the maximum consecutive dry days (CDD) and consecutive wet days (CWD). According to the Copernicus database definition, these indicators are calculated by counting the number of consecutive days when daily precipitation is below 1 mm (CDD), or superior to 1 mm (CWD). Yearly maximum values are then calculated from the timeseries, so that for a specific location, the annual maximum number of consecutive dry days and consecutive wet days can be obtained. In the rest of the report, CDD and CWD will be used to refer to the annual maximum series of maximum consecutive dry days and wet days, respectively.

The bias-adjusted daily precipitation from the NEX-GDDP-CMIP6 dataset at 5-km horizontal resolution was used to obtain projections for both CDD and CWD. The median, 10^{th}, and 90^{th} percentile values were calculated for the ensemble of the different models for the historical and future periods. The calculated ensemble statistics values were then bilinearly interpolated to a higher resolution of 2.5 km. Therefore, ensemble statistics values of CDD and CWD are available for the whole country at a resolution of 2.5 km, and for each climate model at a resolution of 5 km. Most of the study that follows is based on the ensemble statistic values at 2.5 km. Timeseries for the twelve control stations were then created for the historical period and the two scenarios by taking the CDD and CWD values from the grid-point located closest to the station coordinates in the 2.5-km grid.

Similarly, CDD and CWD calculation was made on the precipitation measurements and the CARRA dataset to create timeseries for the twelve control stations with annual maximum CDD and CWD. While the CARRA dataset runs continuously from September 1990 until the end of 2022, a varying number of missing data is present in the observations, as previously shown in Table 1. Thus, missing dates from the measurements were discarded from the reanalysis. In the case of data missing for more than three months within the same year, it was decided to not calculate the yearly maximum.

5 Historical changes of CDD and CWD in the control stations

5.1 Analysis of the CDD and CWD timeseries from the precipitation measurements

As described in the previous section, annual maximum series of CDD and CWD were calculated for the twelve control stations, based on daily precipitation measurements available. Although timeseries are not the same length for all stations, Table 3 shows the minimum, median, and maximum values calculated for each individual station, both for the dry and wet days.

For the consecutive dry days, minimum values vary between 6 and 15 days, meaning that every year of recording shows between about one and two weeks of consecutive days with no precipitation. Overall, the lowest numbers of days are found in Laufbali and Kvísker (respectively 6 and 7 days), which is in accordance with previous studies as both stations are located in the wettest part of Iceland. Other stations, such as Höfn í Hornafirði in the south-east, but also Flateyri and Ísafjörður in the Westfjords have at least two weeks with no precipitation among all the years recorded by the stations. The maximum number of consecutive dry days recorded in a year is 49 in Flateyri in summer 2002, which was also a dry period in the neighbouring stations of Ísafjörður and Súðavík, both with a CDD of 45 days recorded in 2002 (see Appendix I). The lowest number of maximum CDD is found in Kvíkser with a maximum of 22 days (about three weeks) with no rain recorded in 2015. This trend is also noticeable when looking at the median number of CDD, with all stations having a value between 17 and 23 days, except for Laufbali and Kvísker (13 days).

Analysing the annual maximum CWD, it appears that for all the control stations, at least five days of consecutive precipitation were recorded over the time-period covered by the measurements. Again, among all the stations, the wettest is Kvísker, with a minimum value of annual maximum CWD of nine days, and a maximum number of 69 consecutive wet days. Along with Laufbali, Kvísker has a median number of CWD of 17 days, way above the median values in the other stations which are ranging from 9 to 12 days.

Table 3 — Minimum, median, and maximum CDD and CWD as calculated from observations in the twelve control stations. For the time-periods used for the calculation, see Table 1.

	CDD (days)			CWD (days)		
	Minimum	*Median*	*Maximum*	*Minimum*	*Median*	*Maximum*
Eskifjörður	9	21	38	5	9	17
Flateyri	14	20	49	6	11	17
Höfn	15	23	35	6	10	20
Ísafjörður	14	23	45	5	11	27
Kvísker	7	13	22	9	17	69
Laufbali	6	13	32	7	17	32
Neskaupstaður	11	17	28	6	11	22
Ólafsfjörður	13	21	30	6	11	14
Reykjavík	11	17	24	8	11	31
Seyðisfjörður	11	18	33	8	11	20
Siglufjörður	11	17	28	7	12	20
Súðavík	10	21	45	5	10	16

5.2 Comparison between measurements and the CARRA dataset

In order to visualise CDD and CWD timeseries, histograms were created for the twelve control stations. In the histograms, results previously presented in Table 3 can be seen, but in addition, histograms based on simulated CDD and CWD timeseries from the CARRA reanalysis are also shown. Two examples, one for Eskifjörður (Figure 3), the other for Kvísker (Figure 4), are presented, with the others being available in Appendix I.

In Figure 3, for Eskifjörður, results from the measurements and from the CARRA dataset are close overall, especially regarding the general pattern of distribution. Indeed, years with a high CDD number measured by the station correspond to a high number of days in the reanalysis. However, there is a systematic underestimation of the number of dry days in the CARRA dataset: over the 22 years covered by the timeseries, the maximum number of CDD is greater in the CARRA dataset than in the measurements only once, in 2022. This trend is reflected by the median CDD value (horizontal dashed lines), which amounts to 21 days for the observations, and only 13 days for the reanalysis. Regarding the CWD histograms, the opposite trend can be observed, with the CARRA dataset overestimating the number of wet days most years. Overall, the difference between the median values between both datasets is smaller than for the CDD (12 in the CARRA dataset, 9 in the observations).

For Kvísker (Figure 4), results are slightly different. Except for 2010, CDD calculated from the two datasets are comparable. Likewise, for the CWD histograms, except for the two years with a very long period of wet spell (2011 and 2015) recorded by the station, the

reanalysis shows very similar results to the observed timeseries. Those three years (2010, 2011, and 2015) would need to be investigated further.

This general pattern of simulations being wetter than observations (which translates to a smaller number of CDD and larger number of CWD) can be further noticed in the scatterplots shown in Figure 5. In the top panel that shows results for all twelve stations, the trend gives higher CDD values for the measurements, and higher CWD values for the simulations. It can also be noticed in the two individual scatterplots shown for Reykjavík, and Kvísker (scatterplots for the other stations are available in Appendix II). These two stations were selected as Reykjavík shows the smallest bias between measurements and simulations (with low RMSE and MAE) both for the CDD and CWD, while Kvísker shows the largest difference, although this is mainly due to the two outliers observed before on the histograms for the years 2011 and 2015. In Table 4, RMSE and MAE calculated for CWD for each station spread through a smaller interval than for CDD. With the exception of Kvíkser, RMSE values vary between 3.3 (Höfn í Hornafirði) and 8.1 (Laufbali) for CWD, while RMSE for CDD values range from 3.5 (Reykjavík) to 14.2 (Seyðisfjörður). Mean values of RMSE and MAE are also indicated for all stations in the first scatterplot in Figure 5, and both indicators are inferior for CWD than for CDD, even considering the two outliers in Kvísker as discussed earlier.

Table 4 — RMSE and MAE between observation and reanalysis for CDD and CWD timeseries in the twelve control stations.

	CDD (days)		CWD (days)	
	RMSE	*MAE*	*RMSE*	*MAE*
Eskifjörður	10.0	7.2	4.5	3.6
Flateyri	10.3	6.6	4.6	4.2
Höfn í Hornafirði	10.2	8.0	3.3	2.5
Ísafjörður	9.3	7.0	7.0	5.8
Kvísker	6.0	3.8	20.1	10.5
Laufbali	8.0	6.0	8.1	5.9
Neskaupstaður	5.6	4.0	3.7	3.0
Ólafsfjörður	8.0	6.8	5.7	3.7
Reykjavík	3.5	2.8	3.9	2.9
Seyðisfjörður	14.2	7.0	5.1	3.7
Siglufjörður	6.3	4.6	5.0	3.5
Súðavík	8.3	6.0	3.7	2.8

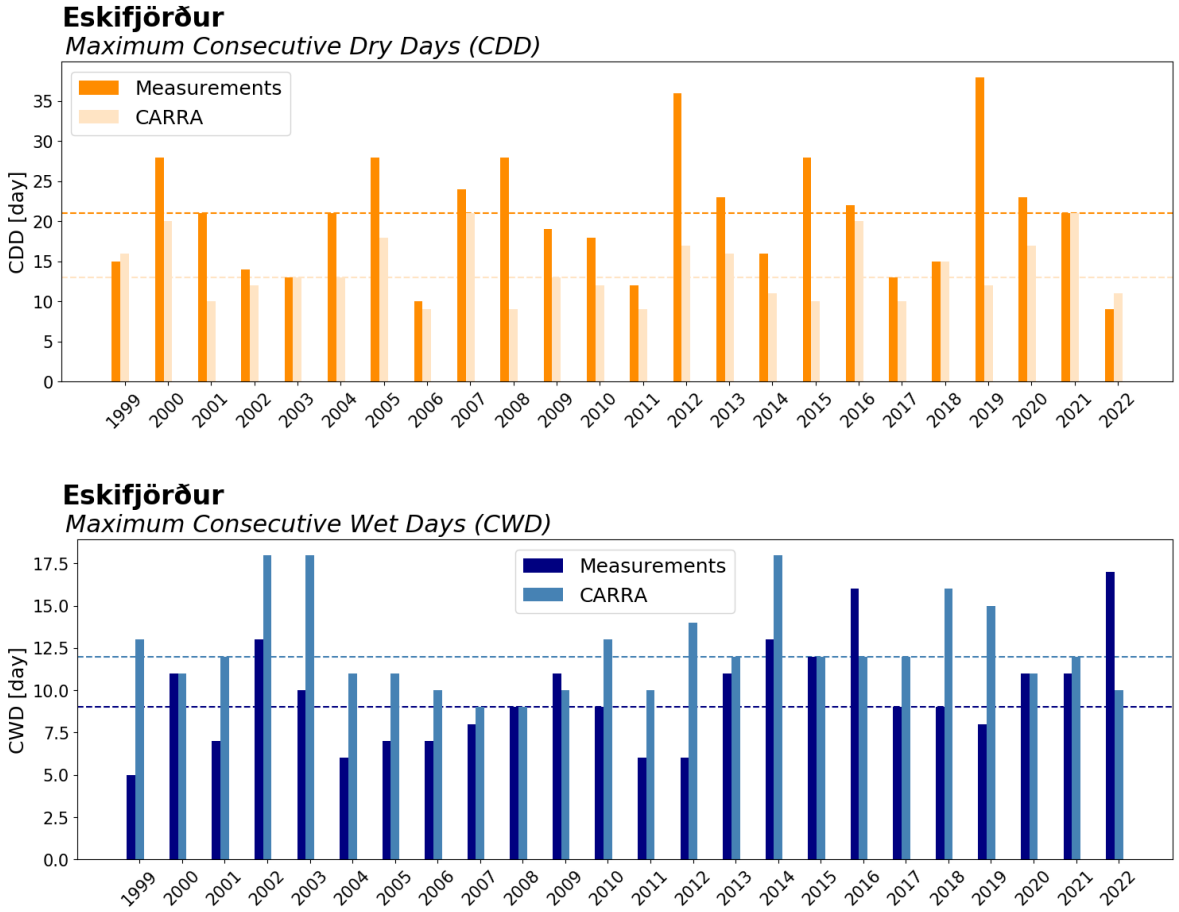

Figure 3 — Histograms showing annual maximum CDD (top) and CWD (bottom) based on observations and reanalysis for station Eskifjörður. Dashed lines indicate the median values over the years covered by the timeseries.

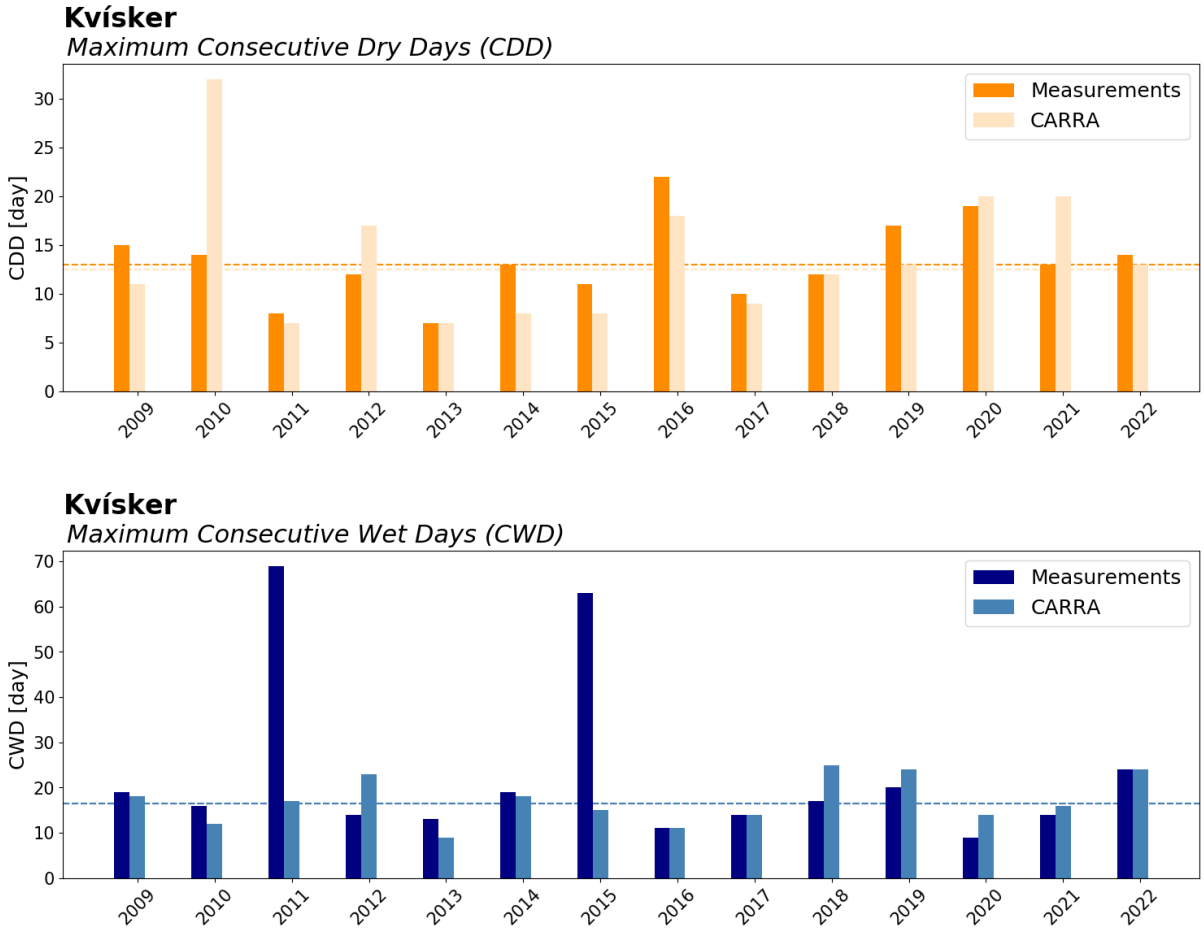

Figure 4 — Histograms showing annual maximum CDD (top) and CWD (bottom) based on observations and reanalysis for station Kvísker. Dashed lines indicate the median values over the years covered by the timeseries.

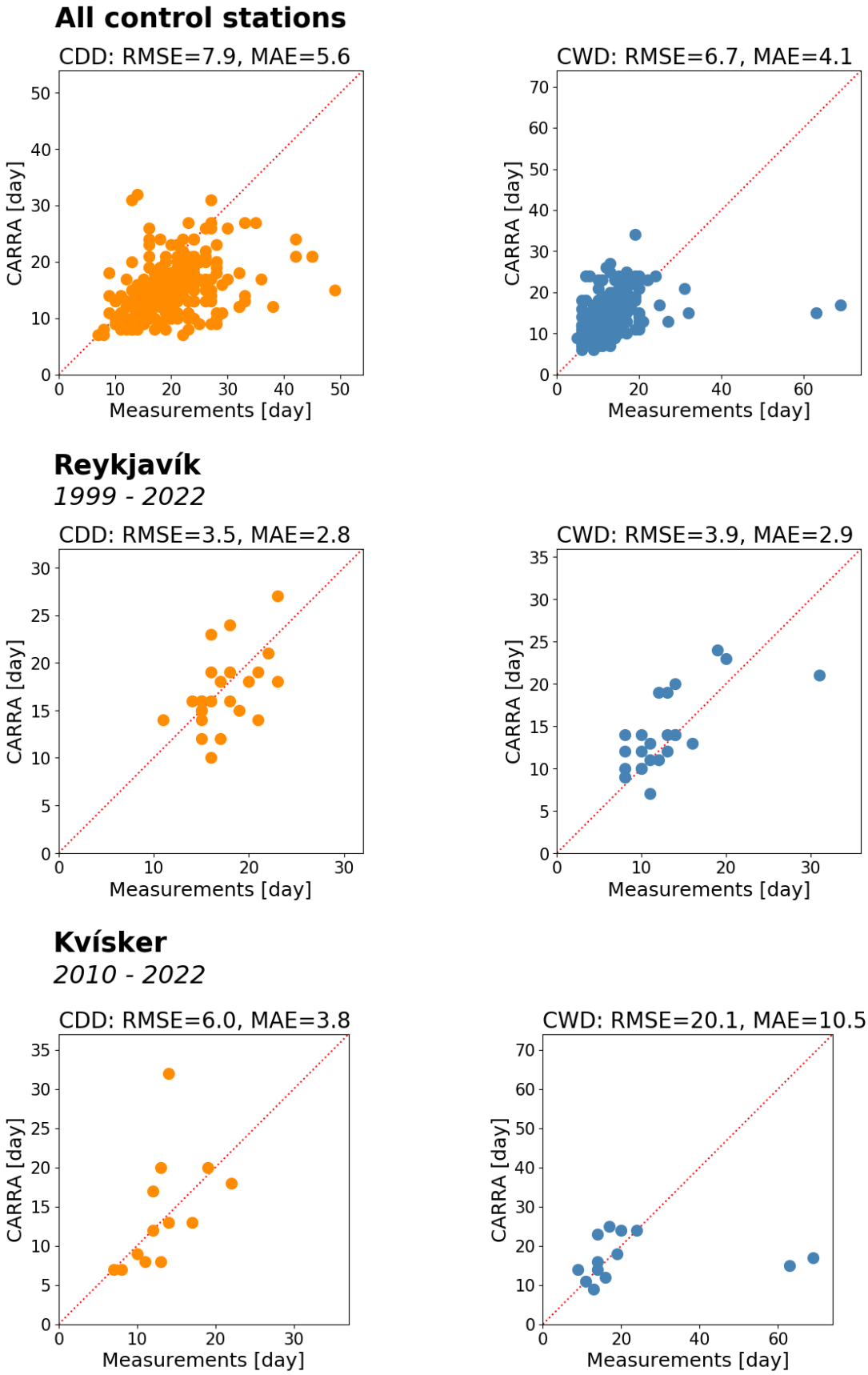

Figure 5 — Scatterplots comparing CDD (left) and CWD (right) timeseries based on observations and reanalysis for all stations (top), Reykjavík (middle) and Kvísker (bottom). RMSE and MAE are also indicated.

5.3 Temporal changes in CDD and CWD for the control stations

In the histograms presented for Eskifjörður and Kvísker in Figure 3 and 4, it is difficult to see trends in CDD and CWD over the years, which is also the case for the other control stations shown in Appendix I. In order to further study whether the situation has changed over the years covered by the control stations, step plots were created, as shown in Figure 6.

In those step plots, shown here for three stations (Eskifjörður, Flateyri, and Seyðisfjörður; others are available in Appendix III), the number of times a threshold is reached is shown by an indent (or step) in the line and plotted against time. In these figures, the thresholds chosen are the median values from the timeseries, as already given in Table 4. In the top left figure, the orange line represents the annual maximum CDD calculated from the observations in Eskifjörður. In this case, as seen in Table 4, the median value of the timeseries is 21 days. The steps shown by the orange line represents the number of times this threshold of 21 days is reached or overcome: in this case, 13 times. The same is done for the timeseries based on the CARRA dataset, represented by the light-orange line (the median value there is reached 12 times). On top of these results, vertical lines denote the year in which half of the total occurrences that the threshold was reached. In the case of the orange line, the vertical line marks the year 2008, as this is the year when the median value has been reached 6 times, representing half the total occurrences that this threshold has been reached (the result was rounded as the total number is 13). Therefore, by studying the years indicated by the vertical lines, indication whether the thresholds were reached more often at the beginning of the timeseries or at the end can be drawn.

In the majority of cases (9 out of 12 stations), the CDD timeseries give a date at which half the total number of times the threshold is reached earlier than for the CWD timeseries. In Figure 6, this is illustrated by stations Eskifjörður and Seyðisfjörður, while for Flateyri, this date is reached later on by the CDD timeseries (2012 for measurements, 2008 for the reanalysis) than by the CWD timeseries (2008 for measurements, 2009 for the reanalysis).

These results tend to indicate that longer periods of dry spells were encountered more frequently during the earlier years covered by the measurements, while longer periods of wet spells are more frequent in recent times. This can also be interpreted from the general shape of the step plots: the CDD tends to have a steeper slope at the beginning and flattens in the latter years covered by the measurements, while the opposite trend is observed for the CWD. Because of the varying lengths of recording between stations, it is difficult to make a general assessment.

However, these results are only a first attempt at quantifying the historical changes in the CDD and CWD timeseries at the stations. It should be noted that in these step plots, the results from the CARRA dataset are in accordance with the observed timeseries. Thus, for a more robust study, the whole time period covered by the CARRA dataset could be used to see if this trend is noticeable over the longer timespan covered by the reanalysis, but this is out of scope for this study.

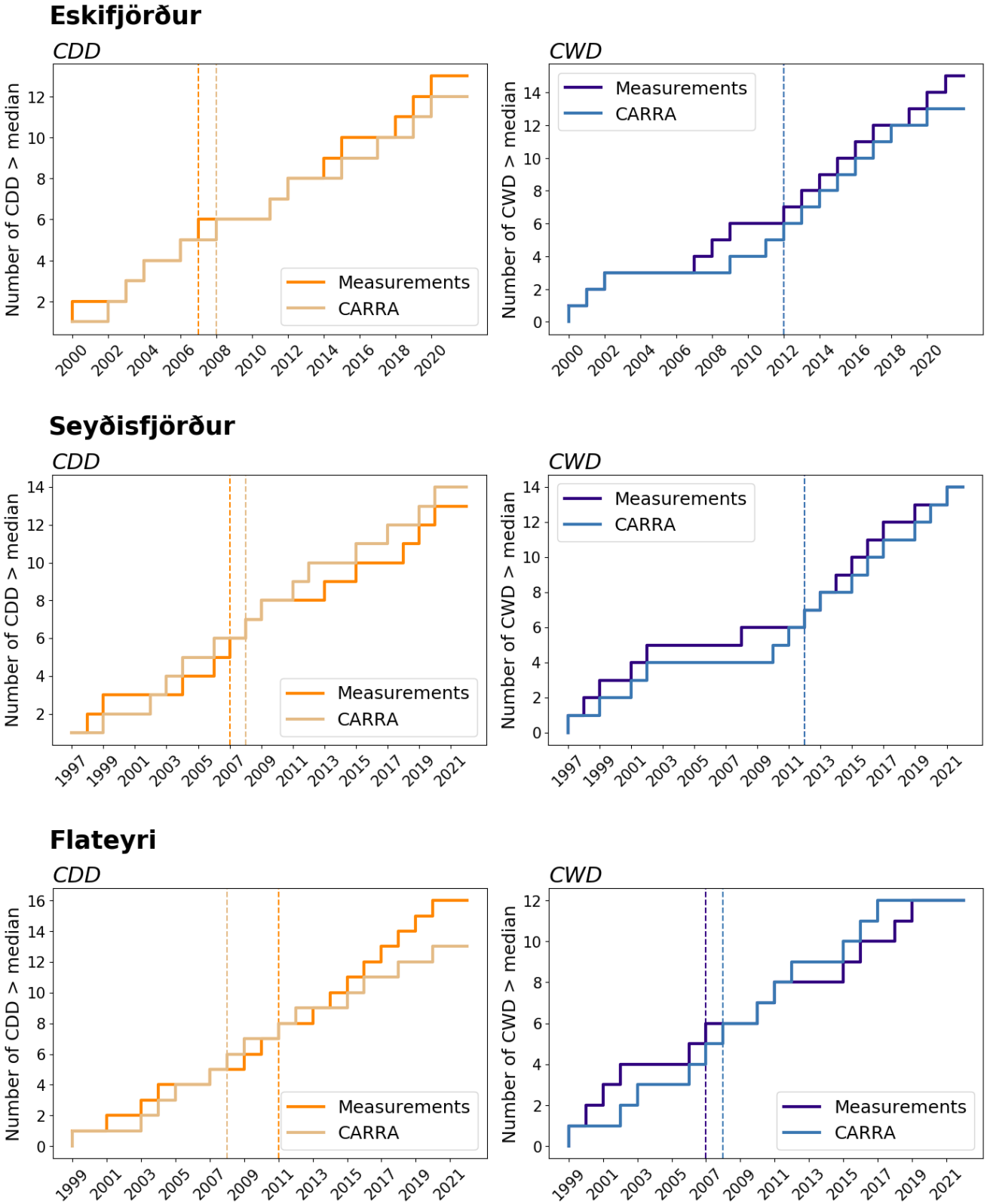

Figure 6 — Step-plots showing the number of times CDD and CWD reach the median value as calculated over all timesteps for stations Eskifjörður (top), Flateyri (middle) and Seyðisfjörður (bottom). For each plot, results are shown both for the measurements and the CARRA timeseries. Vertical dashed lines indicate the year of occurrence when half the total number of times the threshold has been reached.

6 Future CDD and CWD projections from the CMIP6 dataset

6.1 Projections for the control stations

As explained in Section 4, bias-corrected CDD and CWD timeseries were retrieved at the location of the control stations for SSP2-4.5 and SSP5-8.5 and a historical period.

Table 5 gives CDD and CWD values as calculated from the median of the ensemble of climate models for the historical and future periods. Values are calculated for each station based on the median value between 1986 and 2015 for the historical period, and over the period 2091–2100 for the SSP scenarios. These time intervals were chosen to match other studies about climate assessment in Iceland, such as the fourth assessment report from the Scientific Committee on Climate Change (2023).

Comparison of the median historical values with results from Table 3 shows that overall, median CDD values are underestimated in the climate models as values in Table 5 for the historical period ranges from 13 days (Kvísker and Laufbali) to 18 (Súðavík), while results from measurements spread between 13 and 23 days. The same can be noticed for the CWD: median values range from 10 (Höfn) to 14 days (Kvísker, Ísafjörður) in the climate ensemble, against 9 to 17 days in the observation timeseries. Overall, the range reached for the twelve control stations is narrower in the climate models than in the observations. However, the general pattern is respected: wettest stations are Kvísker and Laufbali, with both the largest median CWD values (respectively 15 and 14 days) and the smallest median CDD values (13 days).

Table 5 — CDD and CWD values (days) as calculated from the median of the ensemble of climate models for a historical period (1986–2015) and two scenarios (2091–2100) for the control stations. Median values from Table 3 are added in brackets, although it should be noted that they were calculated on a different time-period.

	CDD (days)			CWD (days)		
	Historical	*SSP2-4.5*	*SSP5-8.5*	*Historical*	*SSP2-4.5*	*SSP5-8.5*
Eskifjörður	15 *(21)*	15	15	12 *(9)*	13	12
Flateyri	17 *(20)*	18	16	15 *(11)*	16	15
Höfn	16 *(23)*	17	17	10 *(10)*	10	10
Ísafjörður	16 *(23)*	18	16	15 *(11)*	15	15
Kvísker	13 *(13)*	14	14	15 *(17)*	14	14
Laufbali	13 *(13)*	12	14	14 *(17)*	14	14
Neskaupstaður	16 *(17)*	17	15	11 *(11)*	11	11
Ólafsfjörður	16 *(21)*	15	15	12 *(11)*	13	14
Reykjavík	17 *(17)*	17	17	13 *(11)*	12	12
Seyðisfjörður	13 *(18)*	14	13	13 *(11)*	14	14
Siglufjörður	15 *(17)*	15	14	13 *(12)*	13	14
Súðavík	18 *(21)*	19	17	13 *(11)*	13	13

In Table 5, median CDD and CWD are also given for the end of the century for SSP2-4.5 and SSP5-8.5. At first sight, results do not change drastically and stay in the same range as the historical values. This is further illustrated by Table 6, that gives the difference in number of days between a projection and the historical period. This is done both for the end of the century (2091–2100) and the middle of the century (2046–2055), each time in regard to the historical period (1986–2015). In order to assess the variability within the ensemble, results are also given for 10th and 90th percentile values. Overall, the changes in number of days is small, regardless of the scenario or the time-period used for the comparison, ranging from -1 day to 2 days. It should be noted that results were rounded to full days.

Regarding the numbers of CDD based on the median of the ensemble, the difference for the end of the century varies between 0 (6 stations) and 2 days (1 station) for SSP2-4.5 with the other stations having a change of 1 day. For SSP5-8.5, the difference ranges from -1 (three stations) to 1 day (3 stations), with 6 stations having no change. Therefore, more stations seems to have a drier trend at the end of the century with the SSP2-4.5 scenario than with SSP5-8.5.

As stated before, the range of change for CWD is the same as for CDD. Again, focusing on the values at the end of the century based on the median, the difference varies between -1 (2 stations) and 1 day (4 stations) for SSP2-4.5, with 6 stations having no change. For SSP5-8.5, the difference ranges from -1 (2 stations) to 2 days (1 station), with 8 stations having no change. Another way of visualising these results is presented in Figure 7 and 8, for two stations. Figure 7 shows the evolution of CDD for both scenarios for Ísafjörður, and Figure 8 shows the evolution of CWD for both scenarios for Ólafsfjörður. Figures for the other stations are shown in Appendix IV. In the figures, median values from the ensemble of models are shown with dots, while mean values are represented by a solid line. The 10th-90th percentile range is also represented by the shaded area. On each plot, the three control periods (historical, middle of the century, end of the century) are emphasized with brighter colours. In Figure 7, focussing on the SSP2-4.5 scenario, the median number of CDD does not change in Ísafjörður in the middle of the century, and increases by 2 days at the end of the century. With the SSP5-8.5 scenario, a difference of 1 day can be observed in the middle of the century, and no change for the end of the century. These results are based on median values (shown by the dots in the figures) and the difference in CDD and CWD can vary for the same station and scenario if a different percentile is considered. In Figure 8, an example of the evolution of CWD under the two climate scenarios is shown for station Ólafsfjörður. For the SSP2-4.5 scenario, the median changes in the middle of the century and at the end of the century are both 1 day when compared to the historical period. Regarding the SSP5-8.5 scenario, no change is found in the middle of the century based on the median values of the ensemble of climate models, but the difference when comparing results at the end of the century with the historical period is 2 days. Again, those results are only based on the median of the ensemble of climate models, and would be different if the 10th or 90th percentile were considered instead.

To further analyse a possible change in the distribution of these two variables, density plots were created, and an example is given in Figure 9 for Neskaupstaður (results for other stations are available in Appendix V). As stated in Section 4, for individual models the resolution is 5 km as only the median and 10th-90th percentile ranges from the ensemble were downscaled to 2.5 km. In the figure, each panel compares the distribution of the twelve GCMs from Table 2 for the historical period (1986–2015), and the end of the century (2091–2100) for both scenarios. Results for CDD are shown in the top plots, while the lower figures show the distribution for CWD. The distribution of the values is shown both with histograms, with each bar indicating the number of occurrences the variable takes a certain value, and with a density curve, to capture the shape of the distribution. Vertical lines indicate the median value for each pool of data. It can be noted that the median values are not exactly the same as the ones presented in Table 5: in Table 5, the median was calculated based on the median of the ensemble data, while here the median is based on the whole ensemble. Although distribution does not vary much between the different periods and scenarios considered, it appears with CDD that for SSP5-8.5, density curves show a higher peak and distribution is contained in a narrower interval than for SSP2-4.5. This is the case for 9 stations out of 12, including Neskaupstaður. For CWD, the shape of the density curves show similar distribution between historical and end of the century model data, and it is more difficult to find a trend among the control stations.

Table 6 — Difference (days) between climate projections over two periods (2046–2055, 2091–2100) as compared to the historical period (1986–2015) for the 10th, 50th, and 90th percentiles of the ensemble of climate models. Results are shown for the twelve control stations for CDD (top table) and CWD (bottom table).

CDD	SSP2-4.5						SSP5-8.5					
	2046-2055			2091-2100			2046-2055			2091-2100		
	10th	*50th*	*90th*	*10th*	*50th*	*90th*	*10th*	*50th*	*90th*	*10th*	*50th*	*90th*
Eskifjörður	0	1	0	0	0	0	0	0	0	0	0	0
Flateyri	0	1	0	1	1	0	0	0	0	-1	-1	-1
Höfn	1	1	3	1	1	1	0	0	0	2	1	1
Ísafjörður	1	0	0	3	2	1	0	1	0	-1	0	0
Kvísker	0	0	0	2	1	1	1	0	1	2	1	0
Laufbali	1	0	-1	0	0	0	1	0	0	1	1	1
Neskaupstaður	0	1	1	0	1	-1	-1	0	0	0	0	0
Ólafsfjörður	0	0	2	0	0	0	1	0	0	-1	0	1
Reykjavík	1	1	1	2	0	1	2	1	1	1	0	0
Seyðisfjörður	1	1	0	0	0	0	0	0	1	0	0	0
Siglufjörður	0	0	2	1	0	-1	0	0	0	0	-1	0
Súðavík	0	0	0	2	1	0	0	0	0	-1	-1	0

CWD	SSP2-4.5						SSP5-8.5					
	2046-2055			2091-2100			2046-2055			2091-2100		
	10th	*50th*	*90th*	*10th*	*50th*	*90th*	*10th*	*50th*	*90th*	*10th*	*50th*	*90th*
Eskifjörður	0	1	0	0	1	0	0	0	0	0	0	1
Flateyri	1	1	0	0	1	0	0	1	0	0	0	0
Höfn	0	1	0	0	0	-1	0	0	0	0	0	-1
Ísafjörður	0	1	1	0	0	0	0	1	1	0	0	0
Kvísker	0	0	0	0	-1	-1	0	-1	0	0	-1	0
Laufbali	1	0	1	0	0	0	0	1	2	-1	0	0
Neskaupstaður	1	1	0	1	0	0	1	0	0	1	0	1
Ólafsfjörður	1	1	1	0	1	1	0	0	0	0	2	2
Reykjavík	1	0	0	0	-1	-1	0	-1	-1	0	-1	0
Seyðisfjörður	0	0	0	0	1	0	0	0	0	0	0	0
Siglufjörður	0	0	2	0	0	0	0	-1	0	0	1	0
Súðavík	0	0	1	0	0	1	0	1	1	0	0	0

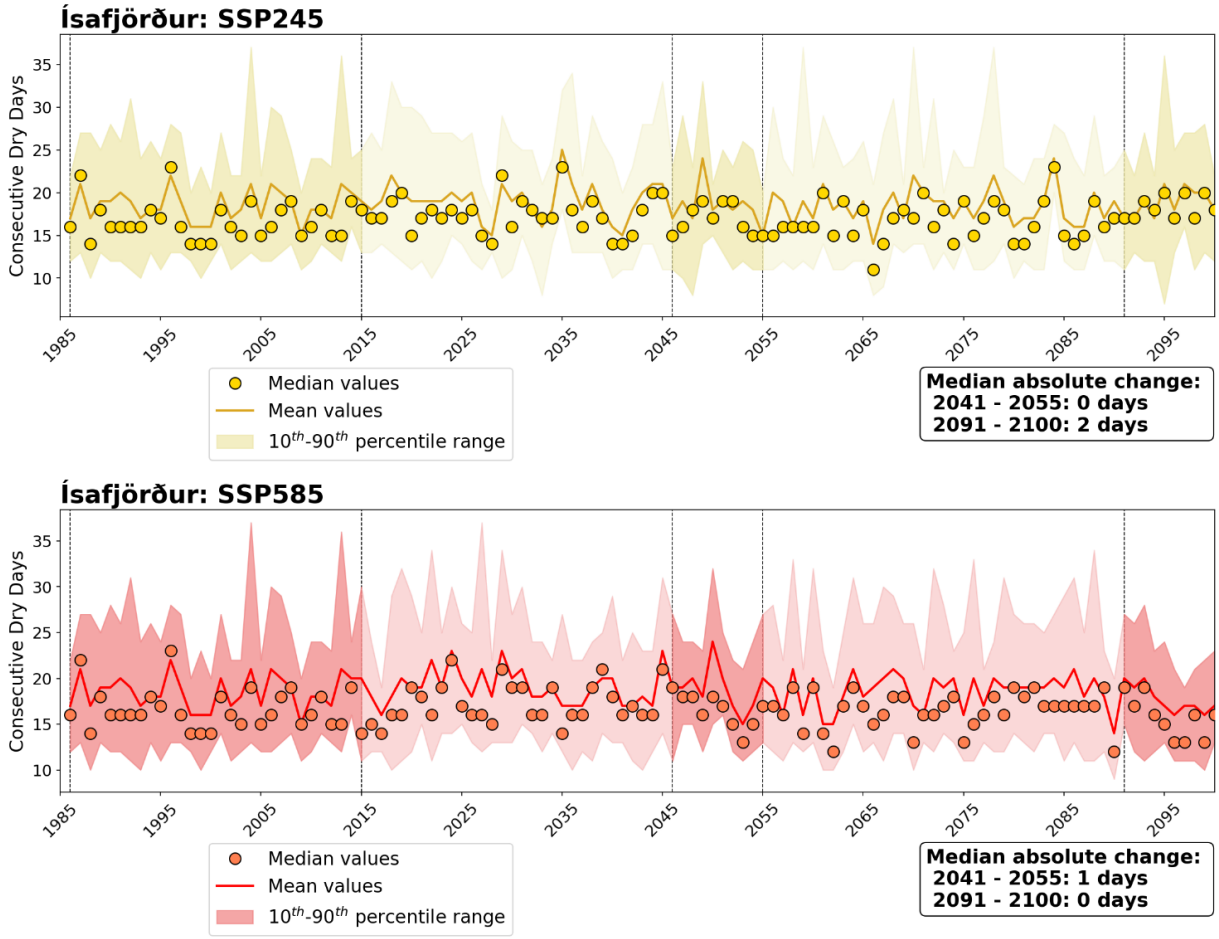

Figure 7 — CDD values for station Ísafjörður as calculated from the median (dots), mean (line), and 10th-90th percentile (shaded area) values of the ensemble of climate models for SSP2-4.5 (top) and SSP5-8.5 (bottom). Median differences for two periods (2041–2055 and 2091–2100) as compared to the historical period (1986–2015) are also indicated.

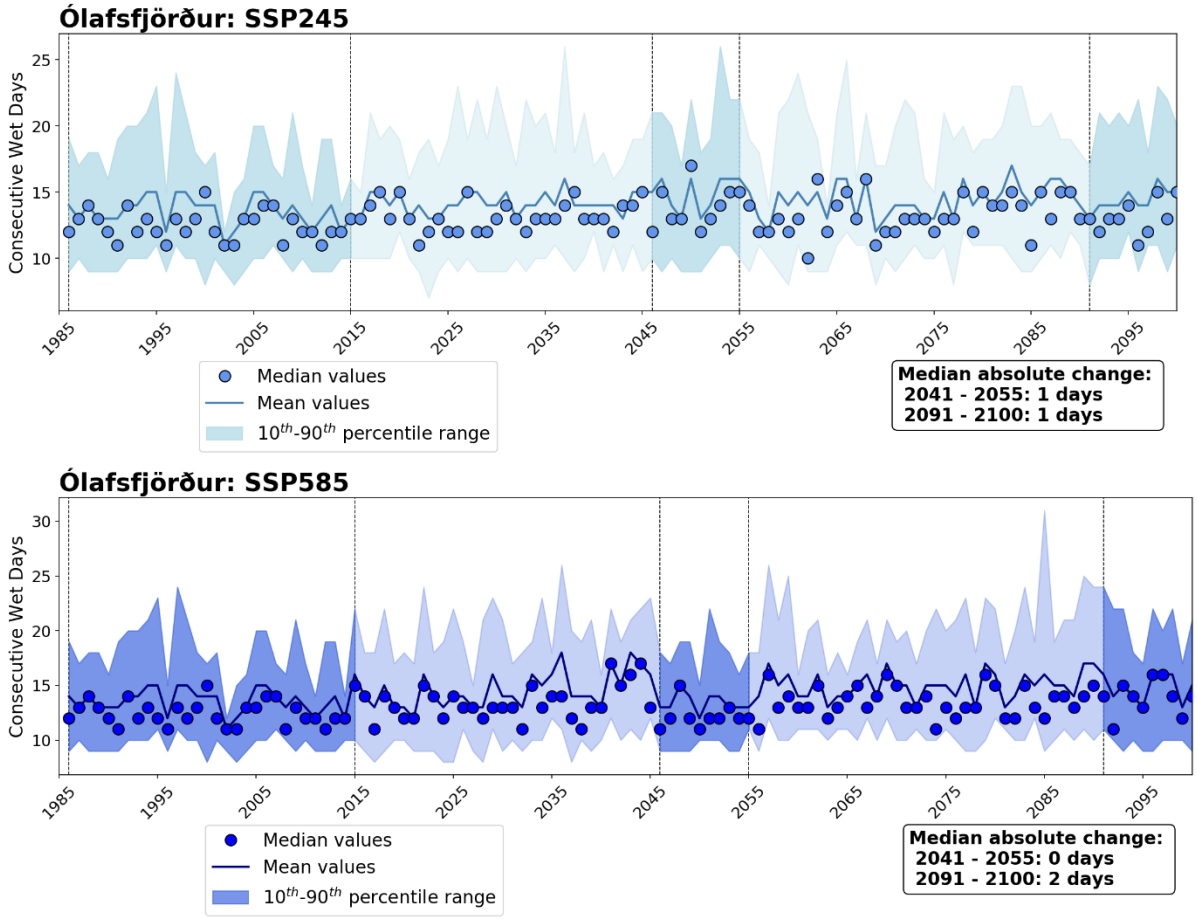

Figure 8 — CWD values for station Ólafsfjörður as calculated from the median (dots), mean (line), and 10th-90th percentile (shaded area) values of the ensemble of climate models for SSP2-4.5 (top) and SSP5-8.5 (bottom). Median differences for two periods (2041–2055 and 2091–2100) as compared to the historical period (1986–2015) are also indicated.

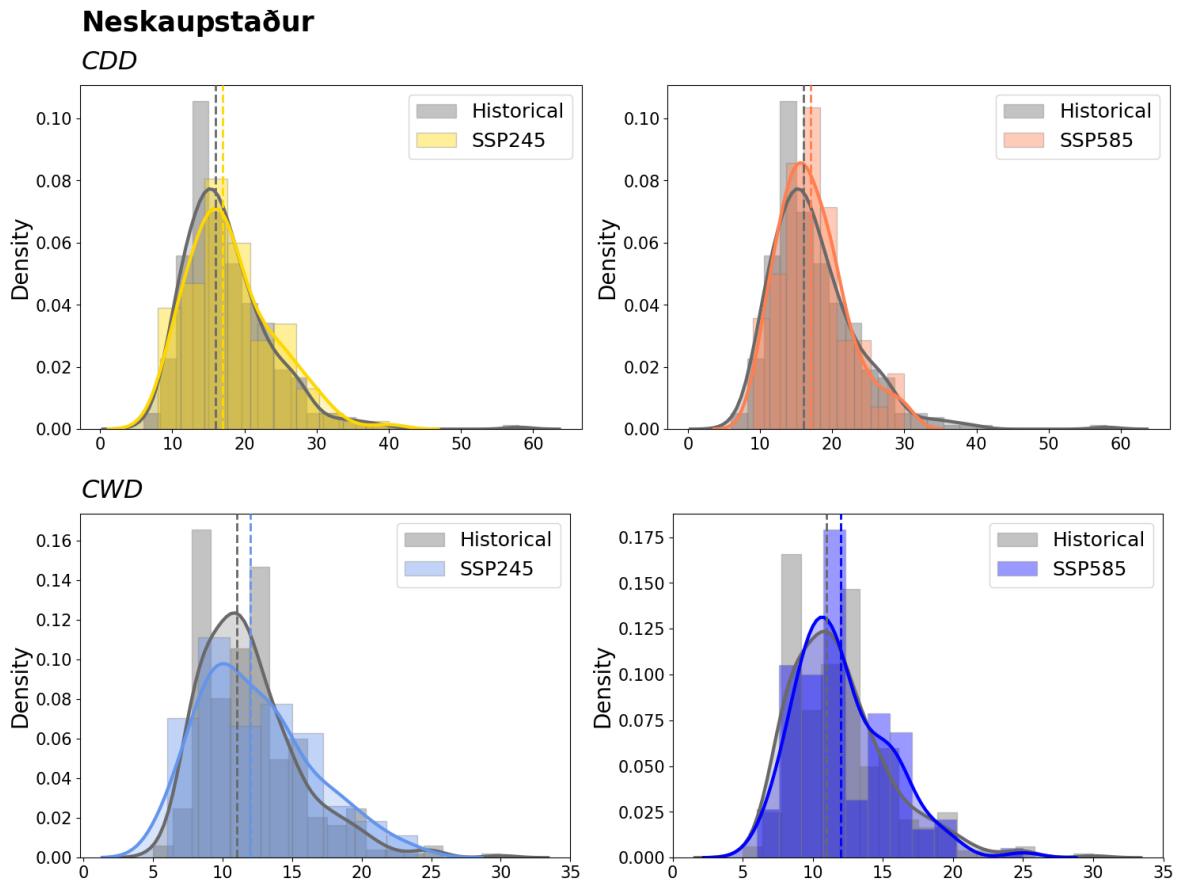

Figure 9 — Density plots and histograms for Neskaupstaður based on individual model values of CDD and CWD for a historical period (1986–2015) and two climate projections (2091–2100).

6.2 Projections for the hydropower catchments

Individual maps were created for each hydropower catchment operated by Landsvirkjun. An example for CDD is shown in Figure 10 for catchment Blöndulón, and an example for CWD is shown in Figure 11 for catchment Hálslón. Results for the other catchments are shown in Appendix VI.

Figure 10 shows CDD maps for Blöndulón. The top panel shows results based on historical data averaged between 1986 and 2015 for the ensemble median (left), and 90th percentile (right). The middle panel shows CDD based on SSP2-4.5 projections for the ensemble median (left) and 90th percentile (right). Finally, the lower panel shows results based on SSP5-8.5 projections for the ensemble median (left) and 90th percentile (right). Values shown on the maps are the mean values for each grid-point between 2091 and 2100. Also indicated on each map is the median value of the CDD values for the grid-points within the catchment. Results show rather small changes when comparing maps based on the ensemble median together, and maps based on the 90th percentile together, with changes in CDD lying in the details. Regarding the maps based on the median ensemble (left column), median CDD values for the catchment is 14 days, both for the historical period,

and for the two scenarios. Values range between 12 and 18 days. Very small changes in the contour lines can be noticed, but it appears for the last map (lower left) that the shaded area with CDD values from 16 to 18 days covers a smaller part of the catchment. The same can be observed in the maps based on the 90th percentile values, with the part of the catchment with values between 24 and 26 days not appearing for the SSP5-8.5 scenario as on the other maps. Median values also show a small decrease in the median CDD (20 days for the SSP5-8.5, against 21 days for both the historical and SSP2-4.5 scenario).

Figure 11 shows similar maps but for catchment Hálslón and CWD values. Again, when compared with the same ensemble percentile under the various scenario, maps look very similar with only small details changing that can lead to a median difference for the whole catchment ranging from 0 to 2 days.

In order to study if a trend is more noticeable in the other catchments, those median values based on the median ensemble models averaged over a historical period (1986–2015) and the end of the century period (2091–2100) are shown in Table 7, both for CDD and CWD. For CDD, when comparing median values from the SSP5-8.5 to the historical period, 7 catchments out of 11 show an increase of 1 day, while the other show no increase. With the SSP2-4.5 scenario, 3 catchments show an increase of 1 day, 4 catchments show a decrease of 1 day and the remaining 4 show no change. For CWD, the table shows an increase of 1 day for 6 catchments with the SSP5-8.5 scenario, with values decreasing by 1 day in one catchment, and three catchments showing no difference in the median CWD. With the SSP2-4.5 scenario, CWD values increases for two catchments by 1 day, decreases for one catchment by 1 day, and stays the same for the remaining 8 catchments.

Table 7 — Median CDD and CWD values for the hydropower catchments calculated from the average over historical (1986–2015) and future (2091–2100) periods.

	Median CDD (days)			Median CWD (days)		
	Historical	*SSP2-4.5*	*SSP5-8.5*	*Historical*	*SSP2-4.5*	*SSP5-8.5*
Blöndulón	14	14	14	13	14	14
Búðarháls	14	13	14	13	13	14
Hágöngulón	12	12	13	15	14	15
Hálslón	12	12	13	16	16	15
Hraunaveita	11	12	13	15	15	15
Kvíslaveita	13	12	13	14	14	15
Sultartangi	14	13	14	13	13	14
Tungnaá	13	14	14	15	15	15
Þingvallavatn	13	13	14	13	13	14
Þórisvatn	13	12	14	14	14	15
Ufsarlón	11	12	12	15	15	15

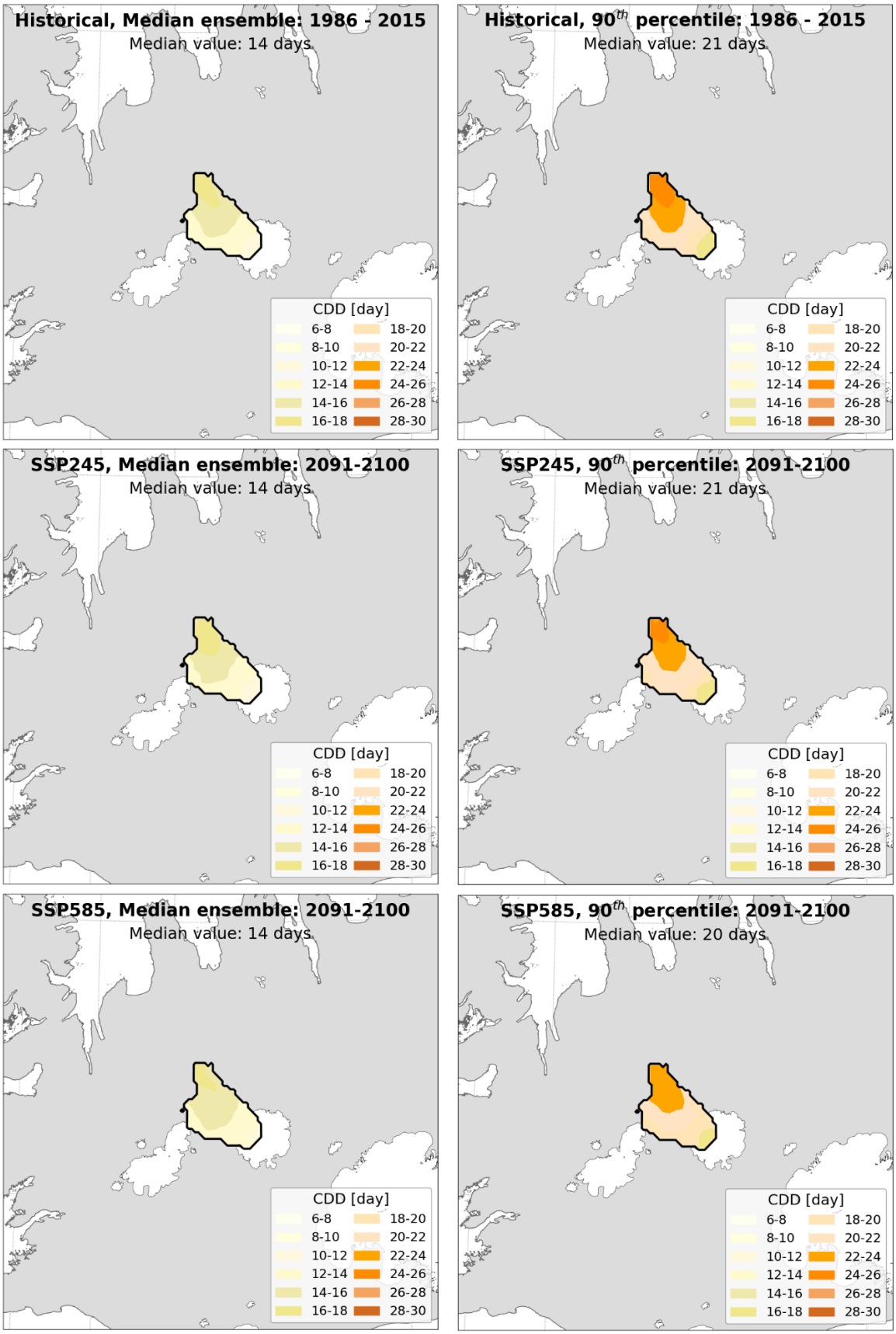

Figure 10 — CDD maps for catchment Blóndulón based on the downscaled CMIP6 dataset averaged over a historical period (1986–2015) and two projections (2091–2100) based on median and 90th percentile of the ensemble of climate models.

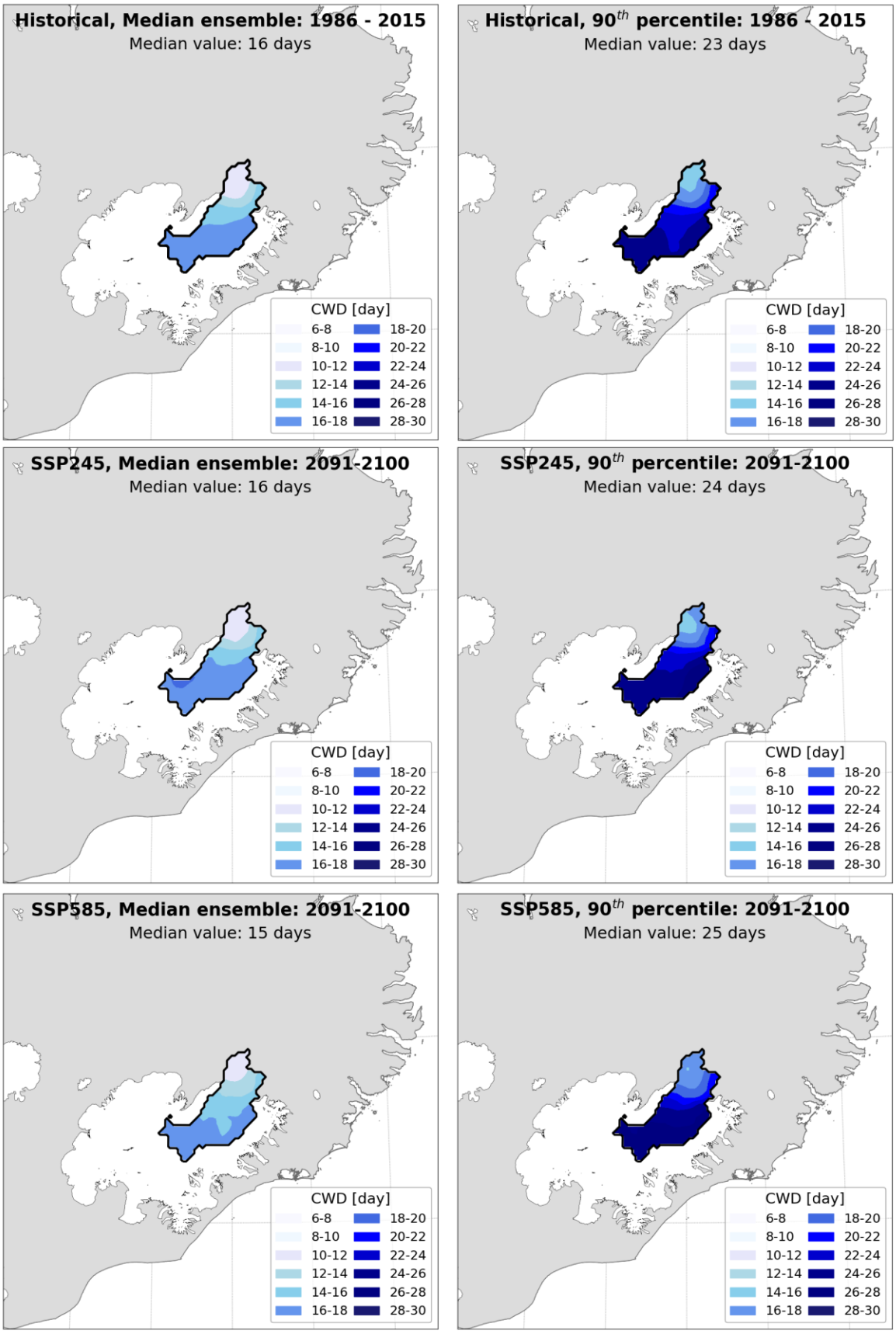

Figure 11 — CWD maps for catchment Hálslón based on the downscaled CMIP6 dataset averaged over a historical period (1986–2015) and two projections (2091–2100) based on median and 90th percentile of the ensemble of climate models.

6.3 Projections for the whole country

Finally, maps for the whole country showing differences between projections and historical period for CDD and CWD data are shown in Figure 12 and 13.

Figure 12 shows four maps: the top left map shows the difference in days for CDD values between SSP2-4.5 for the middle part of the century (values averaged between 2046 and 2055) and the historical period (values averaged between 1986 and 2015). The top right map shows the difference for the same scenario but for the end of the century (values averaged between 2091 and 2100). Lower maps show the differences between SSP5-8.5 and historical periods for the same period in the middle of the century (lower left) and the end of the century (lower right). Figure 13 shows these differences for CWD values.

In Figure 12, with the SSP2-4.5 scenario the changes range from -1 to 1 day for the largest part of the country. The length of the CDD increases in the Westfjords and the south-east up to 2 days, but this trend is smaller at the end of the century compared to the middle of the century for the Eastern part, and larger for the Westfjords. With the SSP5-8.5, variations are within the same range, and changes are slightly more defined geographically for the end of the century, with the northern half having a decrease up to 2 days in the length of CDD, and the southern half having an increase of the length of the dry period.

In Figure 13, it appears that the length of the wet spells increase with the SSP2-4.5 scenario more in the middle of the century than for the end of the century, while with SSP5-8.5, the part of the country covered by an increase of the CWD appears similar for the two time periods, but shifts northwards at end of the century. Out of the four maps, the one showing the most differences is SSP2-4.5 for the middle of the century, with most of the country showing an increase in the length of its wet periods up to 3 days.

Table 8 further reflects those results by showing minimum, maximum, and mean CDD and CWD differences between the scenarios in regard to the historical period for the whole country. For CDD at the end of the century, overall values are slightly higher for SSP2-4.5 (higher minimum, maximum, and mean) than for SSP5-8.5, although results are very close. For CWD difference, results are slightly higher with SSP5-8.5 than SSP2-4.5 for the end of the century, indicating that SSP5-8.5 is slightly wetter overall at the end of the century than SSP2-4.5. However, SSP2-4.5 gives overall higher values in the middle of the century, as was already illustrated by the map in Figure 13.

Table 8 — Minimum, maximum, and mean CDD and CWD difference found in Iceland between the two scenarios for two time periods (2046–2055 and 2091–2100) and the historical period (1986–2015).

	CDD difference				CWD difference			
	SSP2-4.5		*SSP5-8.5*		*SSP2-4.5*		*SSP5-8.5*	
	mid	*end*	*mid*	*end*	*mid*	*end*	*mid*	*end*
Minimum	-1.5	-1.4	-1.2	-2.0	-0.8	-1.8	-1.3	-1.4
Maximum	2.3	2.2	2.1	2.0	3.0	2.3	1.9	2.5
Mean	0.3	0.3	0.3	0.1	0.7	0.3	0.3	0.3

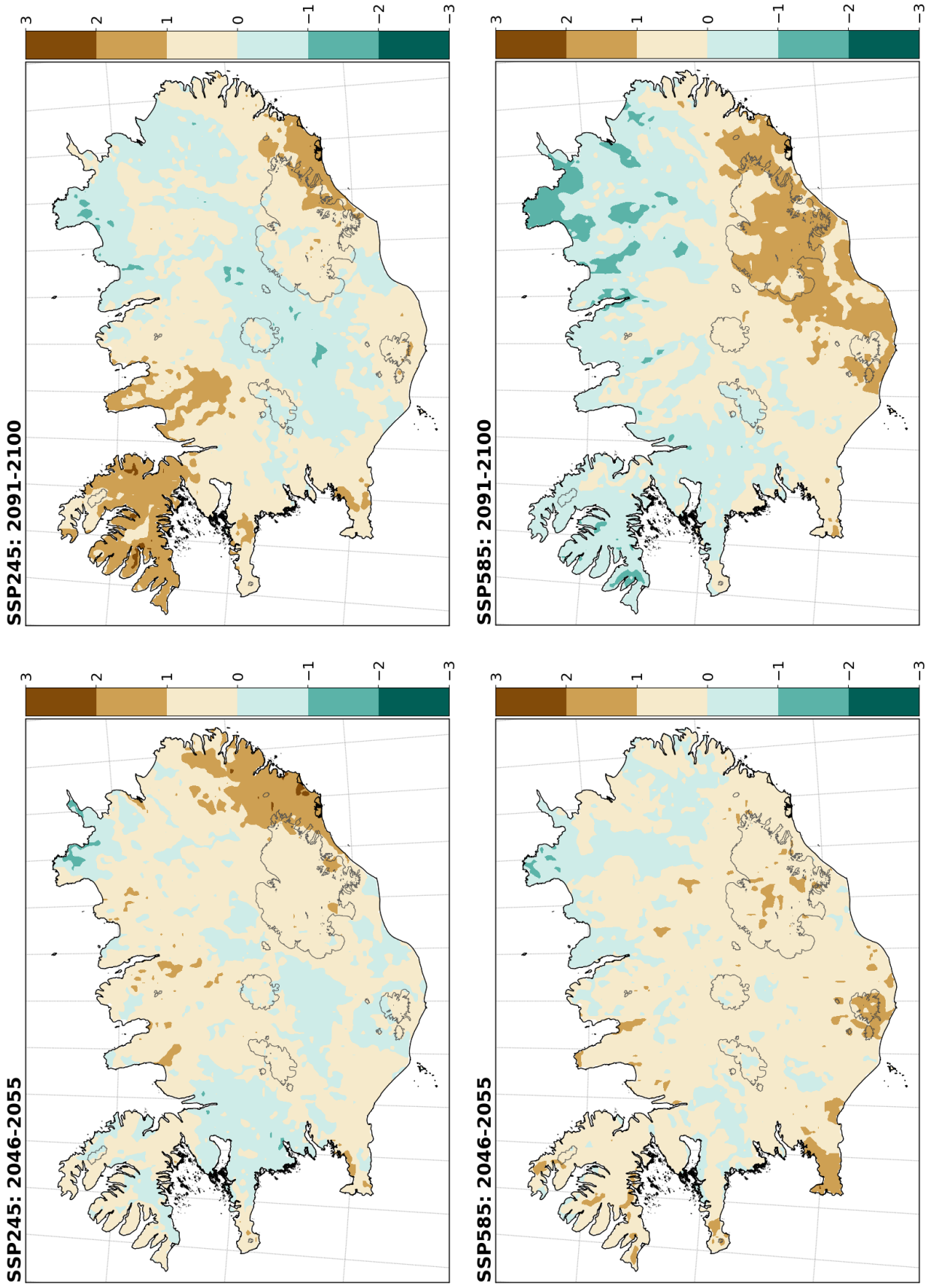

Figure 12 — CDD maps showing the difference between mean values over two periods (2046–2055 and 2091–2100) for two scenarios and mean values over the historical period (1986–2015).

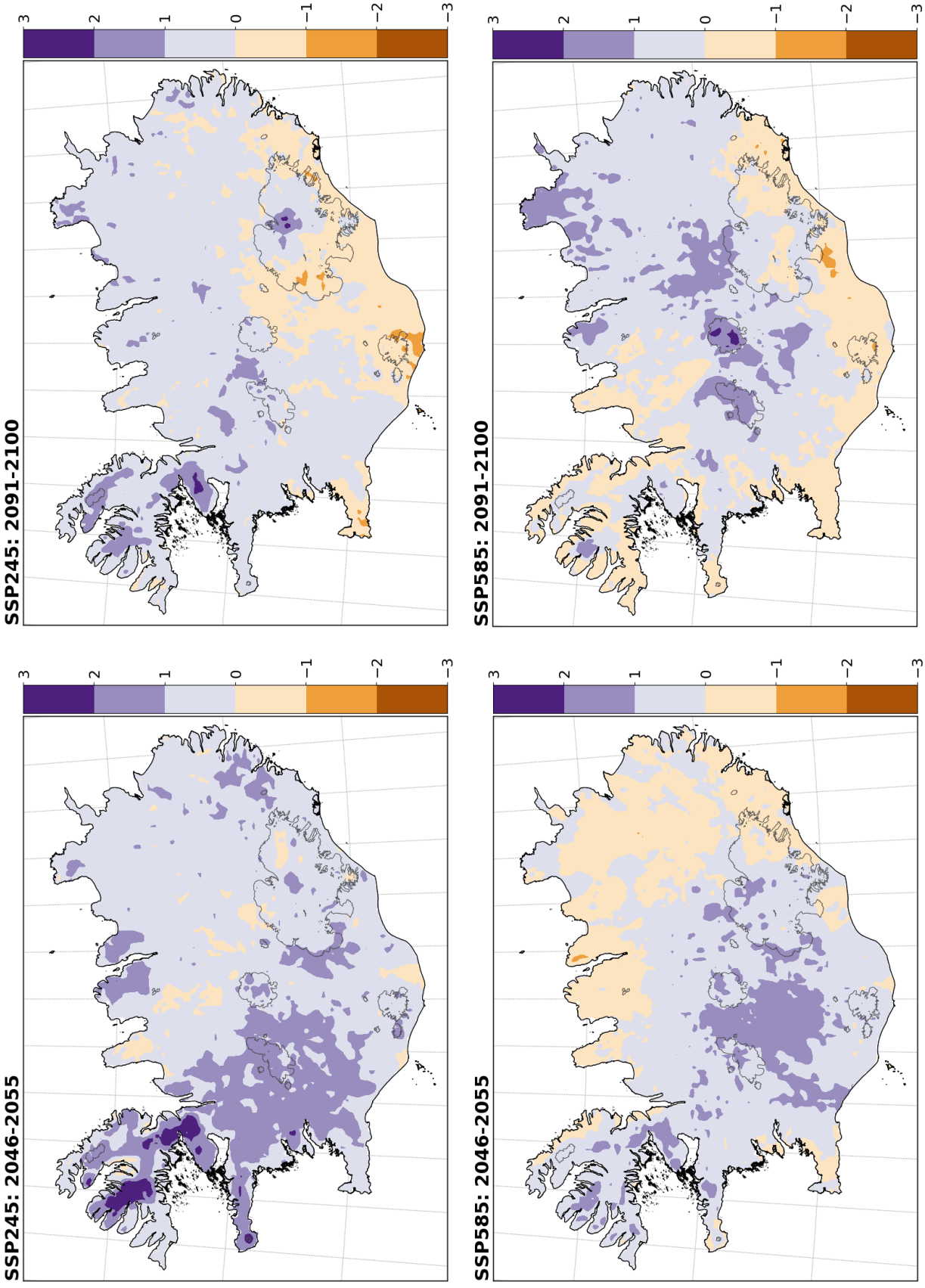

Figure 13 — CWD maps showing the difference between mean values over two periods (2046–2055 and 2091–2100) for two scenarios and mean values over the historical period (1986–2015).

7 Summary

This research addressed two questions: First, are there signs of change in the temporality of CDD and CWD in the control stations selected for this study? Secondly, how are those two extreme climate indicators expected to be affected by the ongoing warming of Arctic regions?

In Section 4, CDD and CWD were calculated for twelve control stations based on precipitation timeseries from observations and the CARRA reanalysis. These indicators were also calculated for the median, 10th, and 90th percentile values of the ensemble of models used in the NEX-GDDP-CMIP6 dataset, interpolated to a 2.5-km grid. These data include both historical (1950–2014) and future periods (2015–2100) for the two emissions scenarios used in this study (SSP2-4.5, and SSP5-8.5).

In Section 5, observed CDD timeseries for the twelve control stations show median values ranging from 13 (Laufbali, Kvísker) to 23 days (Höfn í Hornafirði, Ísafjörður), while CWD median values vary between 9 and 12 days in all stations, with the exception of Laufbali and Kvísker (both 17 days). This is in accordance with the general pattern of precipitation in Iceland, as both those stations are located in the wettest part of the country. Comparison of CDD and CWD timeseries with the CARRA dataset show that the simulations have a smaller number of CDD and a larger number of CWD in most cases, as illustrated by the scatterplots. An early analysis of historical changes of the two climate indicators shows a trend indicating that longer periods of dry spells were encountered more frequently during earlier years covered by the measurements, while longer periods of wet spells are more frequent in recent years. However, more work needs to be done to confirm those results, which could be achieved by making use of the complete time period covered by the CARRA dataset.

Finally, results from CDD and CWD climate projections for two scenarios were shown in Section 6, both for the control stations, the hydropower catchments, and the whole country. For the historical period, the range reached by the median CDD and CWD values for the twelve control stations is narrower in the CMIP6 dataset than in the observations. However, the general pattern is respected, with Kvísker and Laufbali having the highest CWD median values out of all stations. Projections show that for the control stations, the median number of CDD and CWD change between -1 and 2 days when compared to the historical period, regardless of the scenario or the time-period used for the comparison. Median values over the hydropower catchment areas indicate changes for the end of the century within the same range. Projections for the whole country show slightly more variations when CDD and CWD differences are calculated between future and historical periods. For CDD, regions with a change of -2 days are found in the north-eastern part of Iceland with SSP5-8.5 while values increase in the south-east. For CWD, the highest increase is found with the SSP2-4.5 scenario for the middle of the century. With SSP5-8.5, the proportion of the country covered by an increase in CWD appears similar for the two time periods, but shifts northwards at the end of the century.

In conclusion, based on measurements for the twelve control stations, longer periods of CDD seemed more frequent during the earlier years covered by the instruments, while longer periods of CWD are more frequent in the later years. CMIP6 projections indicate that median CDD and CWD values for the selected stations and hydropower catchments show small changes, ranging from -1 to 2 days, when comparing the different climate scenarios to the historical period.

8 References

Bengtsson, L., Andrae, U., Aspelien, T., Batrak, Y., Calvo, J., de Rooy, W. & Køltzow, M.Ø. (2017). The HARMONIE-AROME model configuration in the ALADIN-HIRLAM NWP system. *Mon. Wea. Rev*, 145, 1919–1935

Bintanja, R. (2018) The impact of Arctic warming on increased rainfall. *Scientific Reports*, 8, 16001. https://doi.org/10.1038/s41598-018-34450-3.

Björnsson, H., Sigurðsson, B. D., Davíðsdóttir, B., Ólafsson, J., Ástþórssson, Ó. S., Ólafsdóttir, S., Baldursson, T. & Jónsson, T. (2018). Loftslagsbreytingar og áhrif þeirra á Íslandi – Skýrsla vísindanefndar um loftslagsbreytingar 2018. *Veðurstofa Íslands*.

Crochet P., Johannesson T., Jonsson T., Sigurdsson O., Bjornsson H., Palsson F. & Barstad I. (2007). Estimating the spatial distribution of precipitation in Iceland using a linear model of orographic precipitation. *Journal of Hydrometeorology* 8, 1285–1306.

DMI. (2020). C3S Arctic regional reanalysis – Full system documentation.

Eyring, V., S. Bony, G. A. Meehl, C. A. Senior, B. Stevens, R. J. Stouffer, and K. E. Taylor, 2016: Overview of the Coupled Model Intercomparison Project Phase 6 (CMIP6) experimental design and organization. Geoscientific Model Development, 9, 1937–1958.

Fjórða samantektarskýrsla vísindanefndar um loftslagsbreytingar. (2023). Umfang og afleiðingar hnattrænna loftslagsbrytinga á Íslandi.

(https://cdn.loftslagsbreytingar.is/pdf/2023/10/skyrsla_visindanefndar.pdf)

Gylfadóttir, S. S. (2016). Lágrennslisvísar Greining þurrka og lágrennslistímabila í nokkrum vatnsföllum Landsvirkjunar. *Veðurstofa Íslands (Technical report).*

IPCC (2021). Climate Change 2021: The Physical Science Basis. Contribution of Working Group I to the Sixth Assessment Report of the Intergovernmental Panel on Climate Change [Masson-Delmotte, V., P. Zhai, A. Pirani, S.L. Connors, C. Péan, S. Berger, N. Caud, Y. Chen, L. Goldfarb, M.I. Gomis, M. Huang, K. Leitzell, E. Lonnoy, J.B.R. Matthews, T.K. Maycock, T. Waterfield, O. Yelekçi, R. Yu, and B. Zhou (eds.)]. *Cambridge University Press.* In Press.

Massad, A.-G. R., Petersen, G. N., Þórarinsdóttir, T., Roberts, M. J. (2020). Reassessment of return levels in Iceland. *Veðurstofa Íslands*. VÍ 2020-008.

Massad, A.-G. R., Petersen, G. N., Björnsson, H., Þórarinsdóttir, T., Roberts, M. J. (2022). Extreme precipitation in Iceland: Climate projections and historical changes in precipitation type. *Veðurstofa Íslands*. VÍ 2022-006.

Massad, A.-G. R., Björnsson, H., Petersen, G. N., Þórarinsdóttir, T. (2024). Influence of Iceland's changing climate on extreme precipitation and snow-fraction. *Veðurstofa Íslands.* To be published.

Nawri, N., Pálmason, B., Petersen, G. N., Björnsson, H. & Þorsteinsson, S. (2017). The ICRA atmospheric reanalysis project for Iceland. *Veðurstofa Íslands*. VÍ 2017-005.

O'Neill, B.C., Kriegler, E., Ebi, K. L., Kemp-Benedict, E., Riahi, K., Rothman, D. S., van Ruijven, B. J., van Vuuren, D. P., Birkmann, J., Kok, K., Levy, M., Solecki, W. (2017). The roads ahead: Narratives for shared socioeconomic pathways describing world futures in the 21st century. *Global Environmental Change*, Volume 42, Pages 169-180, ISSN 0959-3780

Sienz, F., Bordi, I., Fraedrich, K., Schneidereit, A. (2007). Extreme dry and wet events in Iceland: Observations, simulations, and scenarios. *Meteorologische Zeitschrift* 16: 9-16.

Thrasher, B., Wang, W., Michaelis, A., Melton, F., Lee, T., & Nemani, R. (2022). NASA Global Daily Downscaled Projections, CMIP6. *Scientific Data*, 9(1), 262.

Wood, A. W., Maurer, E. P., Kumar, A., & Lettenmaier, D. P. (2002). Long-range experimental hydrologic forecasting for the eastern United States. *Journal of Geophysical Research: Atmospheres*, *107*(D20), ACL 6-1-ACL 6-15. https://doi.org/10.1029/2001JD000659

Wood, A. W., Leung, L. R., Sridhar, V., & Lettenmaier, D. P. (2004). Hydrologic Implications of Dynamical and Statistical Approaches to Downscaling Climate Model Outputs. *Climatic Change*, *62*(1), 189–216. https://doi.org/10.1023/B:CLIM.0000013685.99609.9e

Zaqout, T. A. M. (2024). Bias adjustment of the NEX-GDDP-CMIP 6 climate data. *Veðurstofa Íslands*. To be published.

Appendix I. Histograms.

In this appendix, figures similar to Figure 3 and 4 from the report are presented.

Figure I.1–I.12 show annual maximum series of CDD and CWD for the twelve control stations as calculated from observations and from the CARRA dataset. Median values are indicated by the horizontal dashed lines.

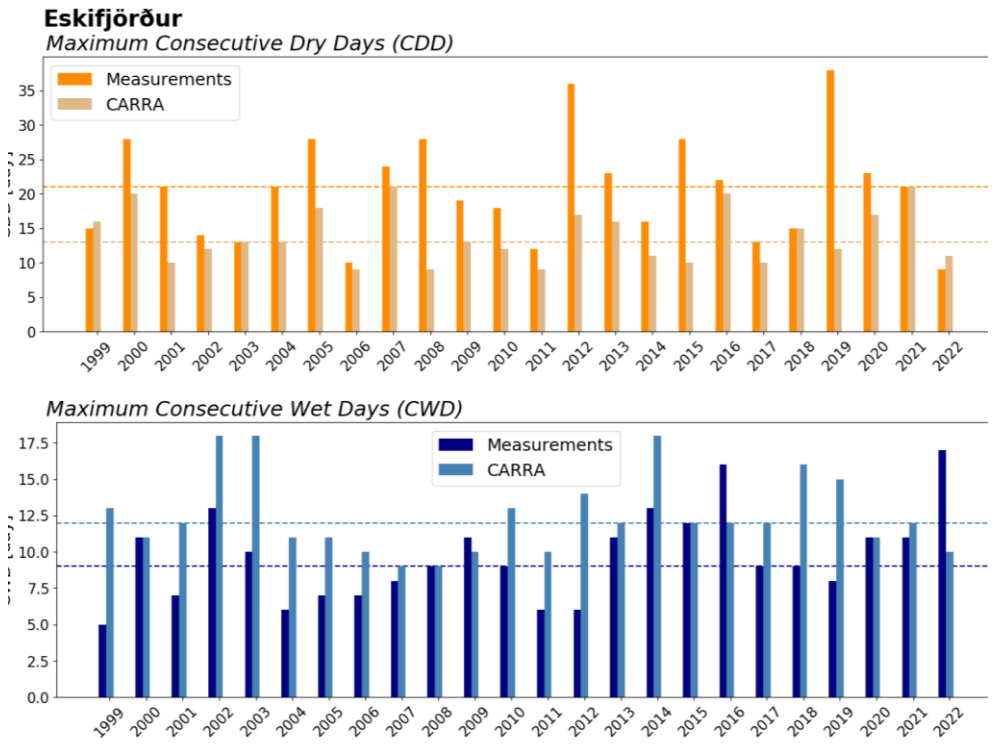

Figure I.1 — Histograms showing annual maximum CDD (top) and CWD (bottom) based on observation timeseries and reanalysis for station Eskifjörður. Dashed lines indicate the median values.

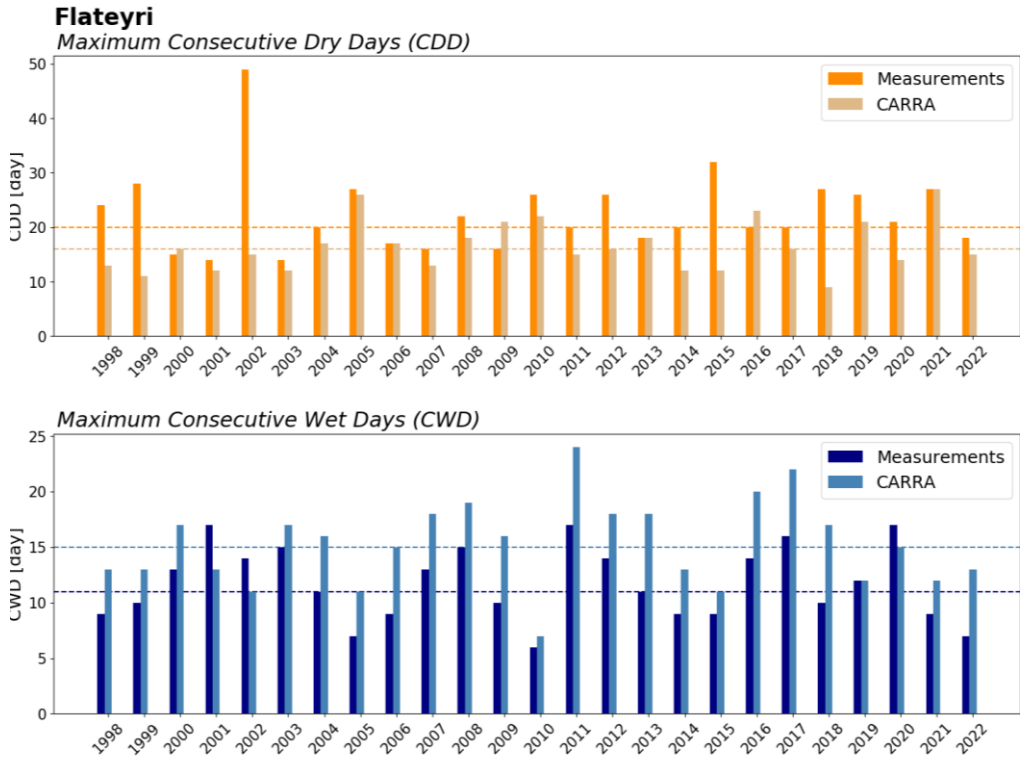

Figure I.2 — Histograms showing annual maximum CDD (top) and CWD (bottom) based on observation timeseries and reanalysis for station Flateyri. Dashed lines indicate the median values.

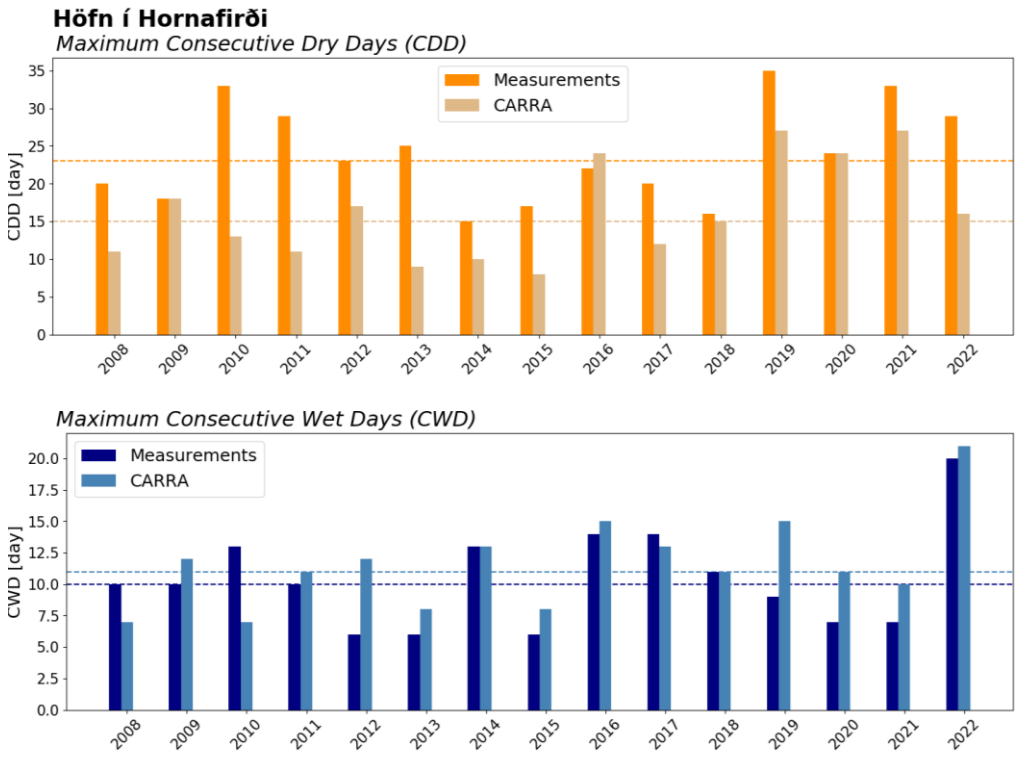

Figure I.3 — Histograms showing annual maximum CDD (top) and CWD (bottom) based on observation timeseries and reanalysis for station Höfn í Hornafirði. Dashed lines indicate the median values.

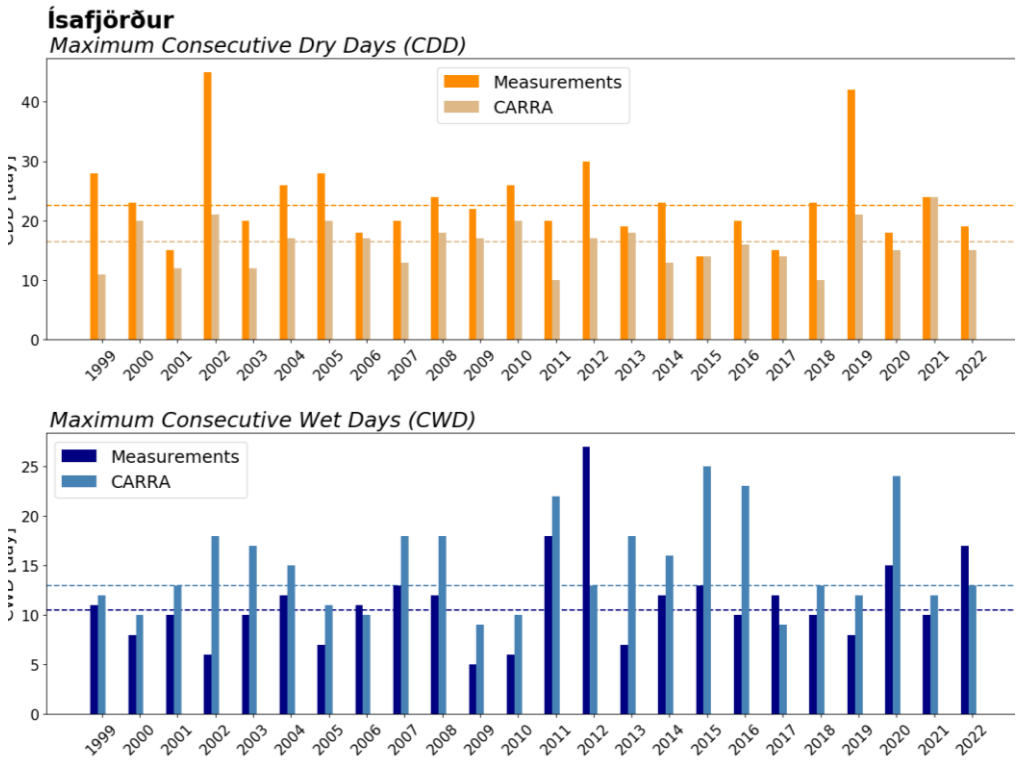

Figure I.4 — Histograms showing annual maximum CDD (top) and CWD (bottom) based on observation timeseries and reanalysis for station Ísafjörður. Dashed lines indicate the median values.

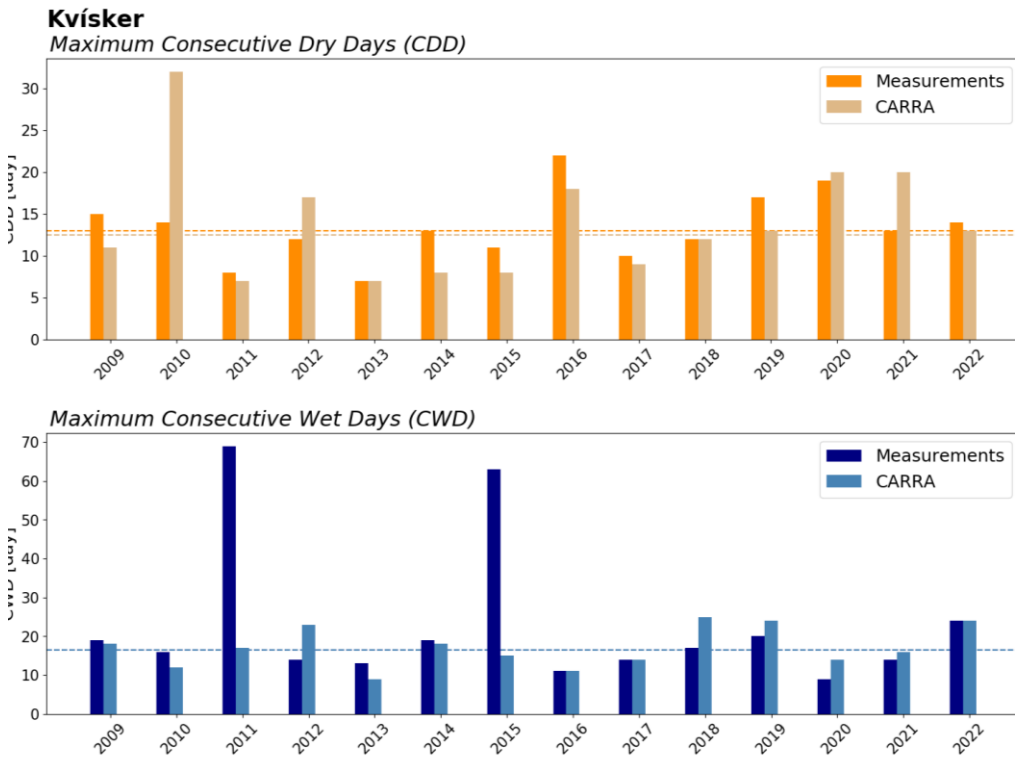

Figure I.5 — Histograms showing annual maximum CDD (top) and CWD (bottom) based on observation timeseries and reanalysis for station Kvísker. Dashed lines indicate the median values.

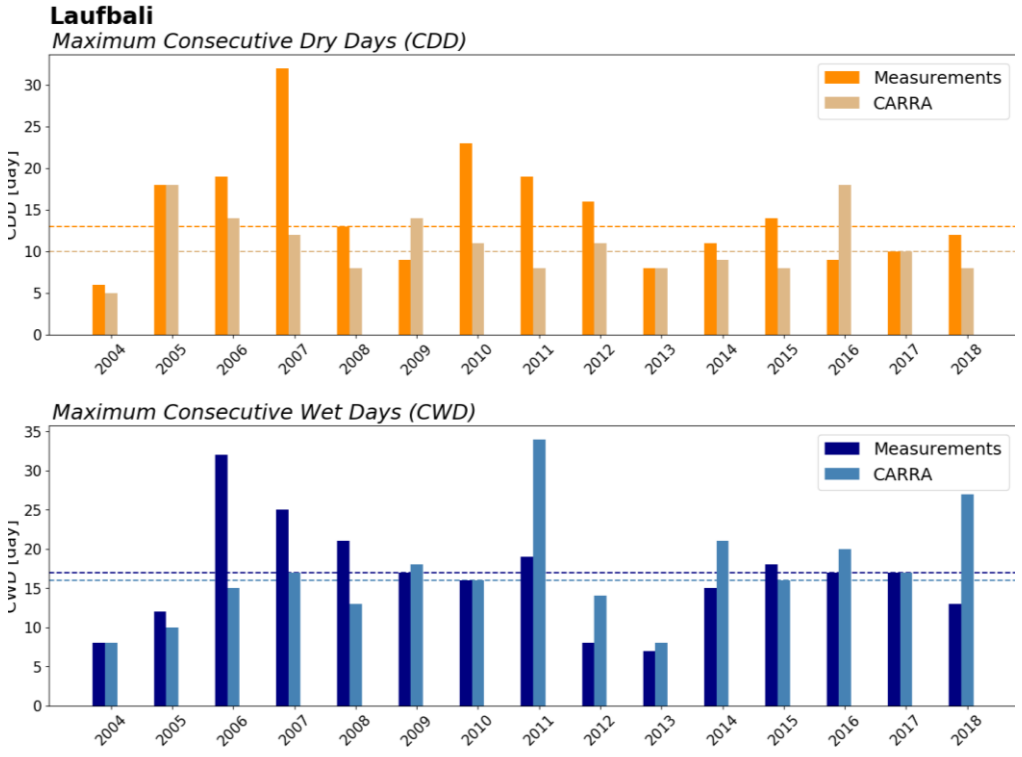

Figure I.6 — Histograms showing annual maximum CDD (top) and CWD (bottom) based on observation timeseries and reanalysis for station Laufbali. Dashed lines indicate the median values.

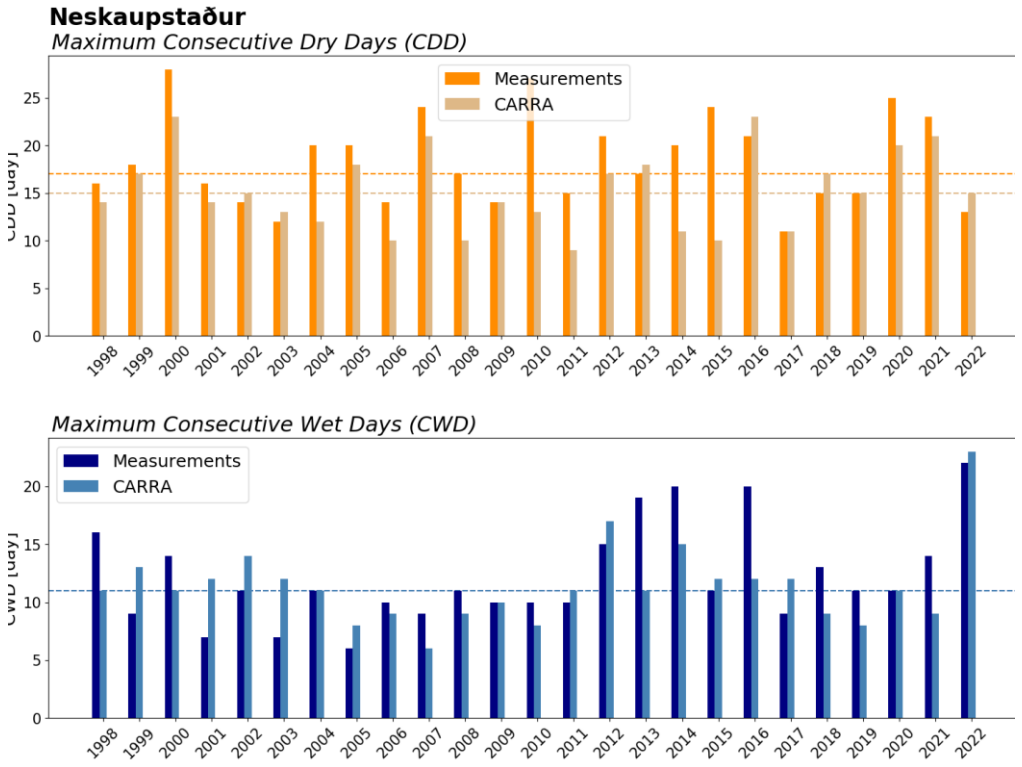

Figure I.7 — Histograms showing annual maximum CDD (top) and CWD (bottom) based on observation timeseries and reanalysis for station Neskaupstaður. Dashed lines indicate the median values.

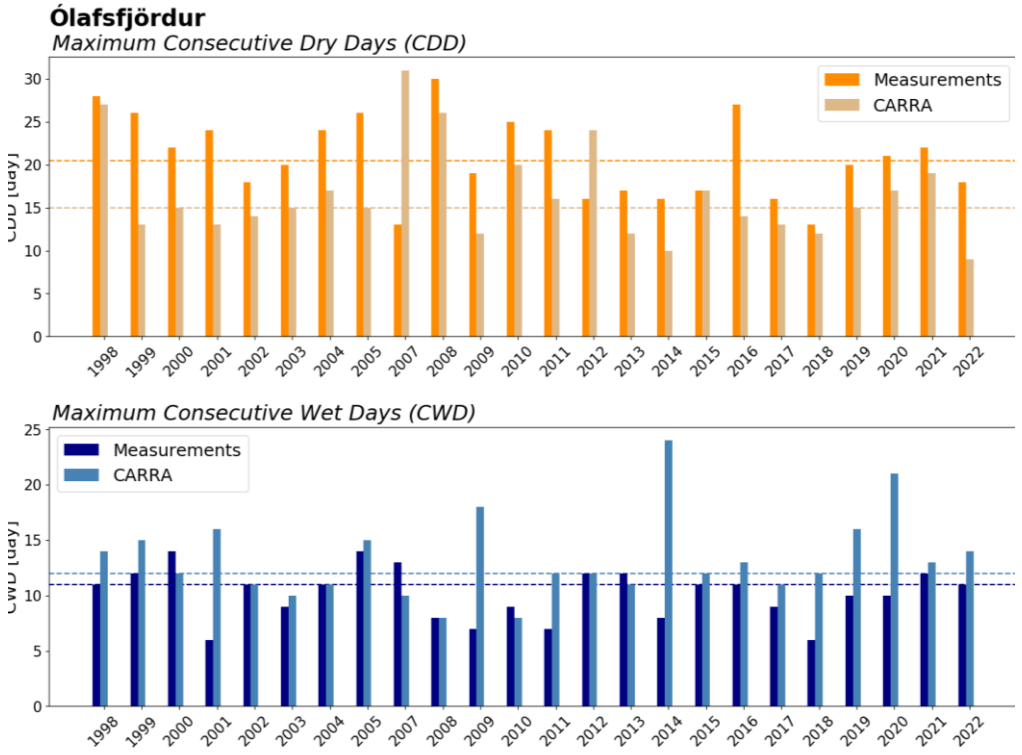

Figure I.8 — Histograms showing annual maximum CDD (top) and CWD (bottom) based on observation timeseries and reanalysis for station Ólafsfjörður. Dashed lines indicate the median values.

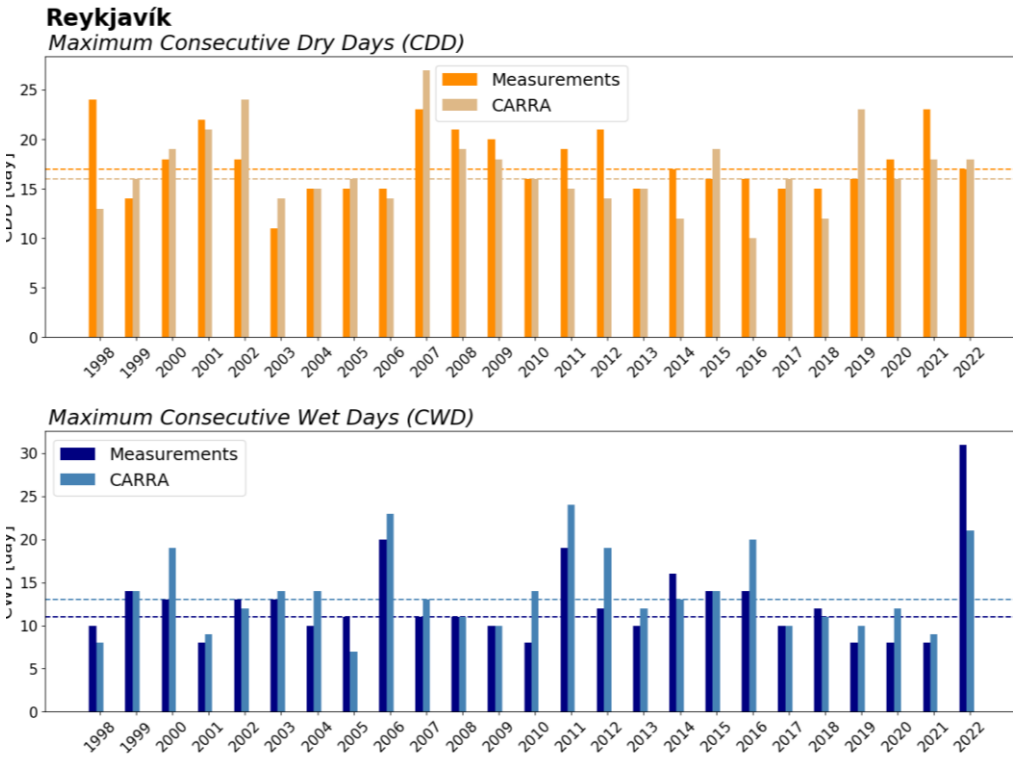

Figure I.9 — Histograms showing annual maximum CDD (top) and CWD (bottom) based on observation timeseries and reanalysis for station Reykjavík. Dashed lines indicate the median values.

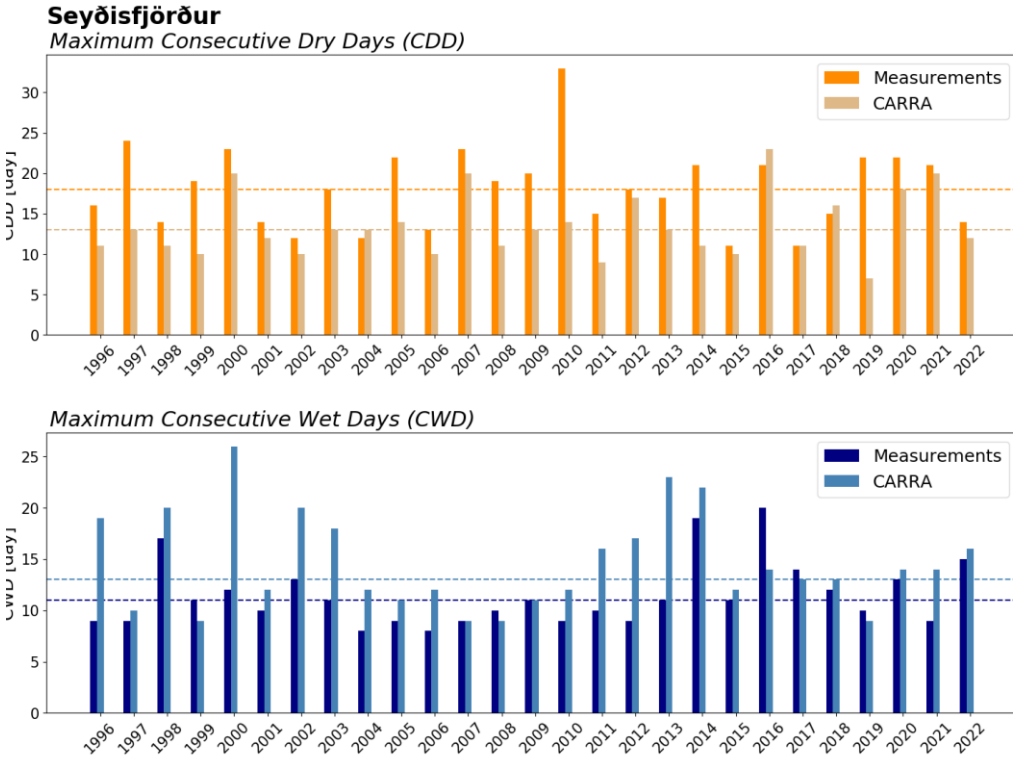

Figure I.10 — Histograms showing annual maximum CDD (top) and CWD (bottom) based on observation timeseries and reanalysis for station Seyðisfjörður. Dashed lines indicate the median values.

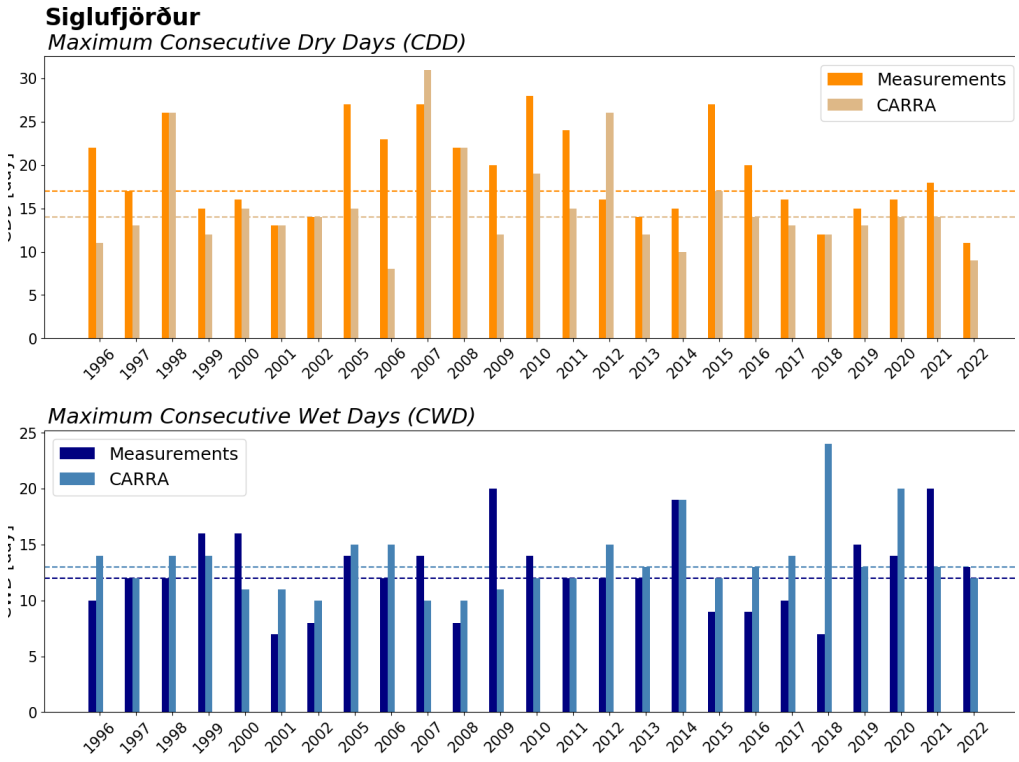

Figure I.11 — Histograms showing annual maximum CDD (top) and CWD (bottom) based on observation timeseries and reanalysis for station Siglufjörður. Dashed lines indicate the median values.

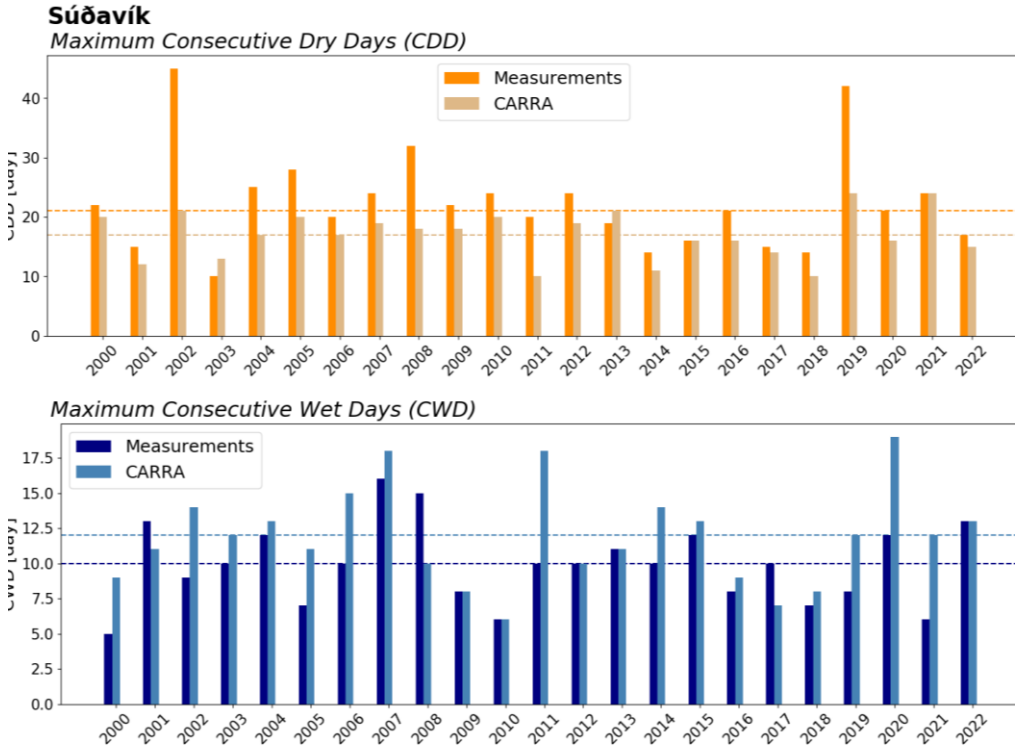

Figure I.12 — Histograms showing annual maximum CDD (top) and CWD (bottom) based on observation timeseries and reanalysis for station Súðavík. Dashed lines indicate the median values.

Appendix II. Scatterplots.

In this appendix, figures similar to Figure 5 from the report are presented.

Scatterplots comparing annual maximum number of CDD (left) and CDW (right) between observations and the CARRA dataset for the twelve control stations. RMSE and MAE are also indicated for each plot.

Eskifjörður

2000 - 2022

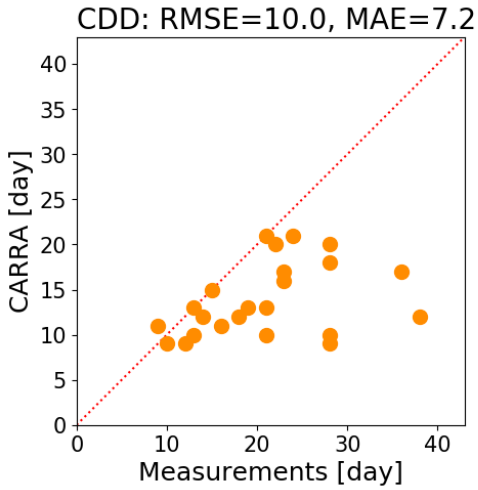

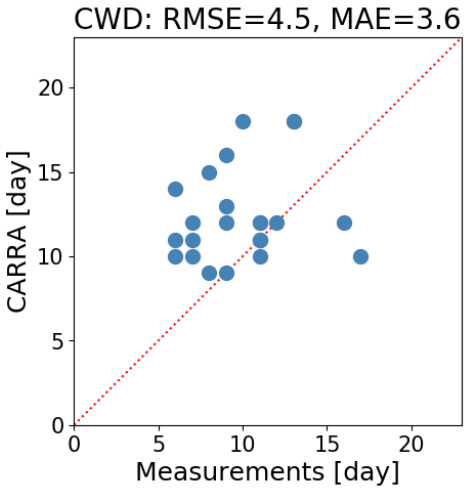

Flateyri

1999 - 2022

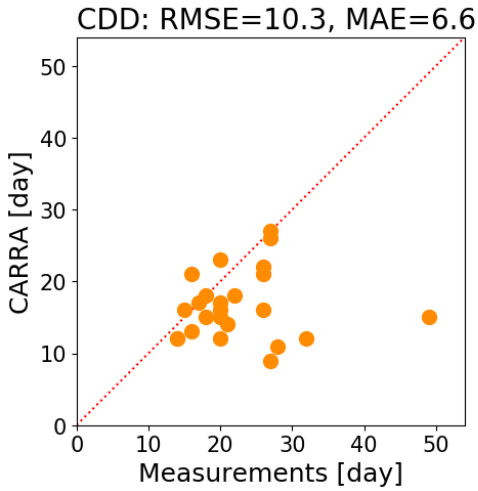

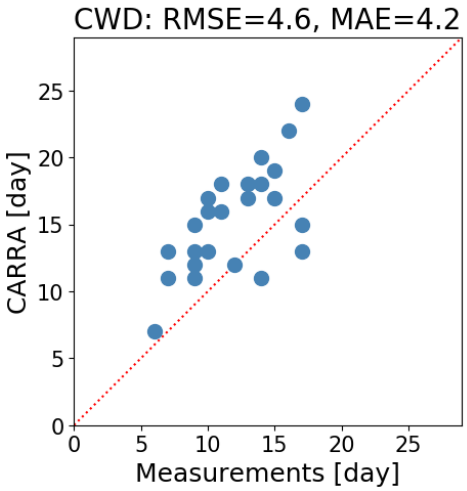

Höfn í Hornafirði

2009 - 2022

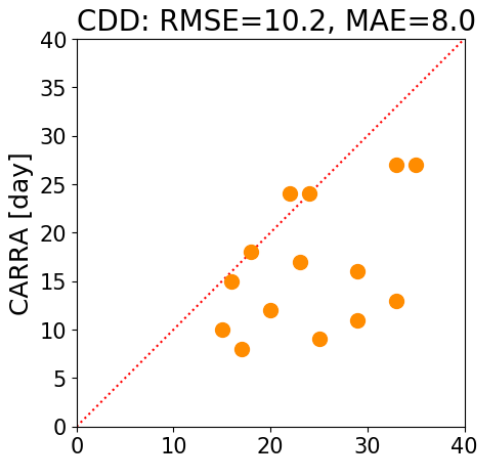

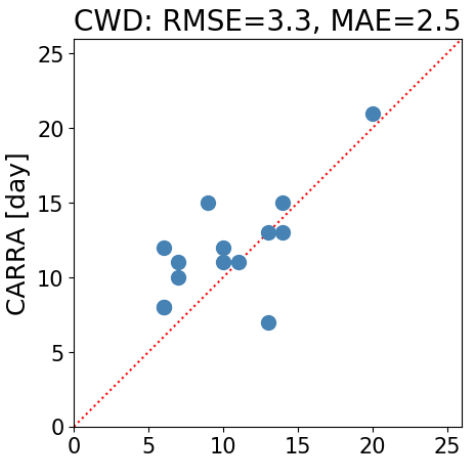

Ísafjörður

2000 - 2022

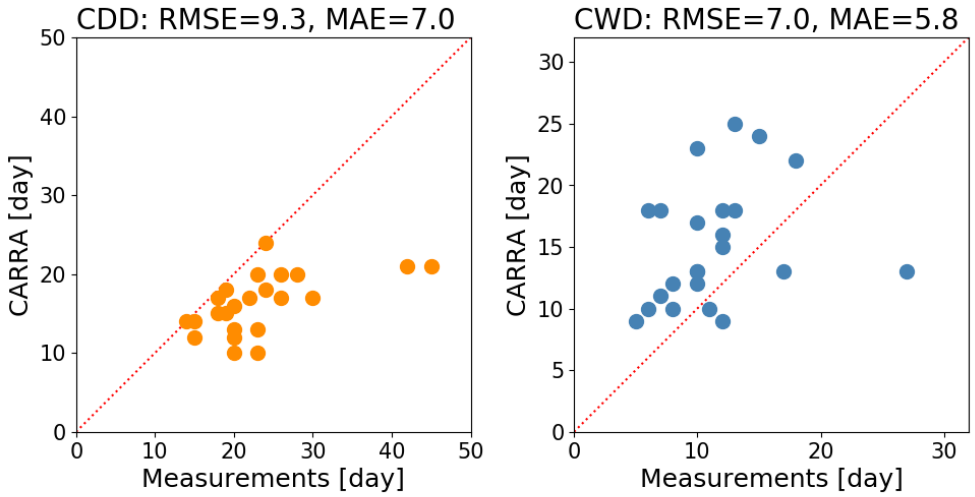

Kvísker

2010 - 2022

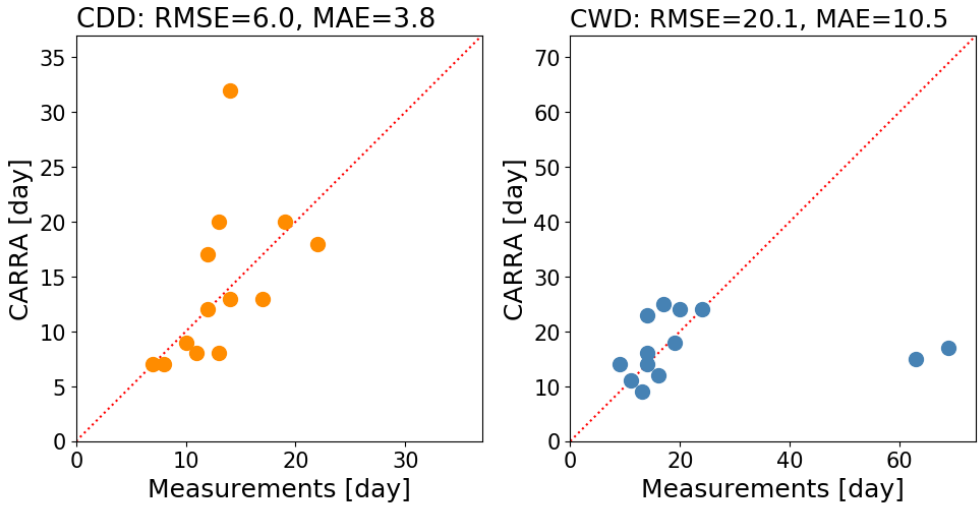

Laufbali

2005 - 2018

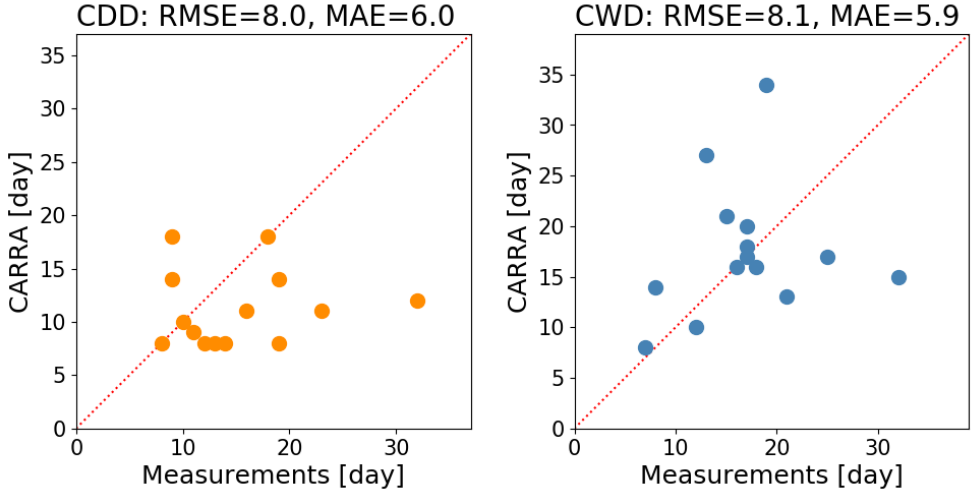

Neskaupstaður

1999 - 2022

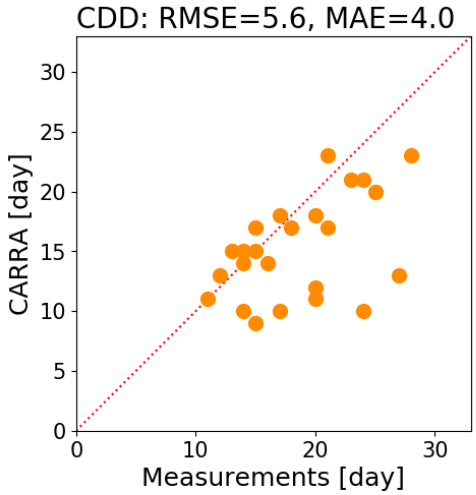

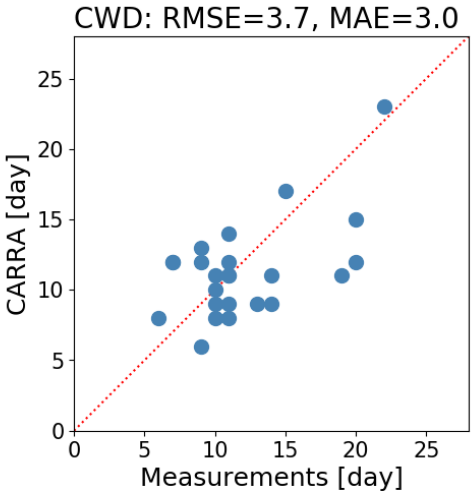

Ólafsfjördur

1999 - 2022

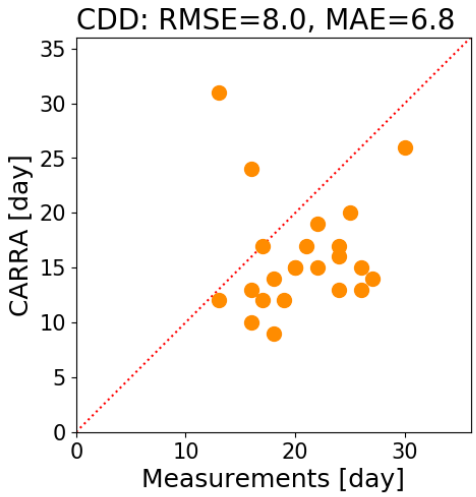

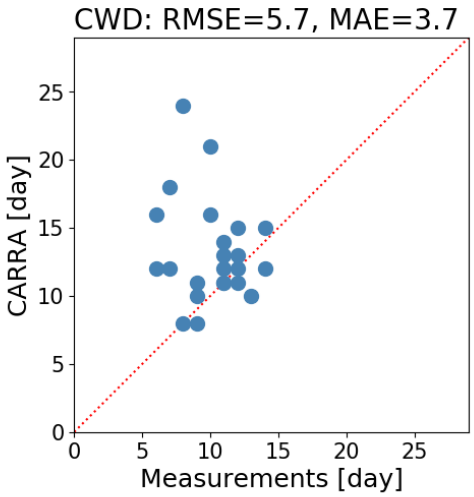

Reykjavík

1999 - 2022

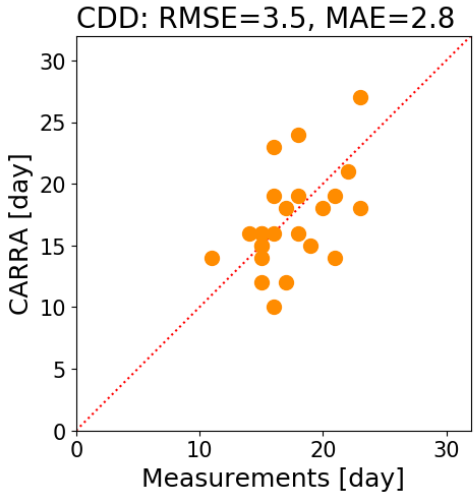

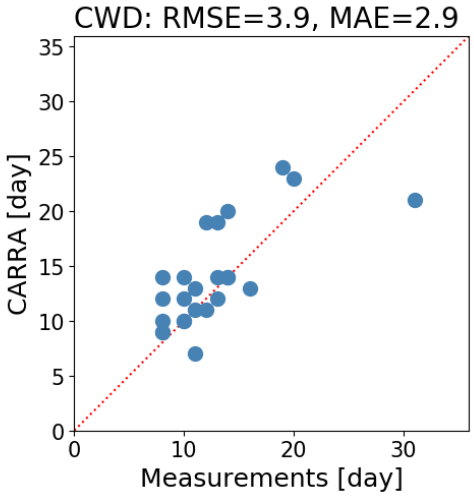

Seyðisfjörður

1997 - 2022

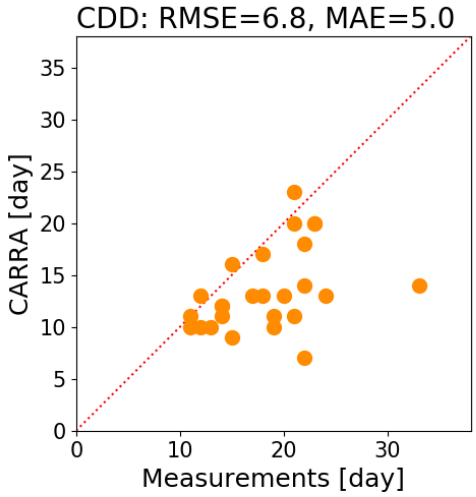

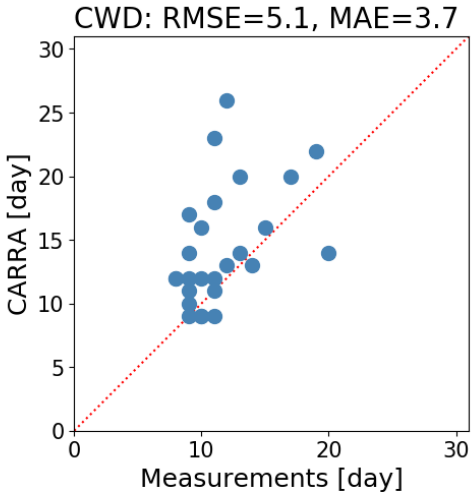

Siglufjörður

1997 - 2022

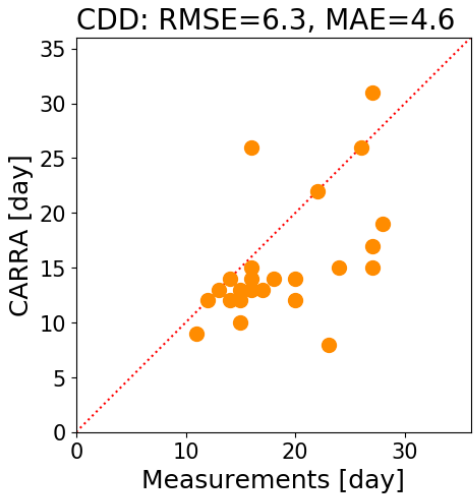

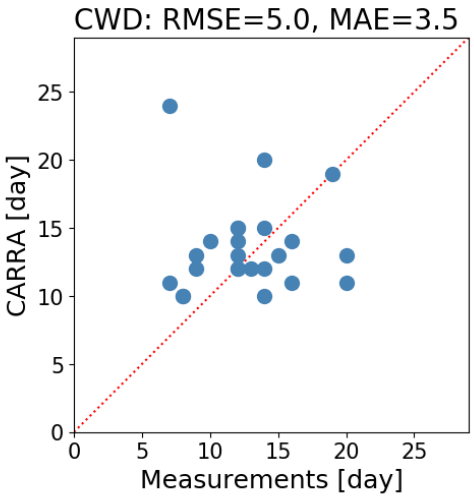

Súðavík

2001 - 2022

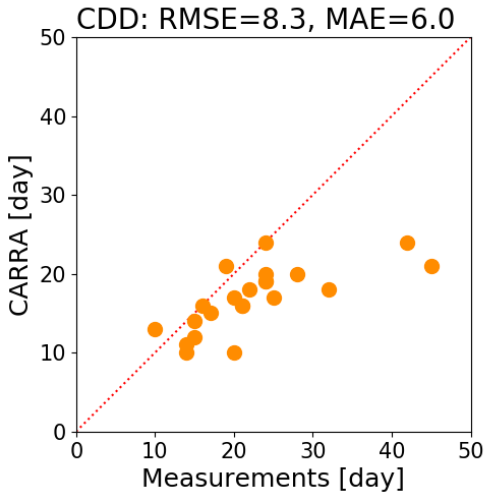

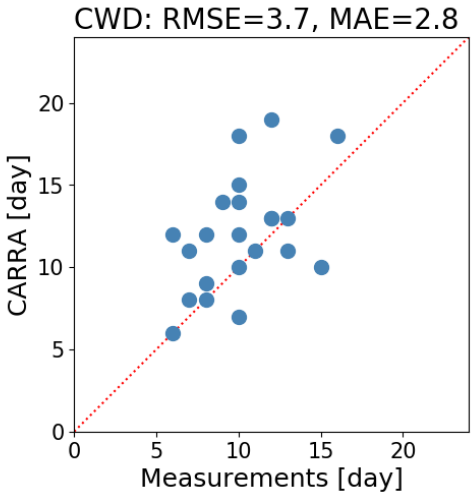

Appendix III. Step plots

In this appendix, figures similar to Figure 6 from the report are presented.

These figures show step plots for the twelve control stations based on the annual maximum series of CDD (left) and CWD (right). On these plots, the number of times a threshold is reached is shown by an indent (or step) in the line and plotted against time. Here, the thresholds chosen are the median values from the timeseries, and given in Table 4. In the top left figure, the orange line represents the annual maximum CDD calculated from the observations timeseries. The light-orange line shows the results based on the CARRA dataset, and so forth. On top of these results, vertical lines indicate the year of occurrence when half the total number of times the threshold has been reached.

Eskifjörður

CDD

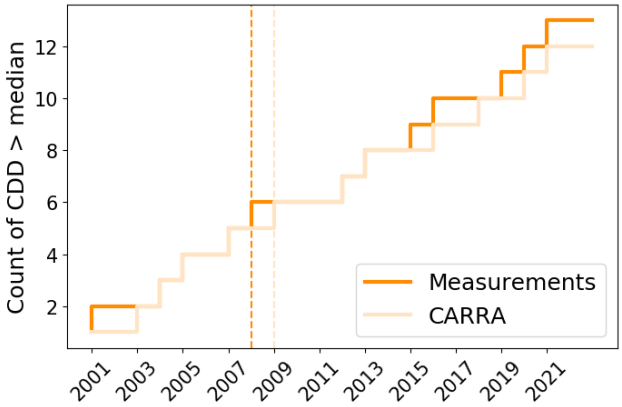

CWD

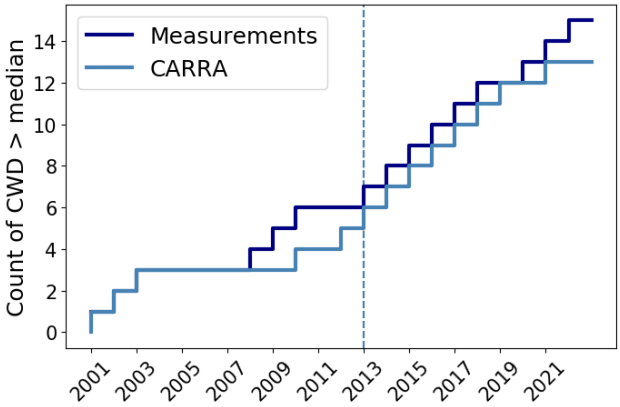

Flateyri

CDD

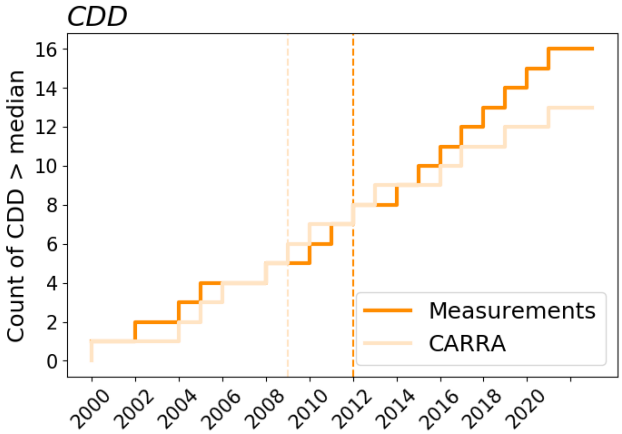

CWD

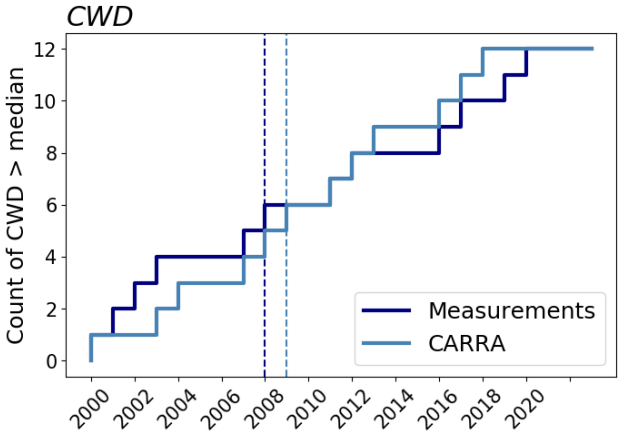

Höfn í Hornafirði

CDD

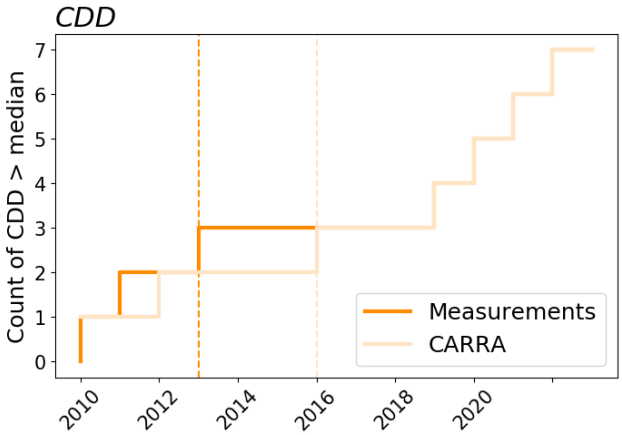

CWD

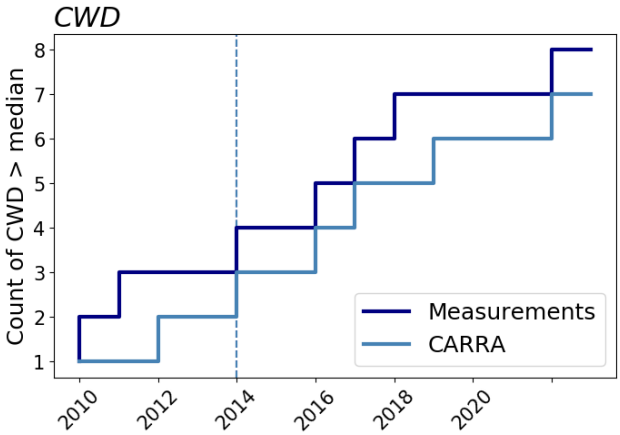

Ísafjörður

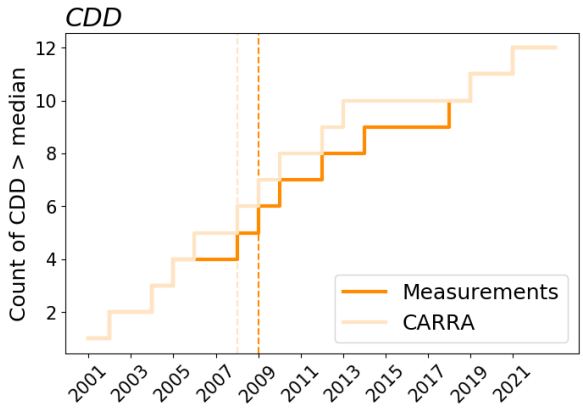

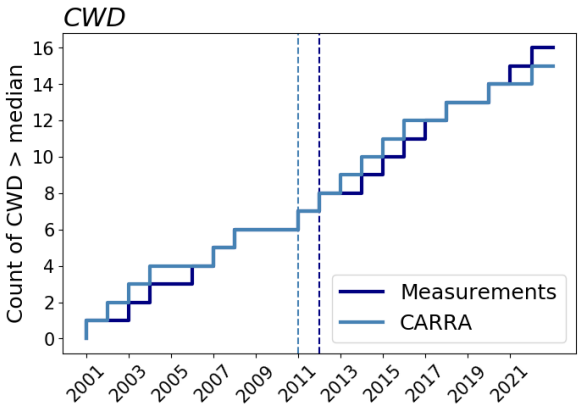

Kvísker

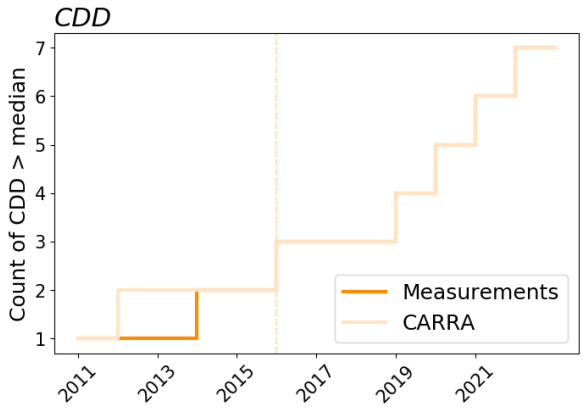

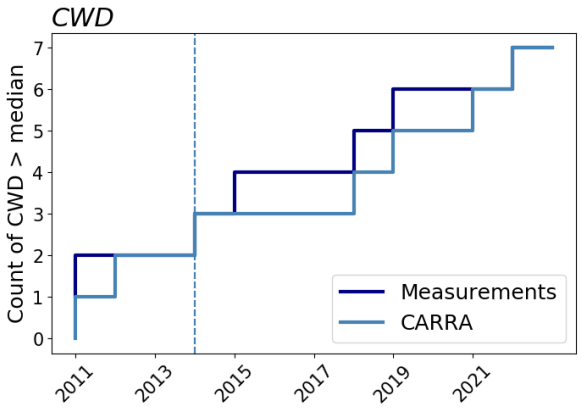

Laufbali

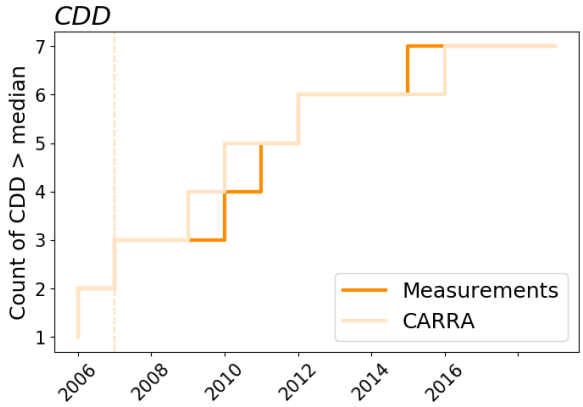

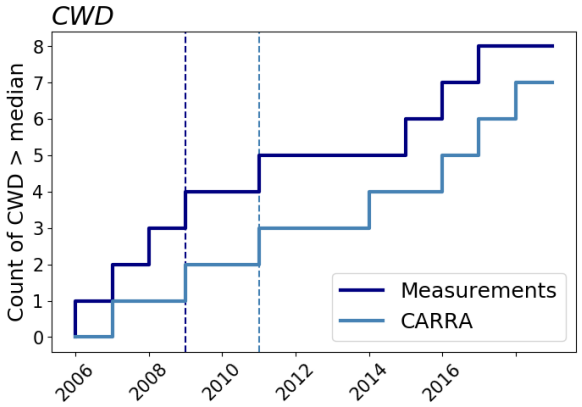

Neskaupstaður

CDD

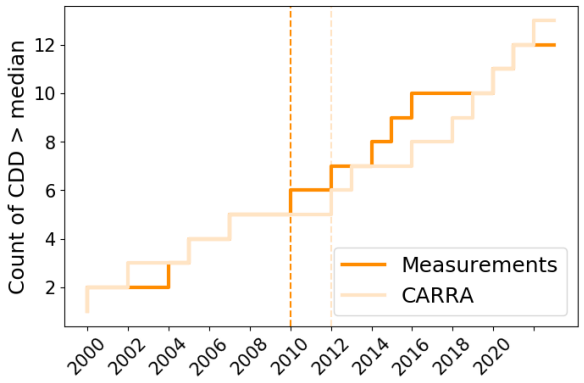

CWD

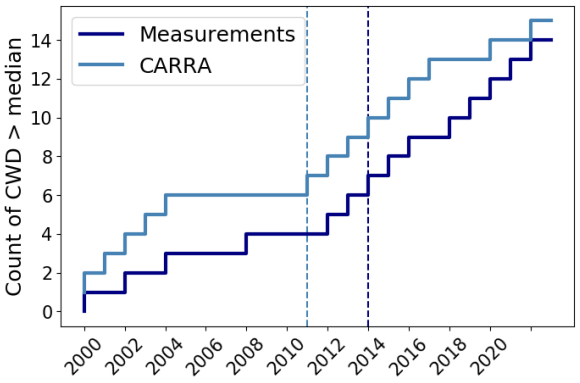

Ólafsfjördur

CDD

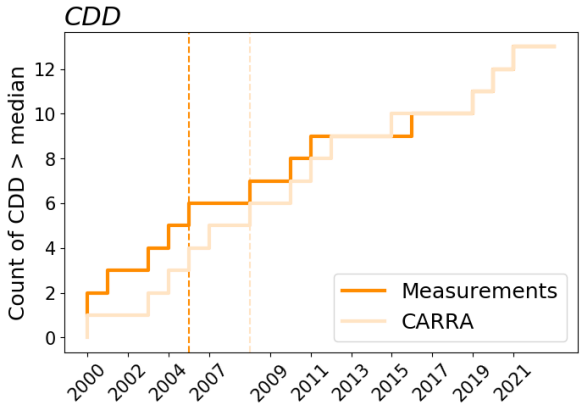

CWD

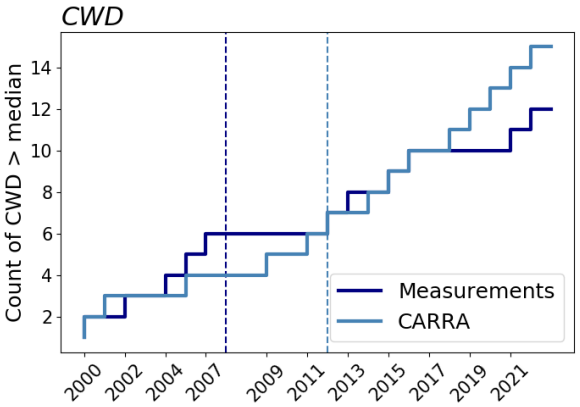

Reykjavík

CDD

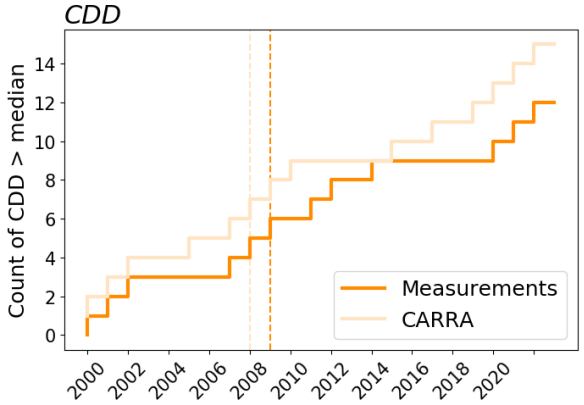

CWD

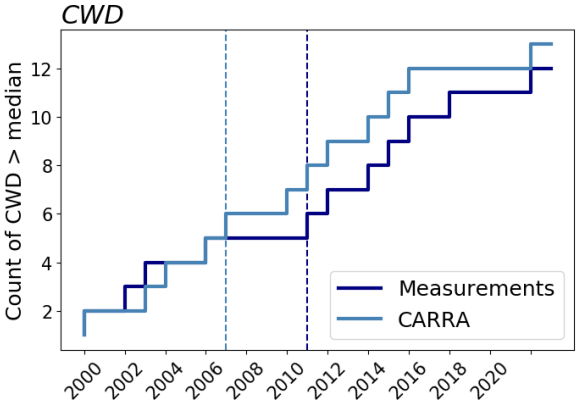

Seyðisfjörður

CDD

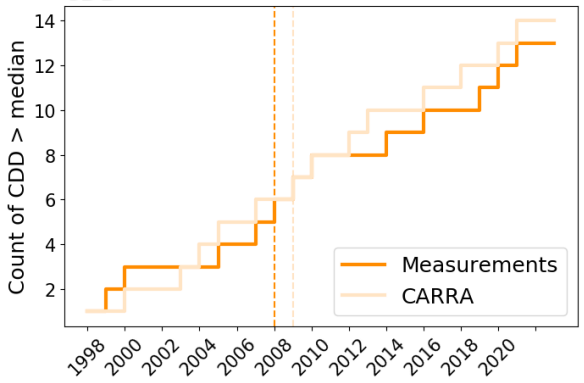

CWD

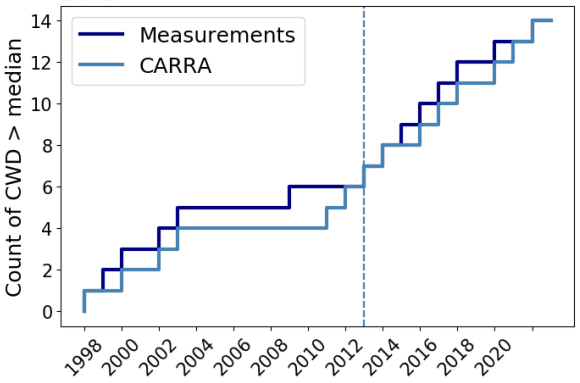

Siglufjörður

CDD

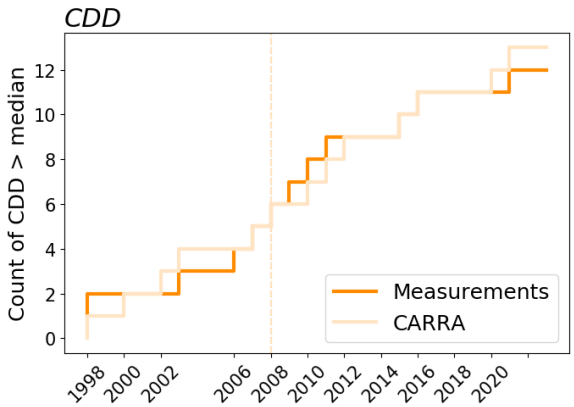

CWD

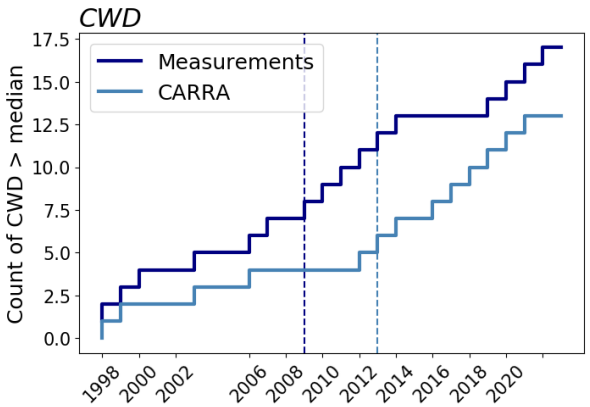

Súðavík

CDD

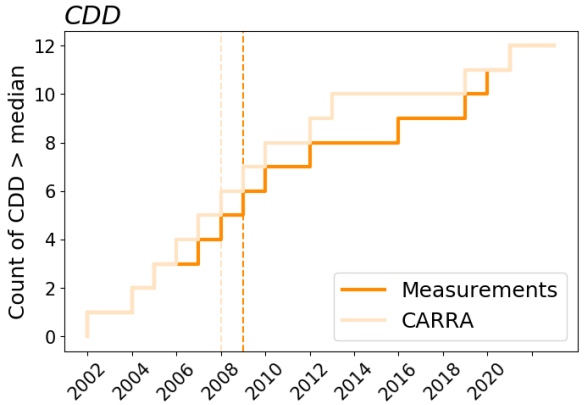

CWD

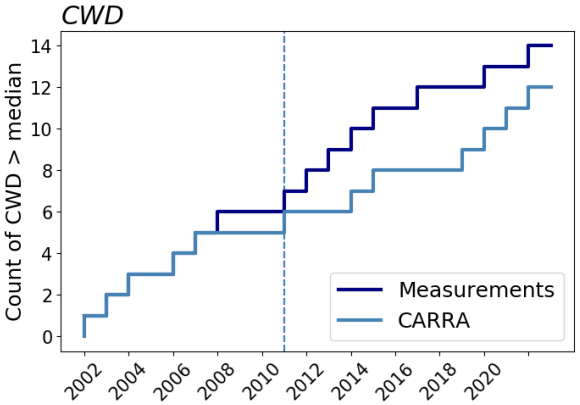

Appendix IV. CDD and CWD projections

In this appendix, figures similar to Figure 7 and 8 from the report are presented.

Figure IV.1–IV.12 show CDD (first two plots) and CWD (last two plots) values for the control stations as calculated from the median (dots), mean (line), and 10th-90th percentile (shaded area) values of the ensemble of climate models for SSP2-4.5 (top) and SSP5-8.5 (bottom) for the twelve control stations. Median absolute differences for two periods (2041–2055 and 2091–2100) as compared to the historical period (1986–2015) are also indicated.

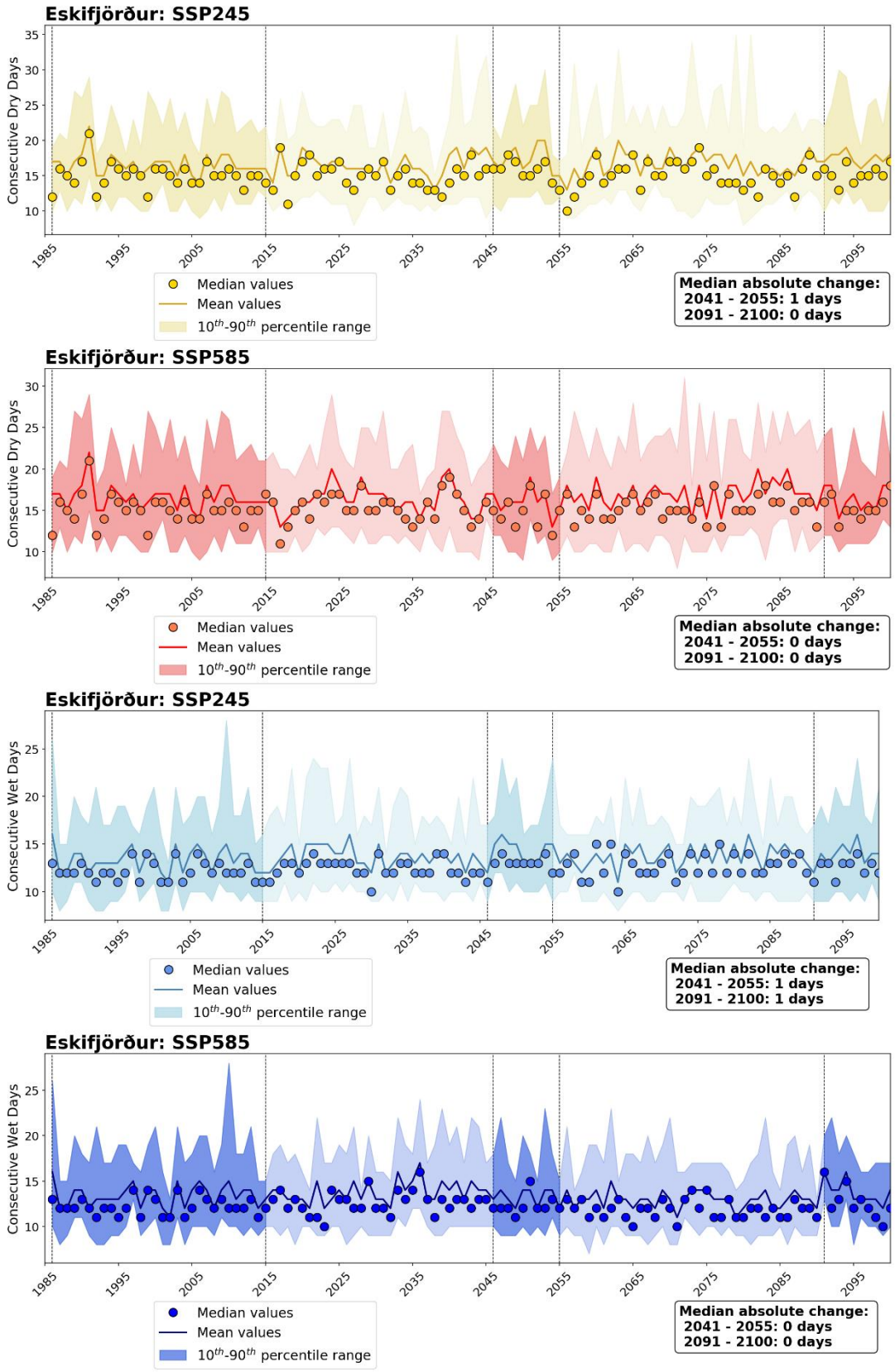

Figure IV.1 — CDD and CWD values for Eskifjörður as calculated from the median (dots), mean (line), and 10th-90th percentile (shaded area) values of the ensemble of climate models for SSP245 and SSP585. Median differences for two future periods (2041–2055 and 2091–2100) as compared to the historical period (1986–2015) are also indicated.

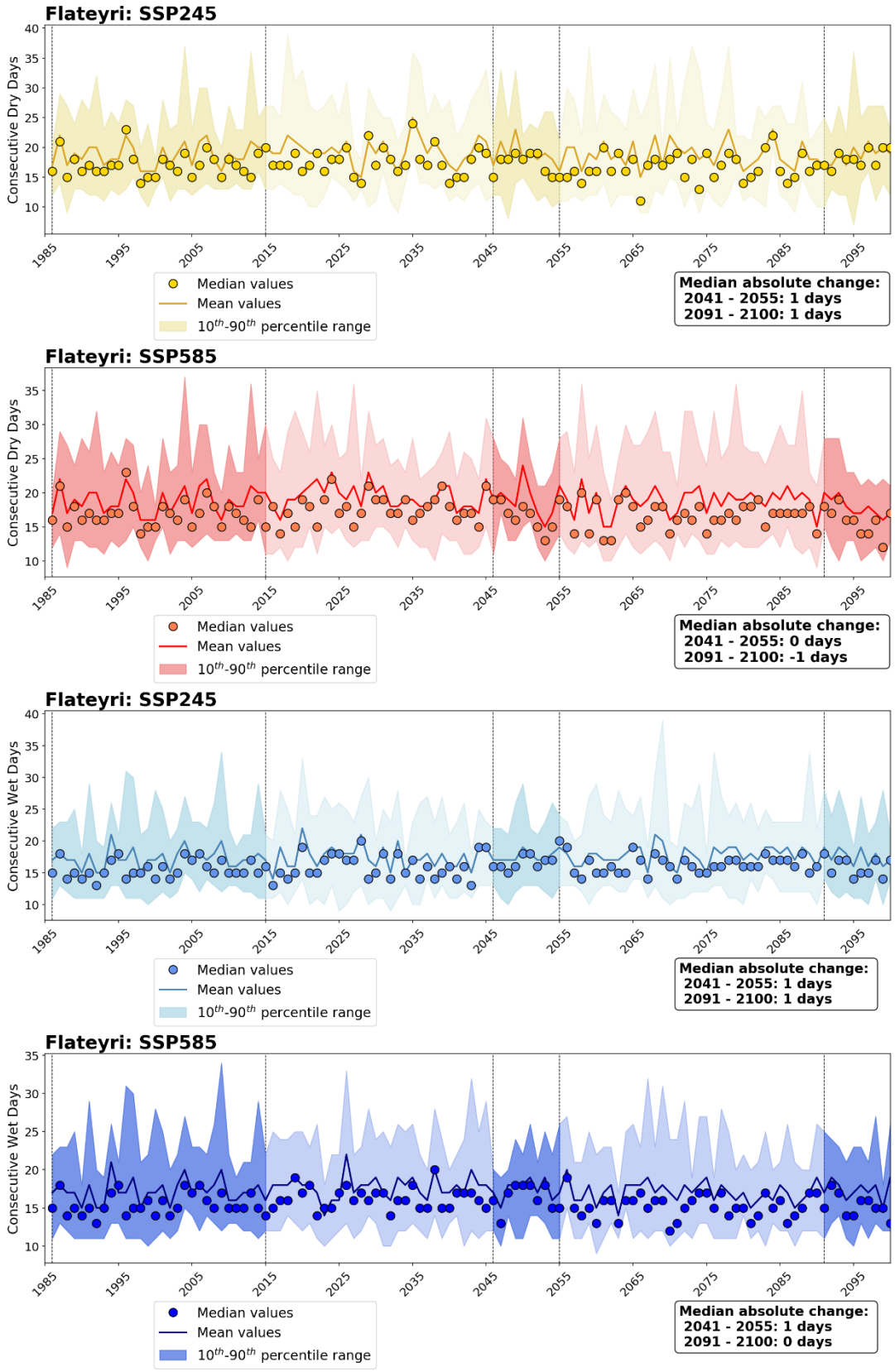

Figure IV.2 — CDD and CWD values for Flateyri as calculated from the median (dots), mean (line), and 10th-90th percentile (shaded area) values of the ensemble of climate models for SSP245 and SSP585. Median differences for two future periods (2041–2055 and 2091–2100) as compared to the historical period (1986–2015) are also indicated.

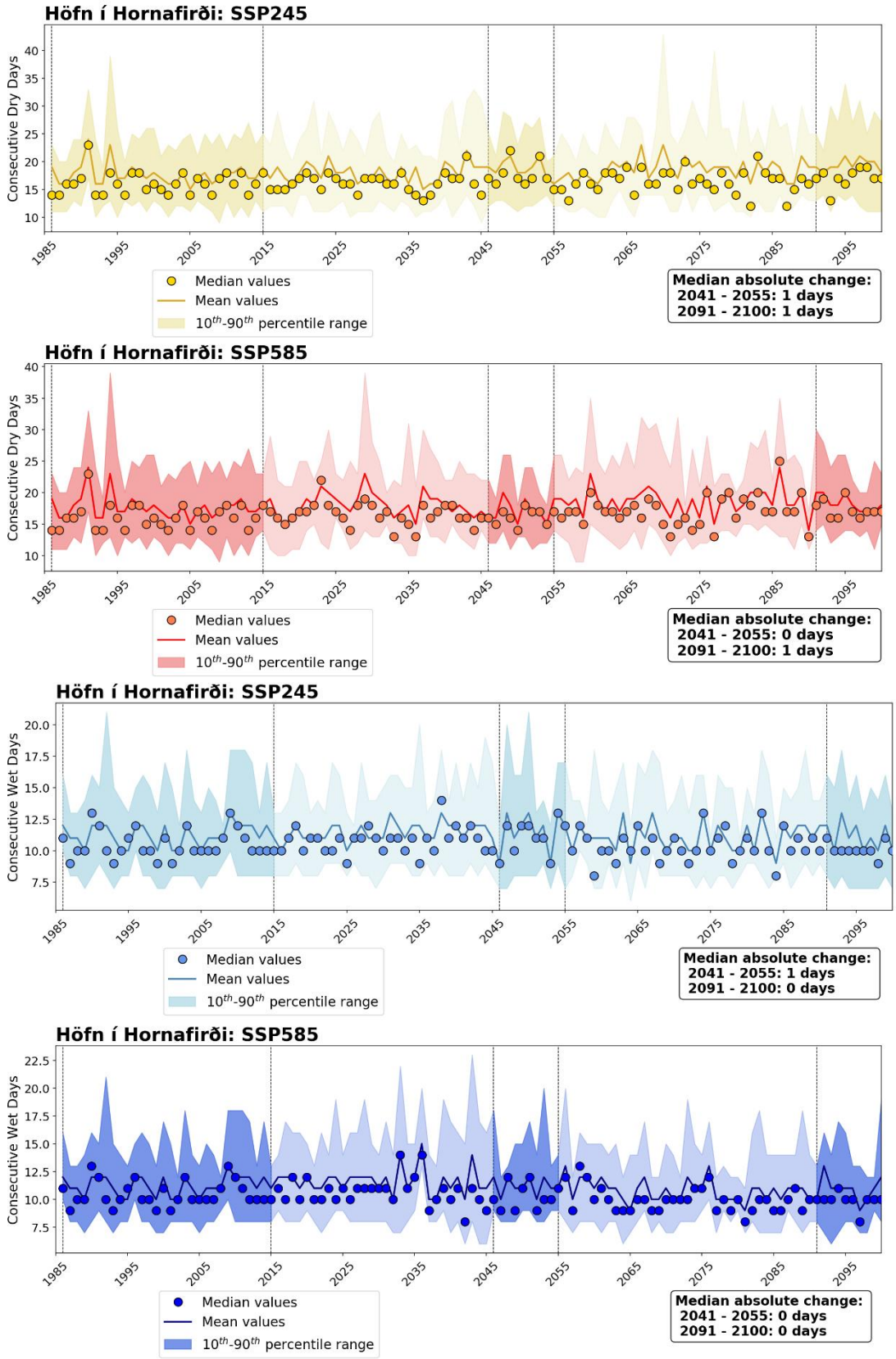

Figure IV.3 — CDD and CWD values for Höfn as calculated from the median (dots), mean (line), and 10th-90th percentile (shaded area) values of the ensemble of climate models for SSP245 and SSP585. Median differences for two future periods (2041–2055 and 2091–2100) as compared to the historical period (1986–2015) are also indicated.

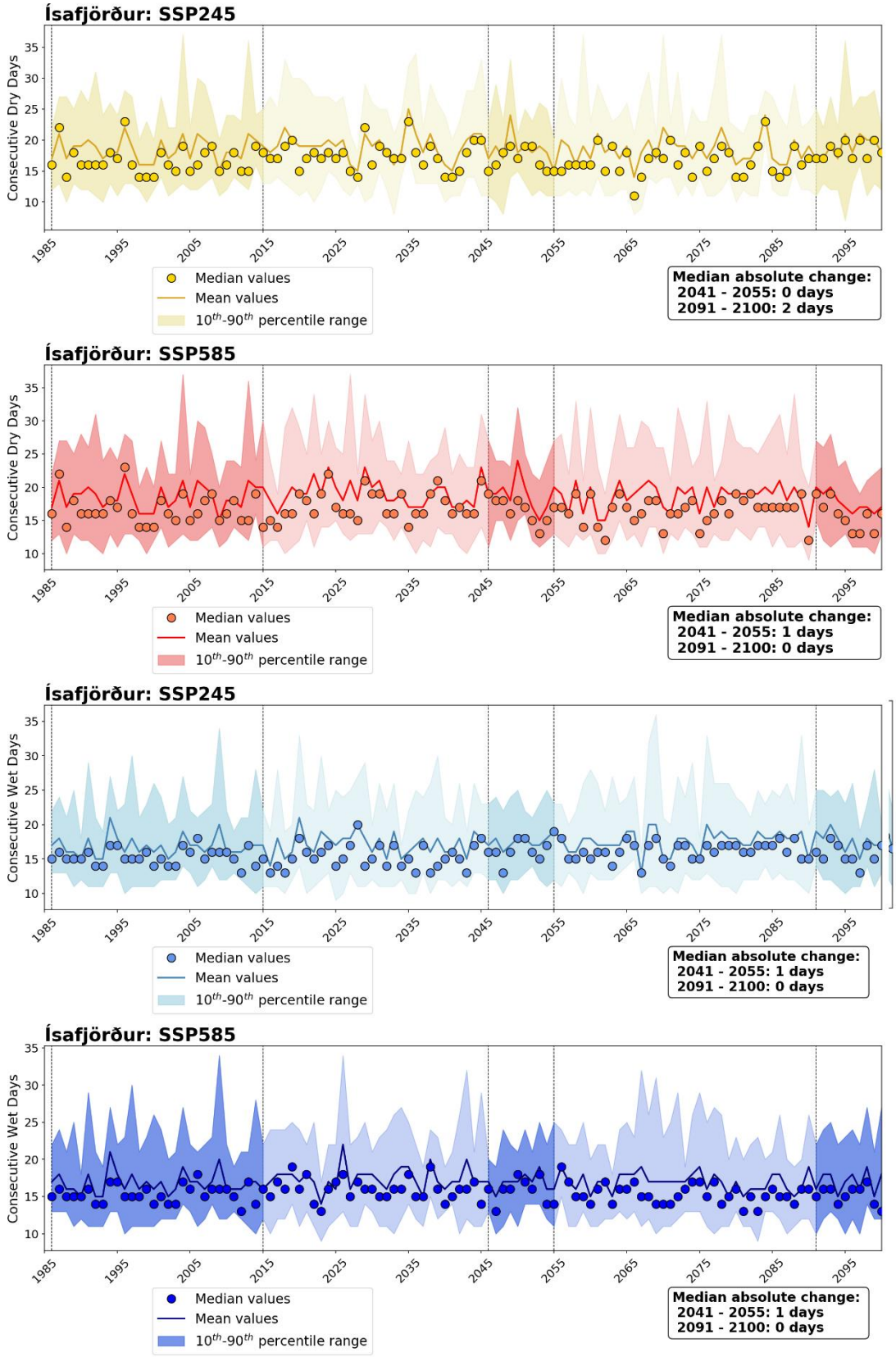

Figure IV.4 — CDD and CWD values for Ísafjörður as calculated from the median (dots), mean (line), and 10th-90th percentile (shaded area) values of the ensemble of climate models for SSP245 and SSP585. Median differences for two future periods (2041–2055 and 2091–2100) as compared to the historical period (1986–2015) are also indicated.

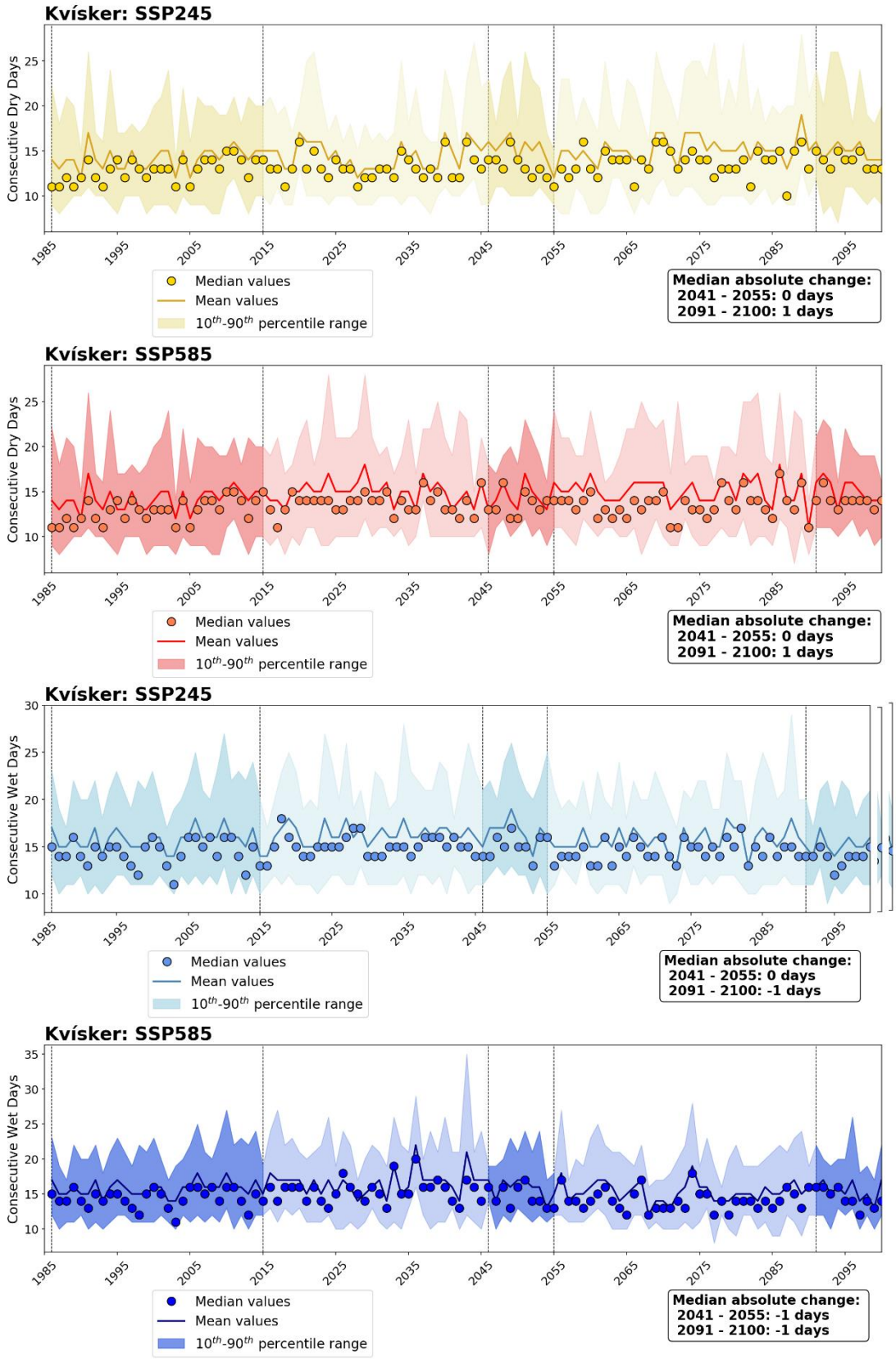

Figure IV.5 — CDD and CWD values for Kvísker as calculated from the median (dots), mean (line), and 10th-90th percentile (shaded area) values of the ensemble of climate models for SSP245 and SSP585. Median differences for two future periods (2041–2055 and 2091–2100) as compared to the historical period (1986–2015) are also indicated.

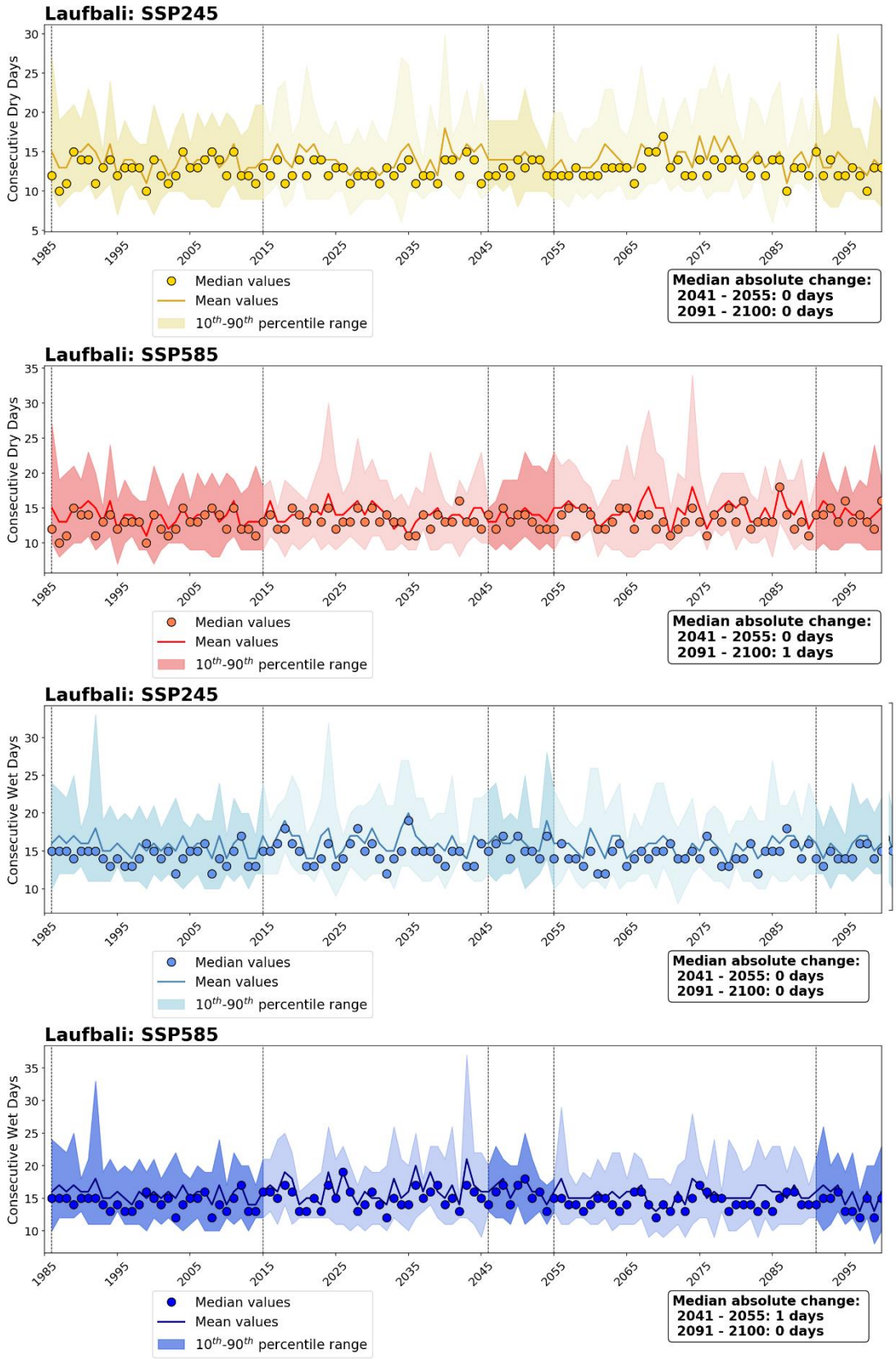

Figure IV.6 — CDD and CWD values for Laufbali as calculated from the median (dots), mean (line), and 10th-90th percentile (shaded area) values of the ensemble of climate models for SSP245 and SSP585. Median differences for two future periods (2041–2055 and 2091–2100) as compared to the historical period (1986–2015) are also indicated.

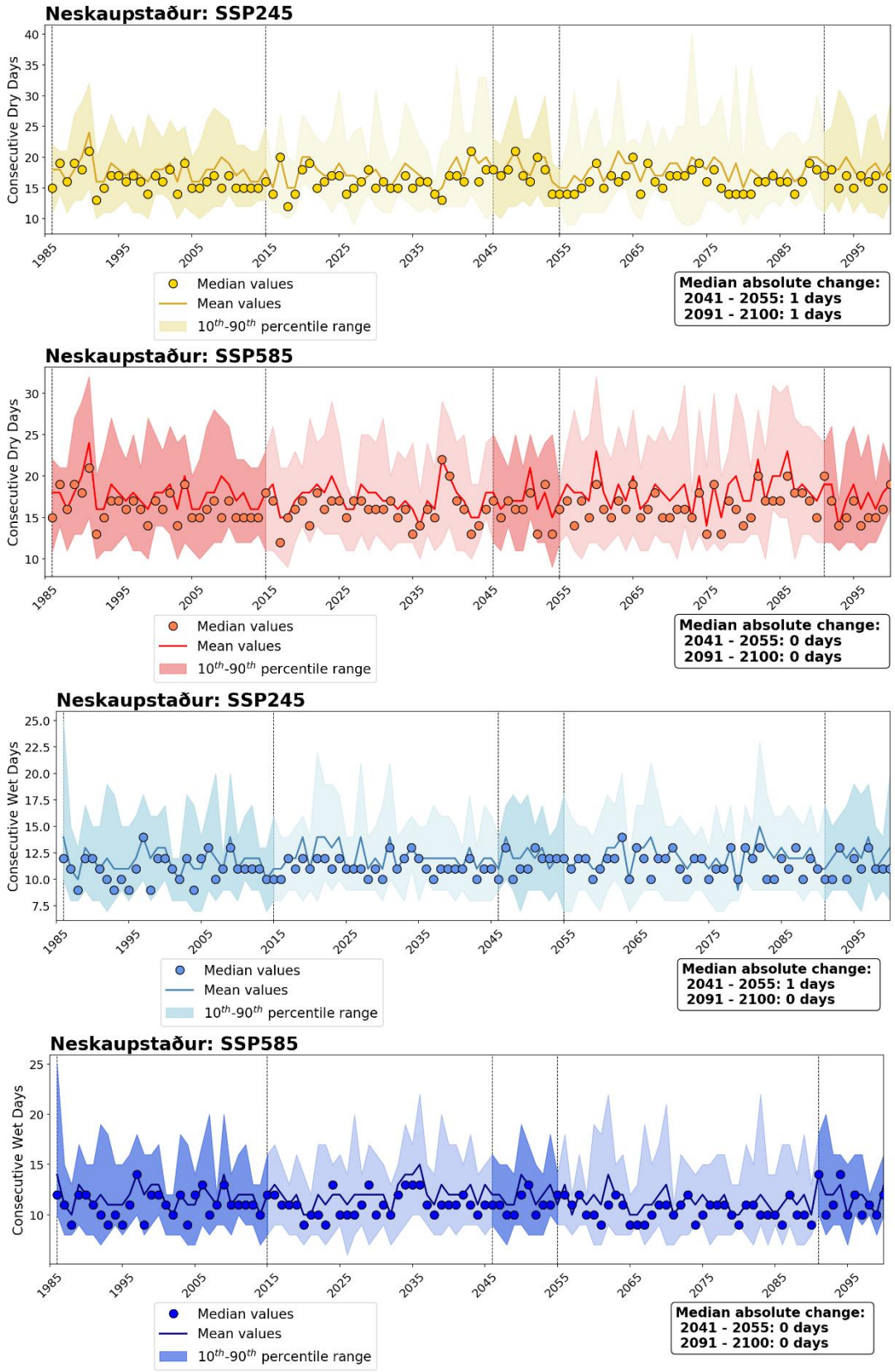

Figure IV.7 — CDD and CWD values for Neskaupstaður calculated from the median (dots), mean (line), and 10th-90th percentile (shaded area) values of the ensemble of climate models for SSP245 and SSP585. Median differences for two future periods (2041–2055 and 2091–2100) as compared to the historical period (1986–2015) are also indicated.

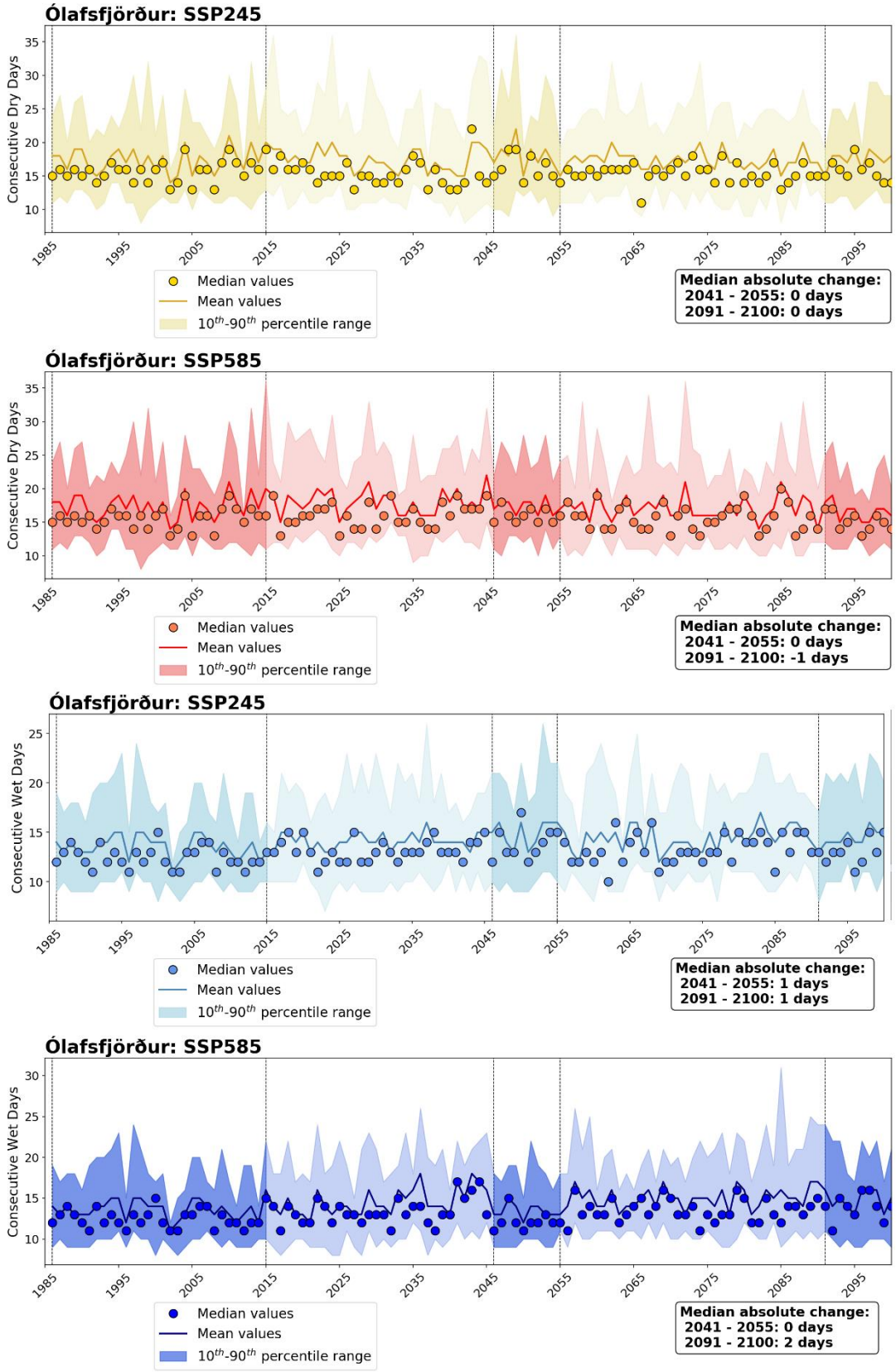

Figure IV.8 — CDD and CWD values for Ólafsfjörður as calculated from the median (dots), mean (line), and 10th-90th percentile (shaded area) values of the ensemble of climate models for SSP245 and SSP585. Median differences for two future periods (2041–2055 and 2091–2100) as compared to the historical period (1986–2015) are also indicated.

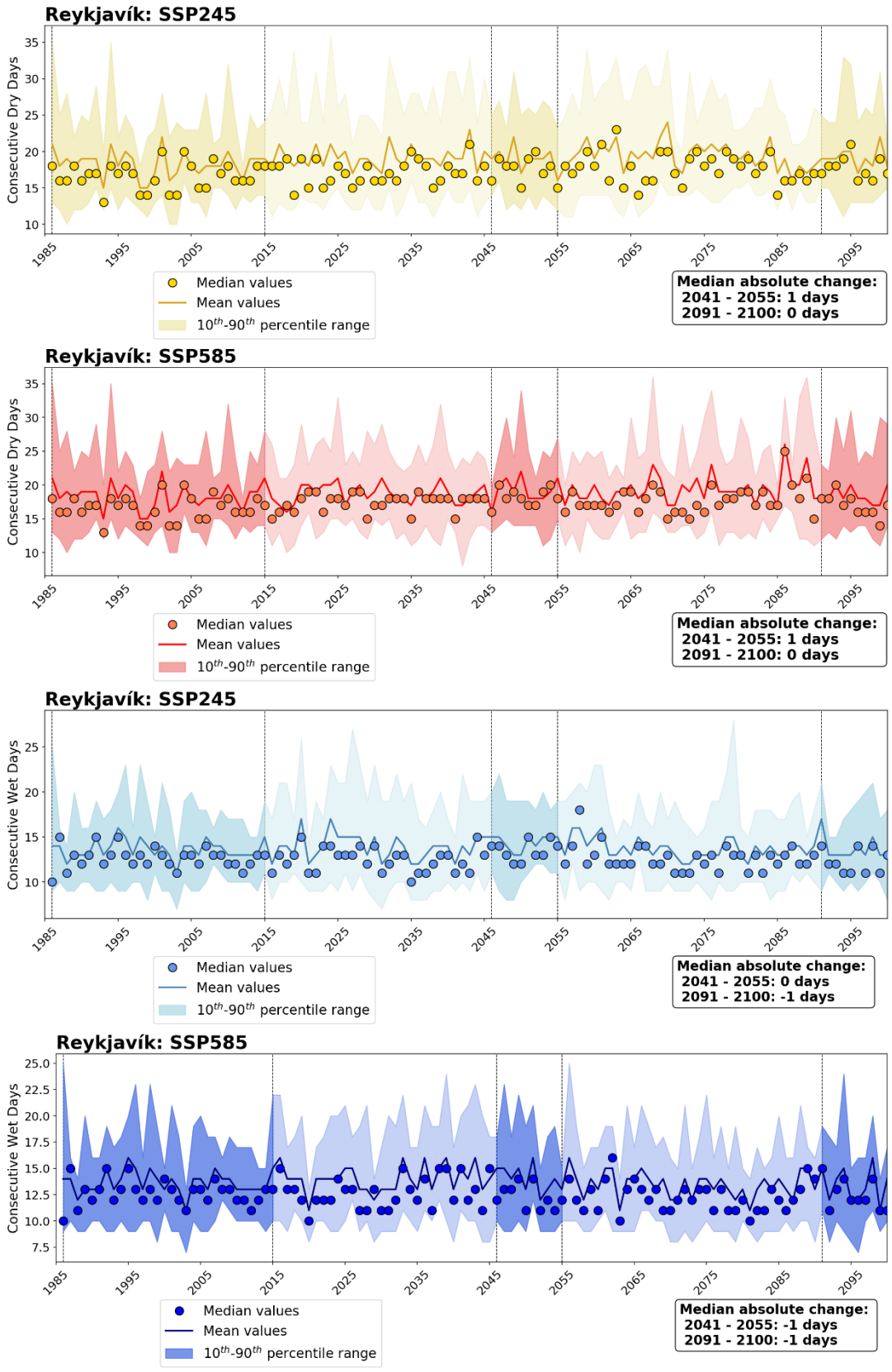

Figure IV.9 — CDD and CWD values for Reykjavík as calculated from the median (dots), mean (line), and 10th-90th percentile (shaded area) values of the ensemble of climate models for SSP245 and SSP585. Median differences for two future periods (2041–2055 and 2091–2100) as compared to the historical period (1986–2015) are also indicated.

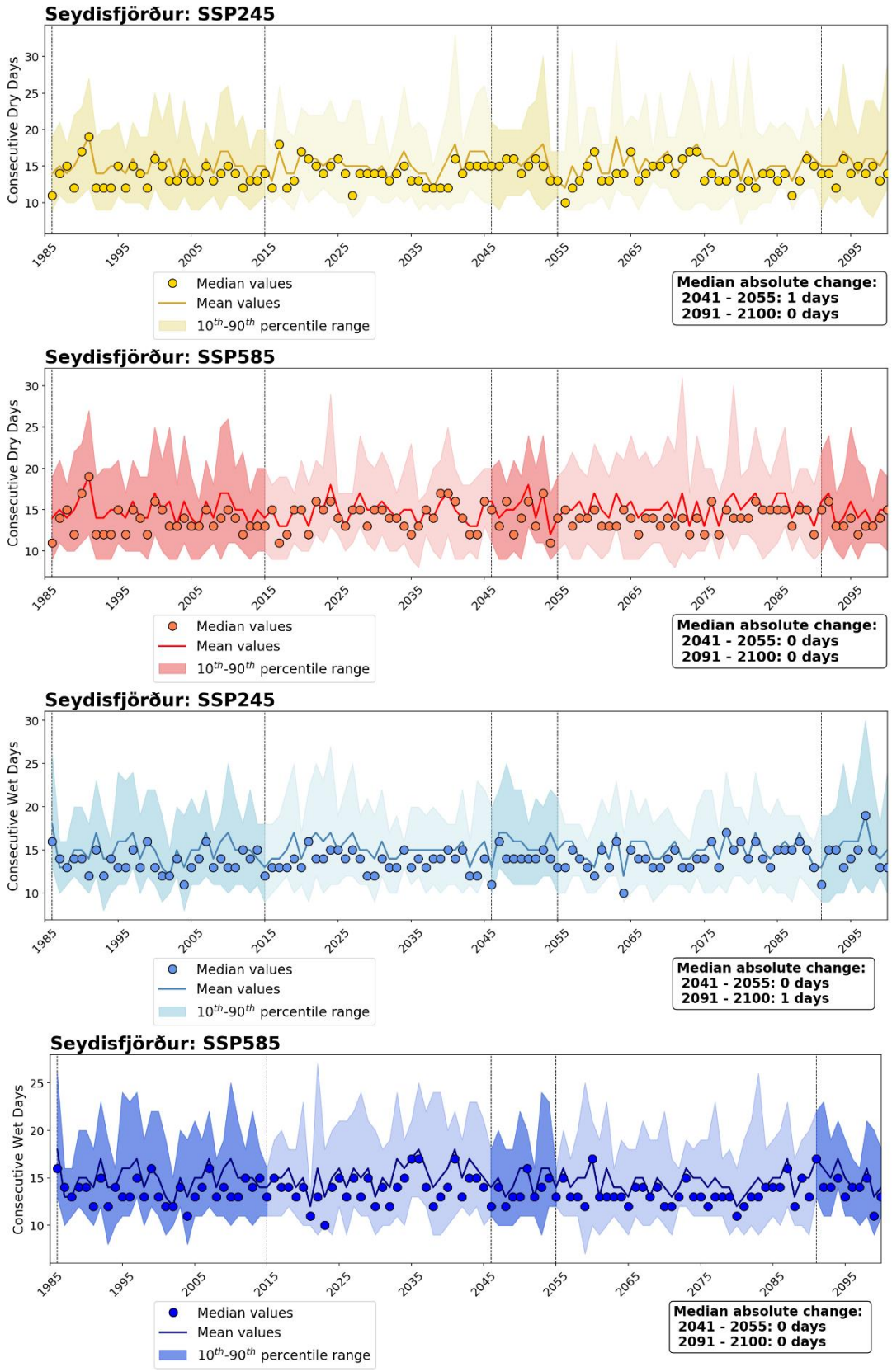

Figure IV.10 — CDD and CWD values for Seyðisfjörður calculated from the median (dots), mean (line), and 10th-90th percentile (shaded area) values of the ensemble of climate models for SSP245 and SSP585. Median differences for two future periods (2041–2055 and 2091–2100) as compared to the historical period (1986–2015) are also indicated.

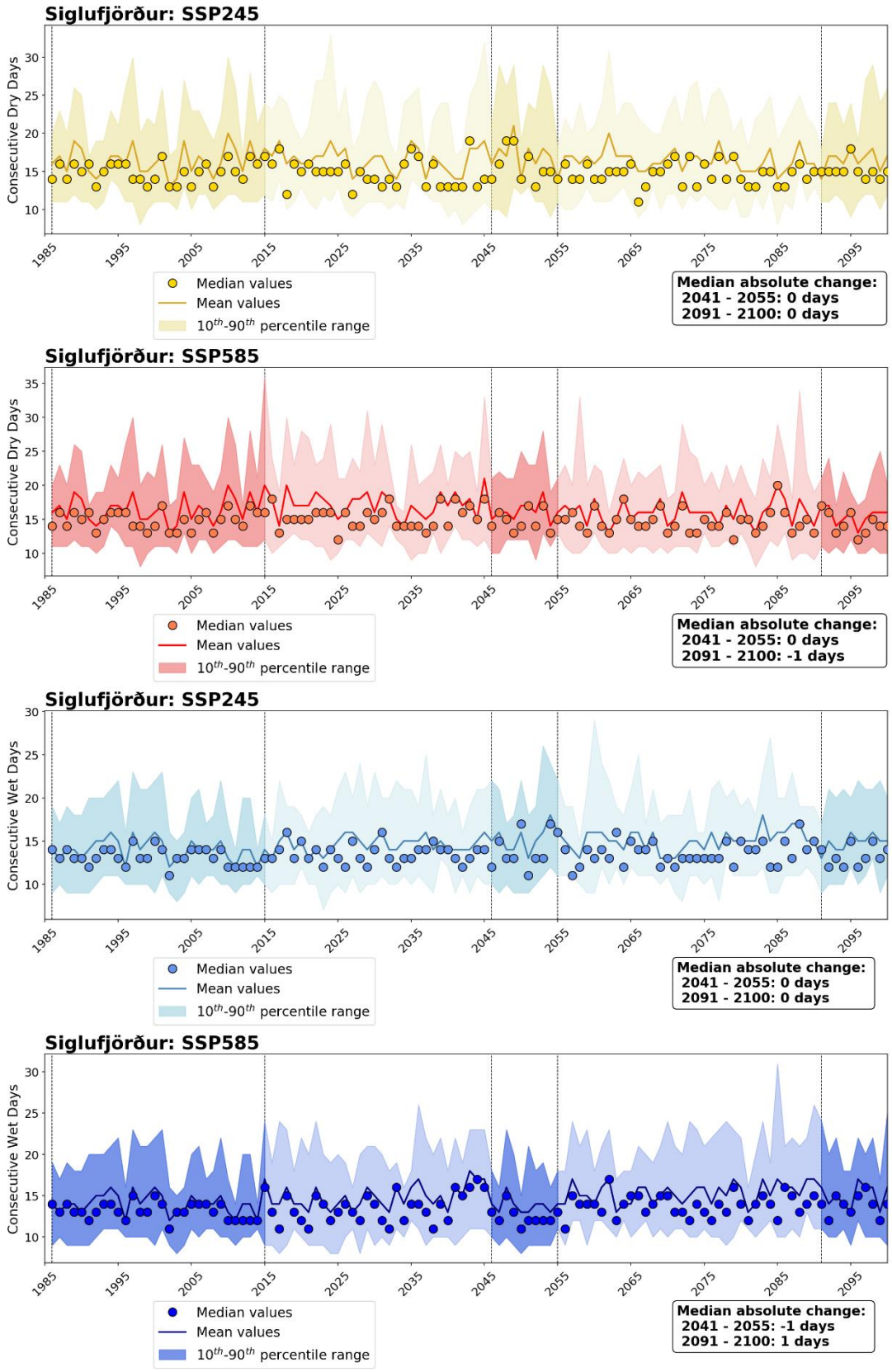

Figure IV.11 — CDD and CWD values for Siglufjörður calculated from the median (dots), mean (line), and 10th-90th percentile (shaded area) values of the ensemble of climate models for SSP245 and SSP585. Median differences for two future periods (2041–2055 and 2091–2100) as compared to the historical period (1986–2015) are also indicated.

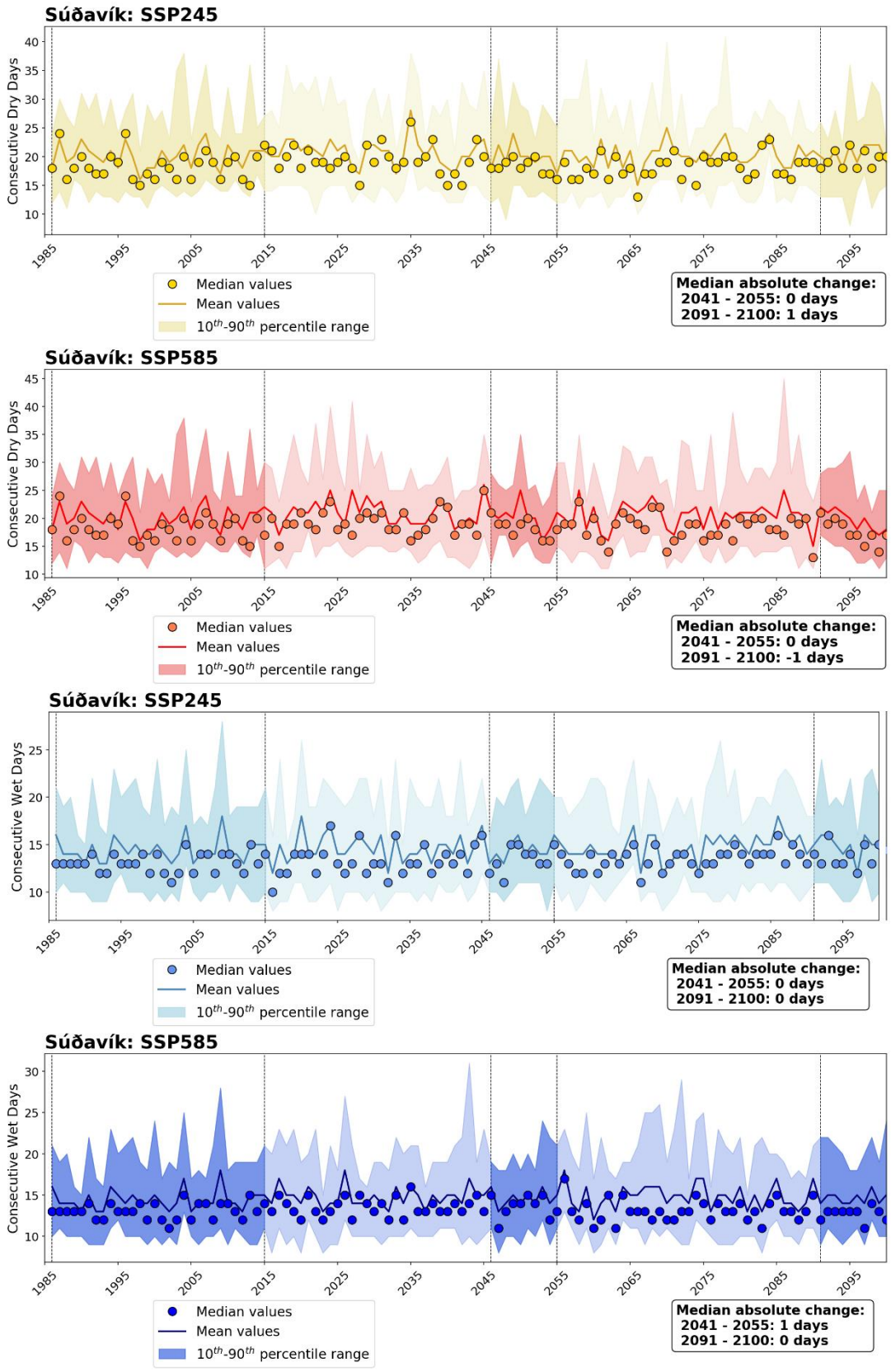

Figure IV.12 — CDD and CWD values for Súðavík as calculated from the median (dots), mean (line), and 10th-90th percentile (shaded area) values of the ensemble of climate models for SSP245 and SSP585. Median differences for two future periods (2041–2055 and 2091–2100) as compared to the historical period (1986–2015) are also indicated.

Appendix V. Density plots

In this appendix, figures similar to Figure 9 from the report are presented.

In these figures, each panel compares the distribution of the twelve GCMs from Table 2 for the historical period (between 1986 and 2015), and the end of the century (2091–2100) for both scenarios (SSP2-4.5 and SSP5-8.5), with histograms and density lines.

Eskifjörður

CDD

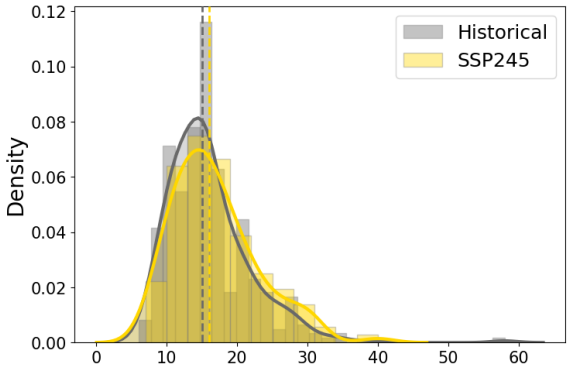

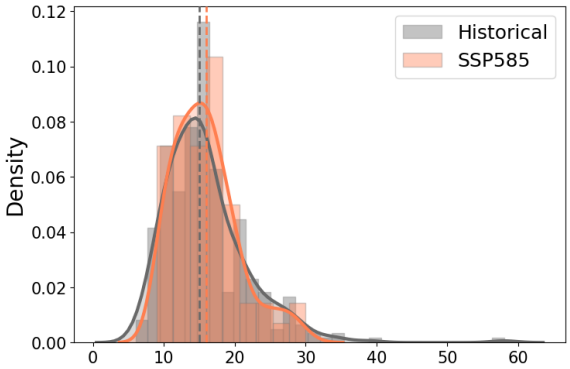

CWD

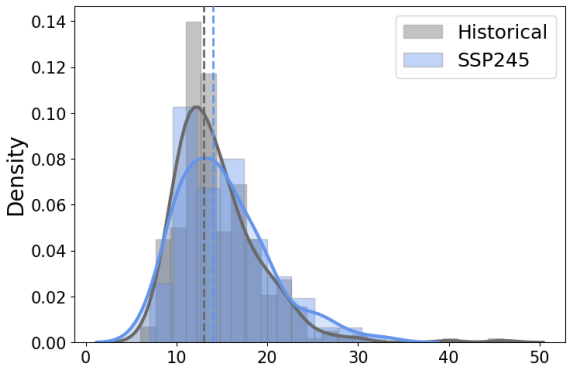

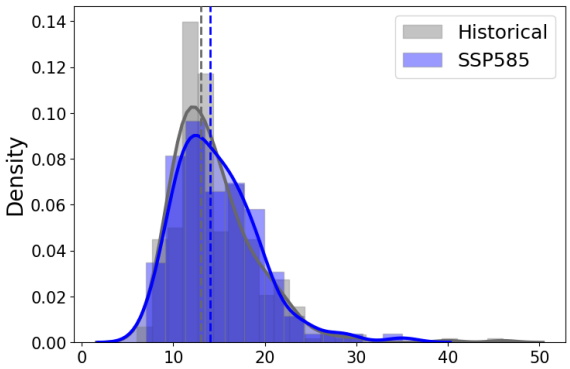

Flateyri

CDD

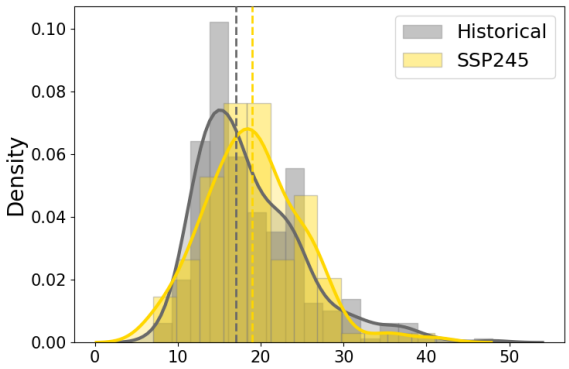

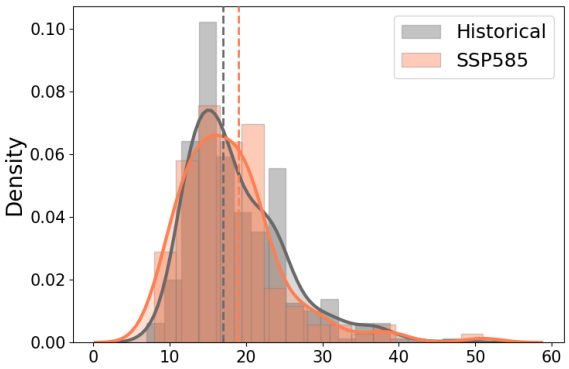

CWD

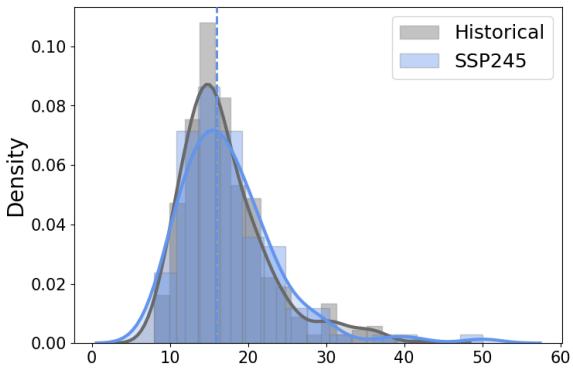

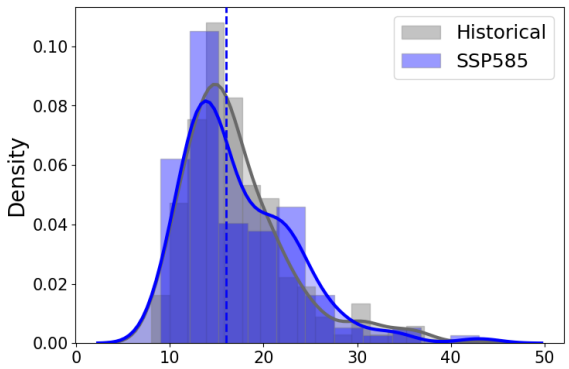

Höfn í Hornafirði

CDD

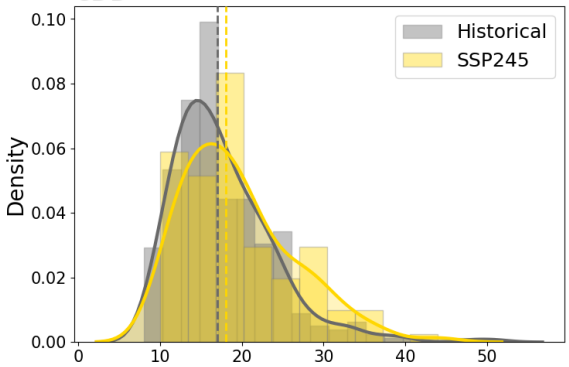

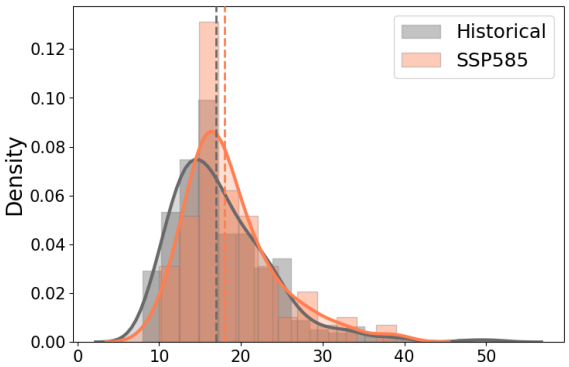

CWD

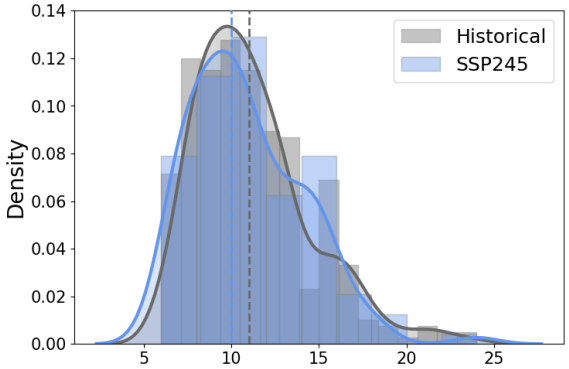

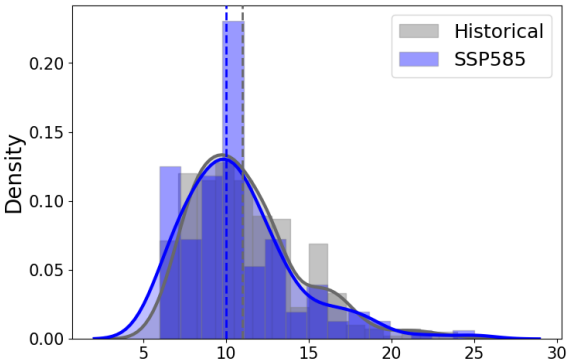

Ísafjörður

CDD

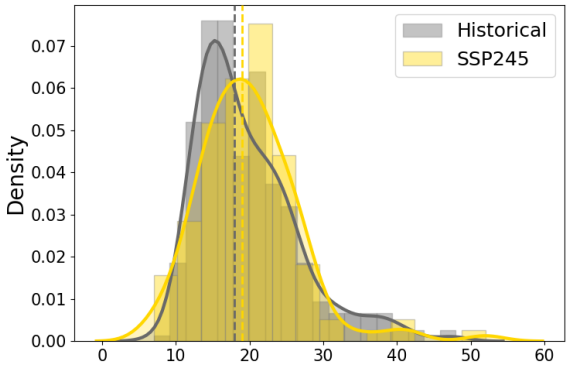

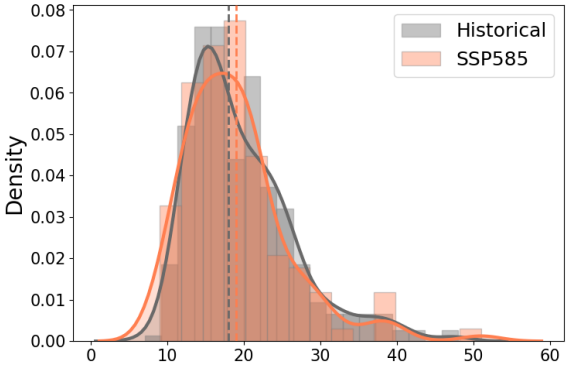

CWD

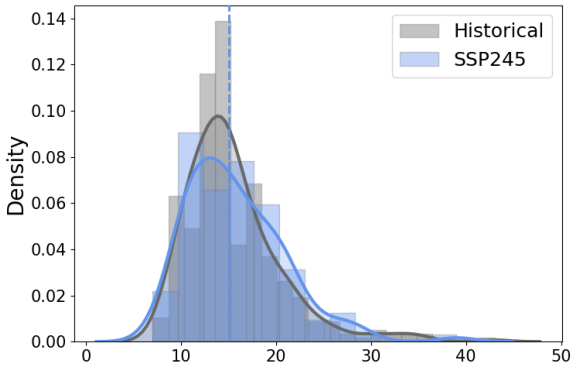

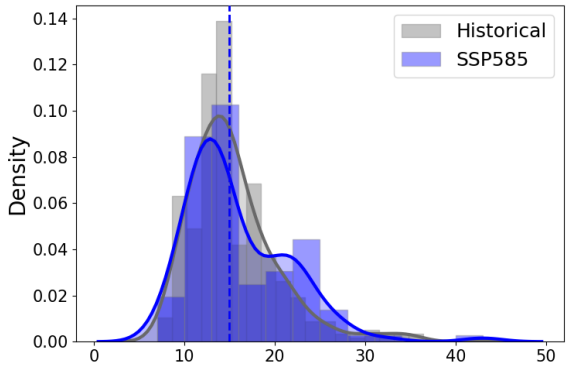

Kvísker

CDD

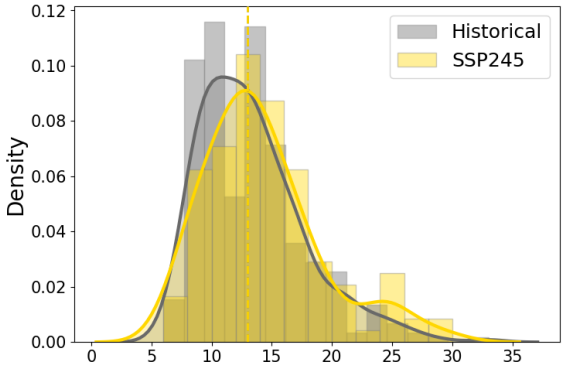

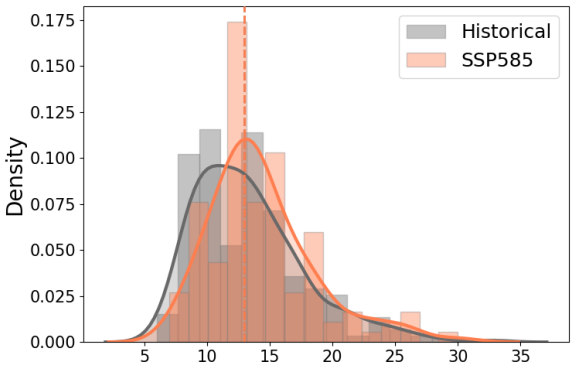

CWD

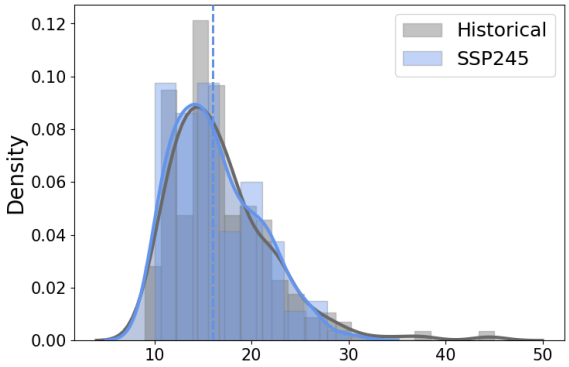

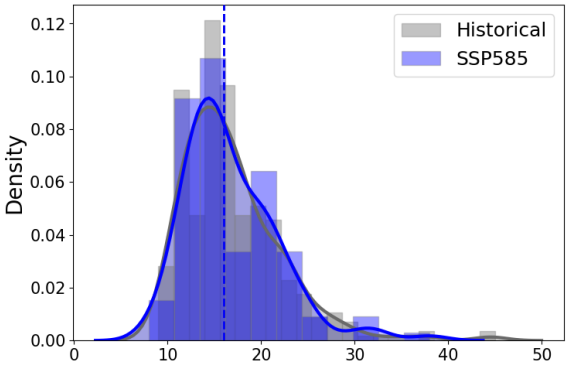

Laufbali

CDD

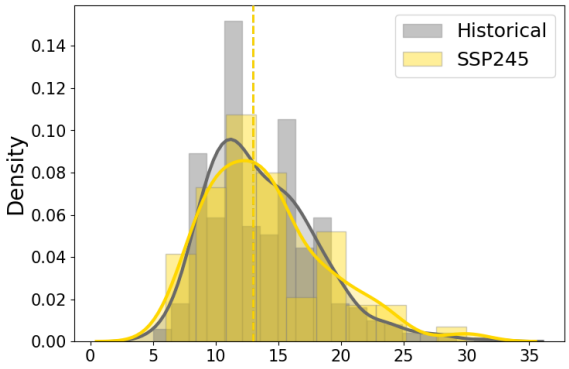

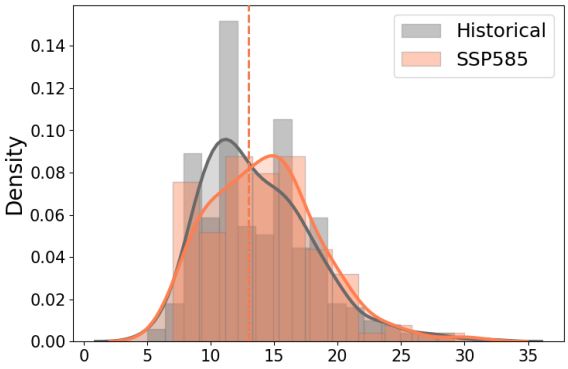

CWD

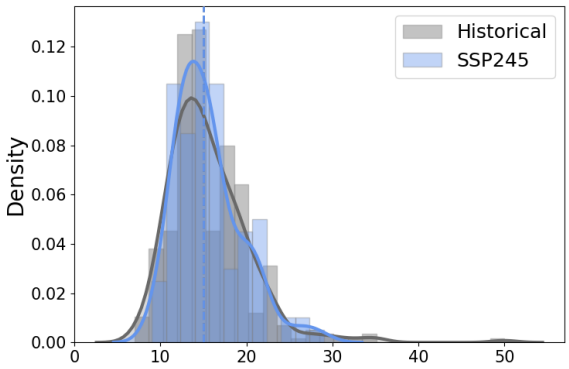

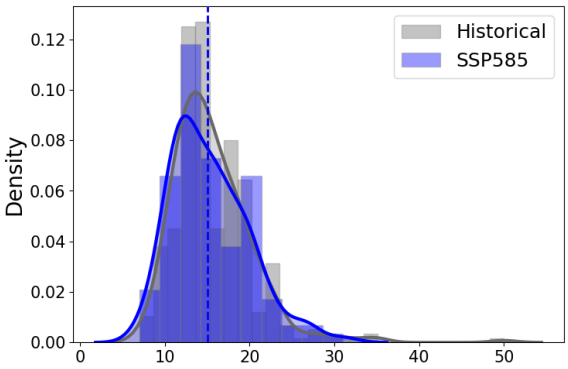

Neskaupstaður

CDD

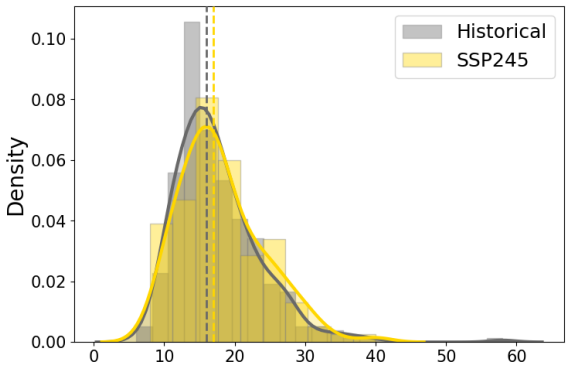

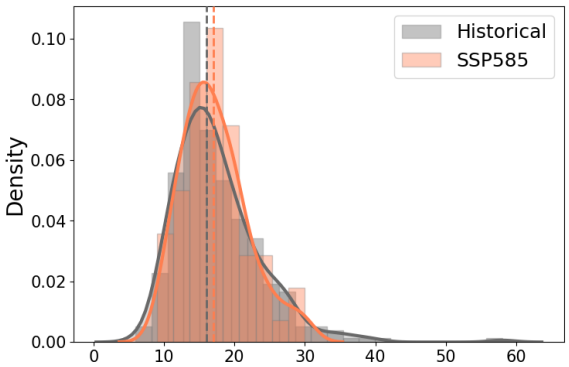

CWD

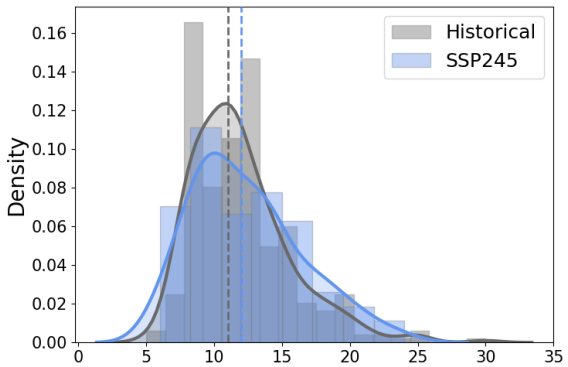

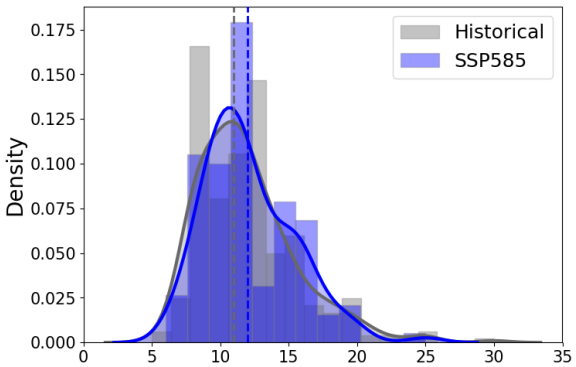

Ólafsfjörður

CDD

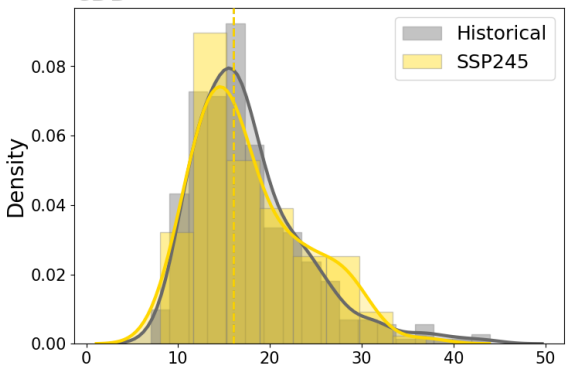

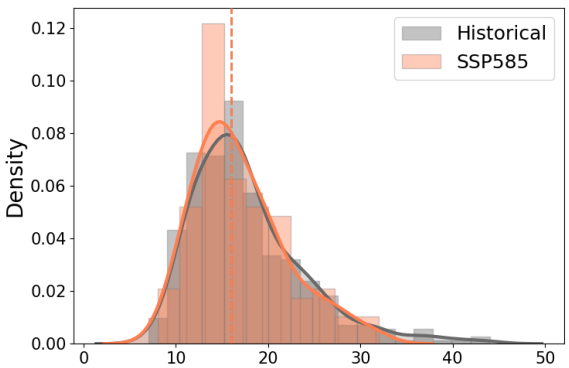

CWD

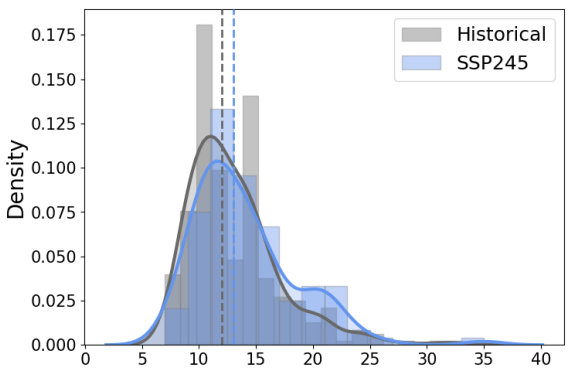

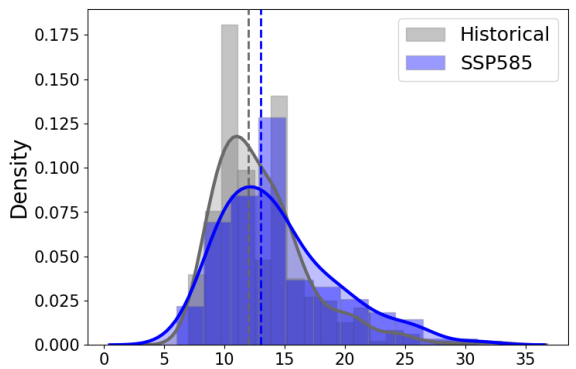

Reykjavík

CDD

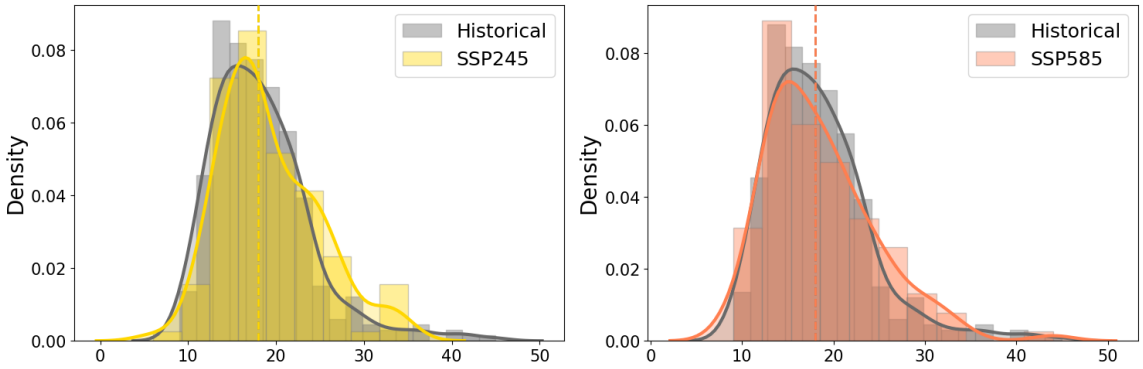

CWD

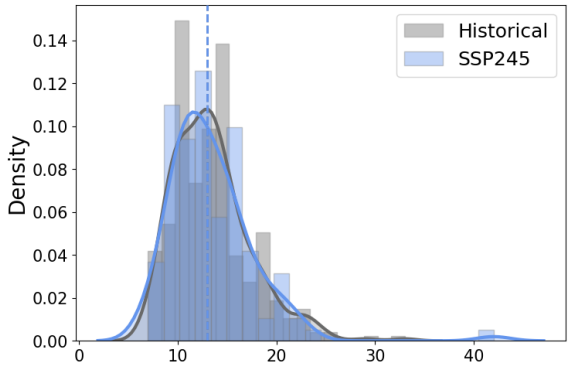

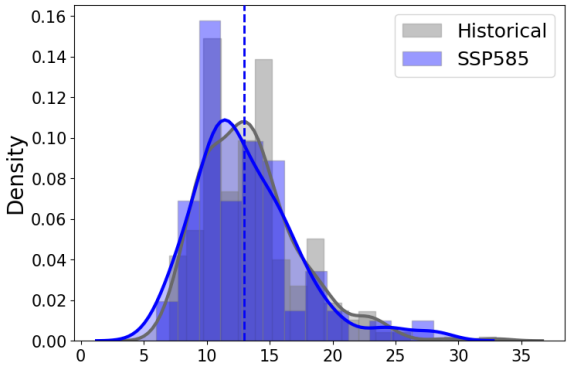

Seydisfjörður

CDD

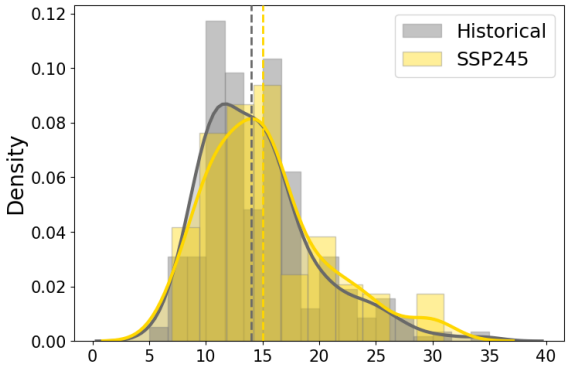

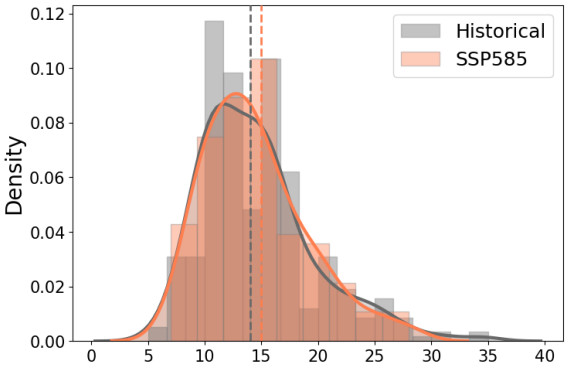

CWD

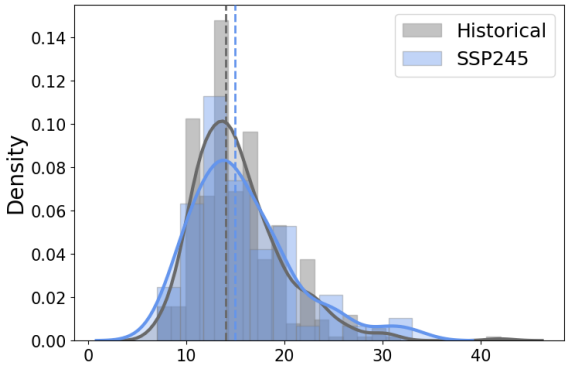

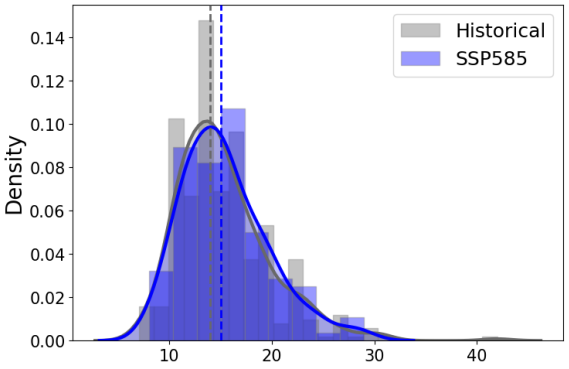

Siglufjörður

CDD

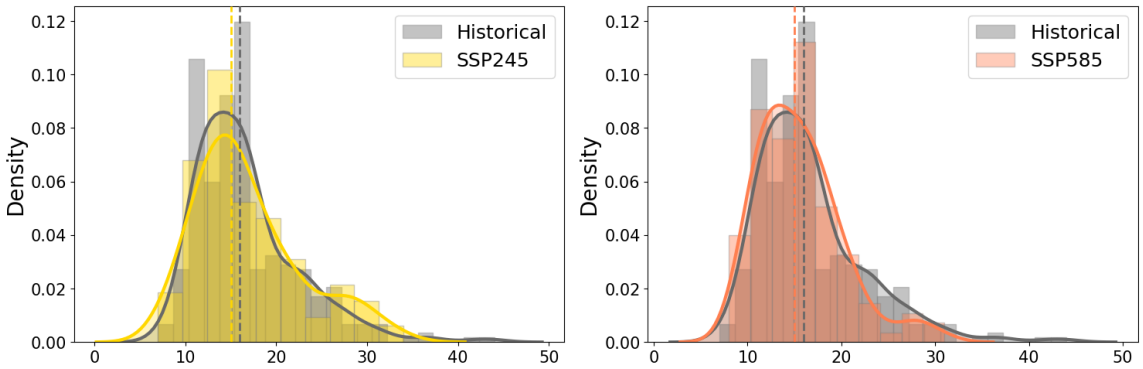

CWD

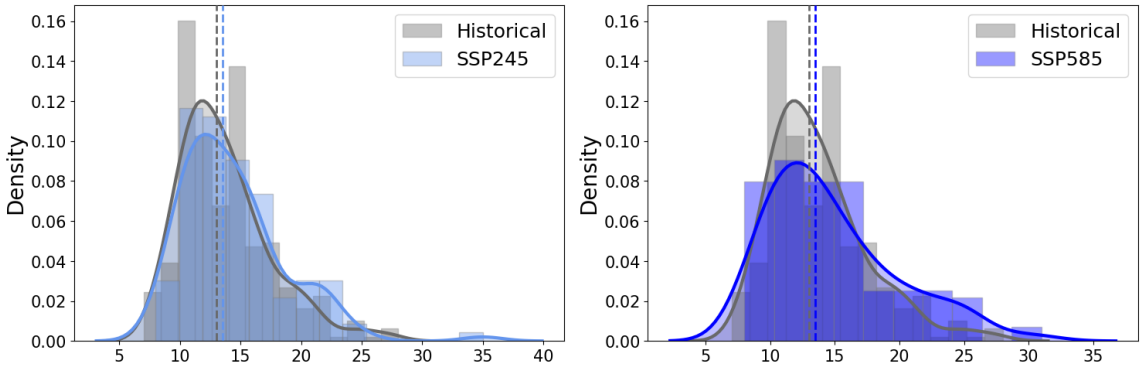

Súðavík

CDD

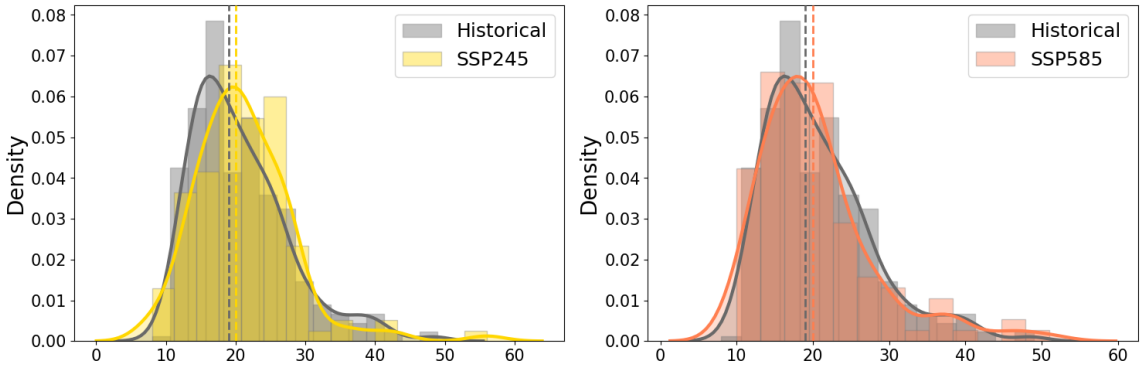

CWD

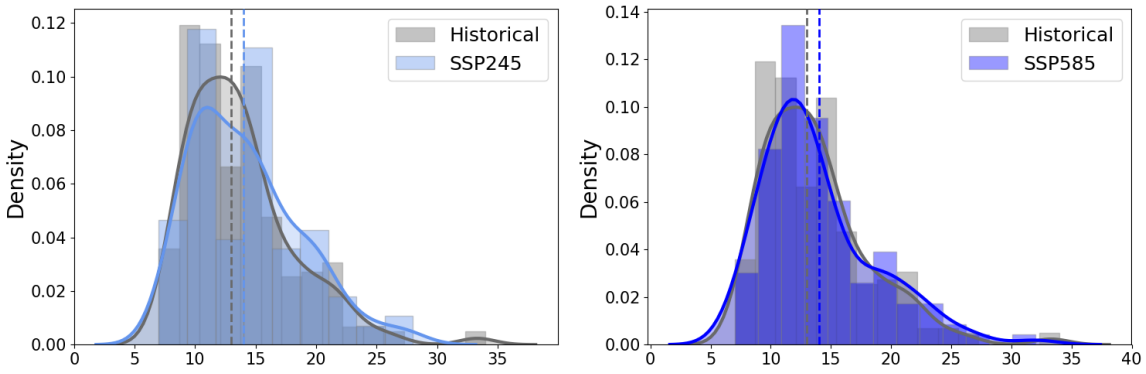

Appendix VI. Catchment-scale CDD and CWD maps

In this appendix, figures similar to Figure 10 and 11 in the report are presented.

In the figures, the top panel shows results based on historical data averaged between 1986 and 2015 for the ensemble median (left), and 90th percentile (right). The middle panel shows CDD based on SSP2-4.5 projections for the ensemble median (left) and 90th percentile (right). Finally, the lower panel shows results based on SSP5-8.5 projections for the ensemble median (left) and 90th percentile (right). Projections are shown for the end of the century, using the mean value for each grid-points between 2091 and 2100. Indicated on each map is the median value of the CDD values displayed on the map.

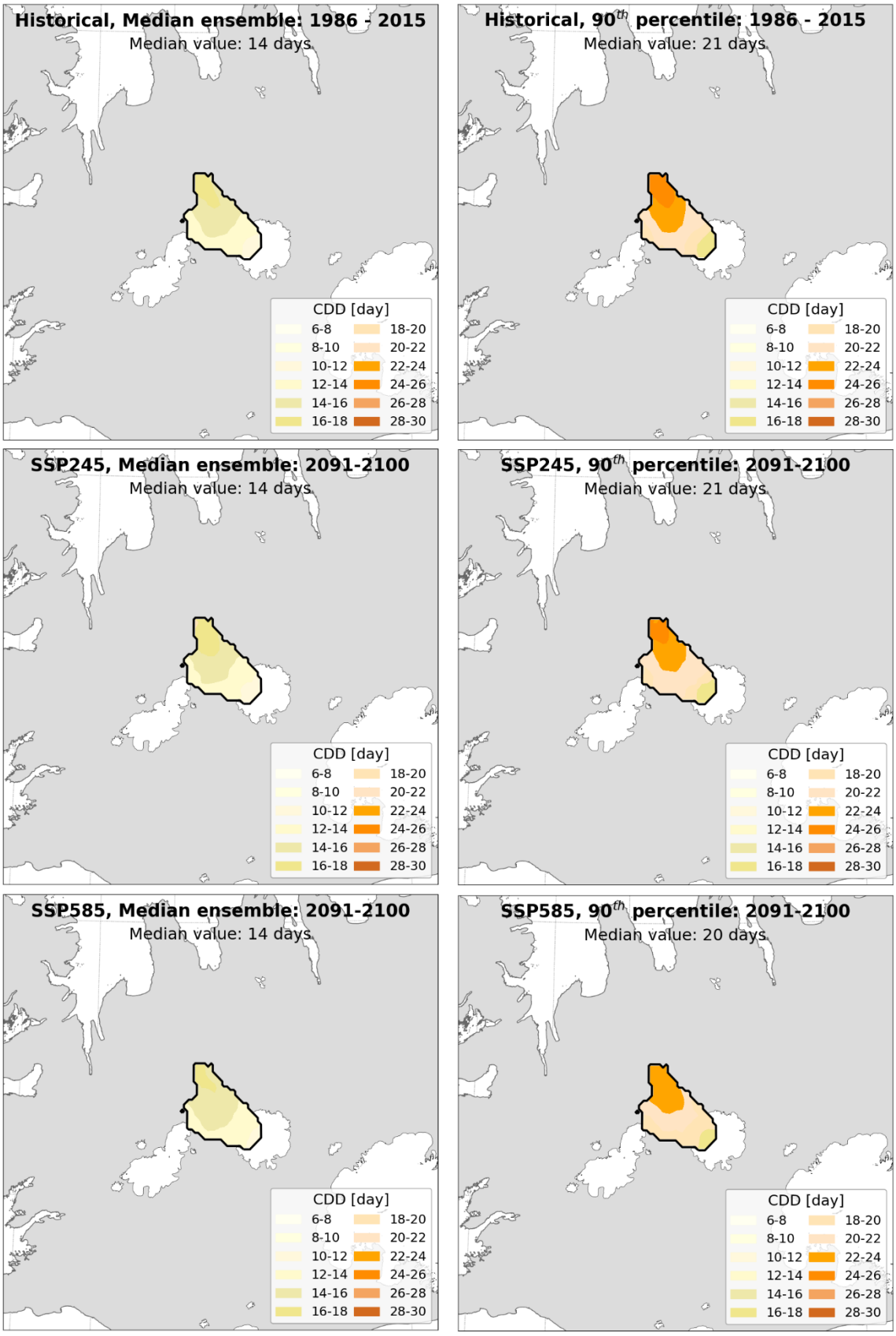

Figure VI.1 — CDD maps for catchment Blóndulón based on the downscaled CMIP6 dataset averaged over a historical period (1986–2015) and two projections (2091–2100) based on median and 90th percentile of the ensemble of climate models.

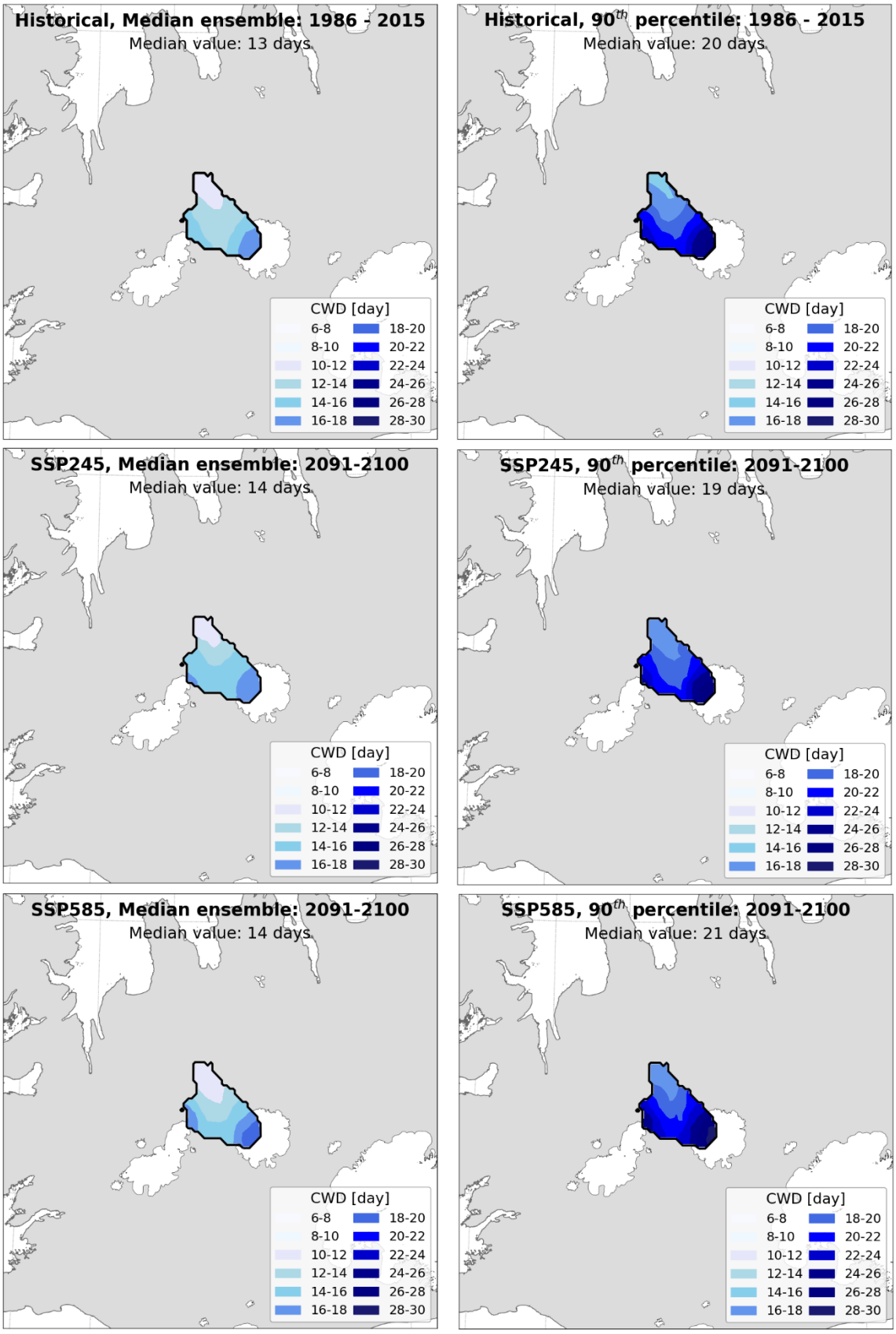

Figure VI.2 — CWD maps for catchment Blöndulón based on the downscaled CMIP6 dataset averaged over a historical period (1986–2015) and two projections (2091–2100) based on median and 90th percentile of the ensemble of climate models.

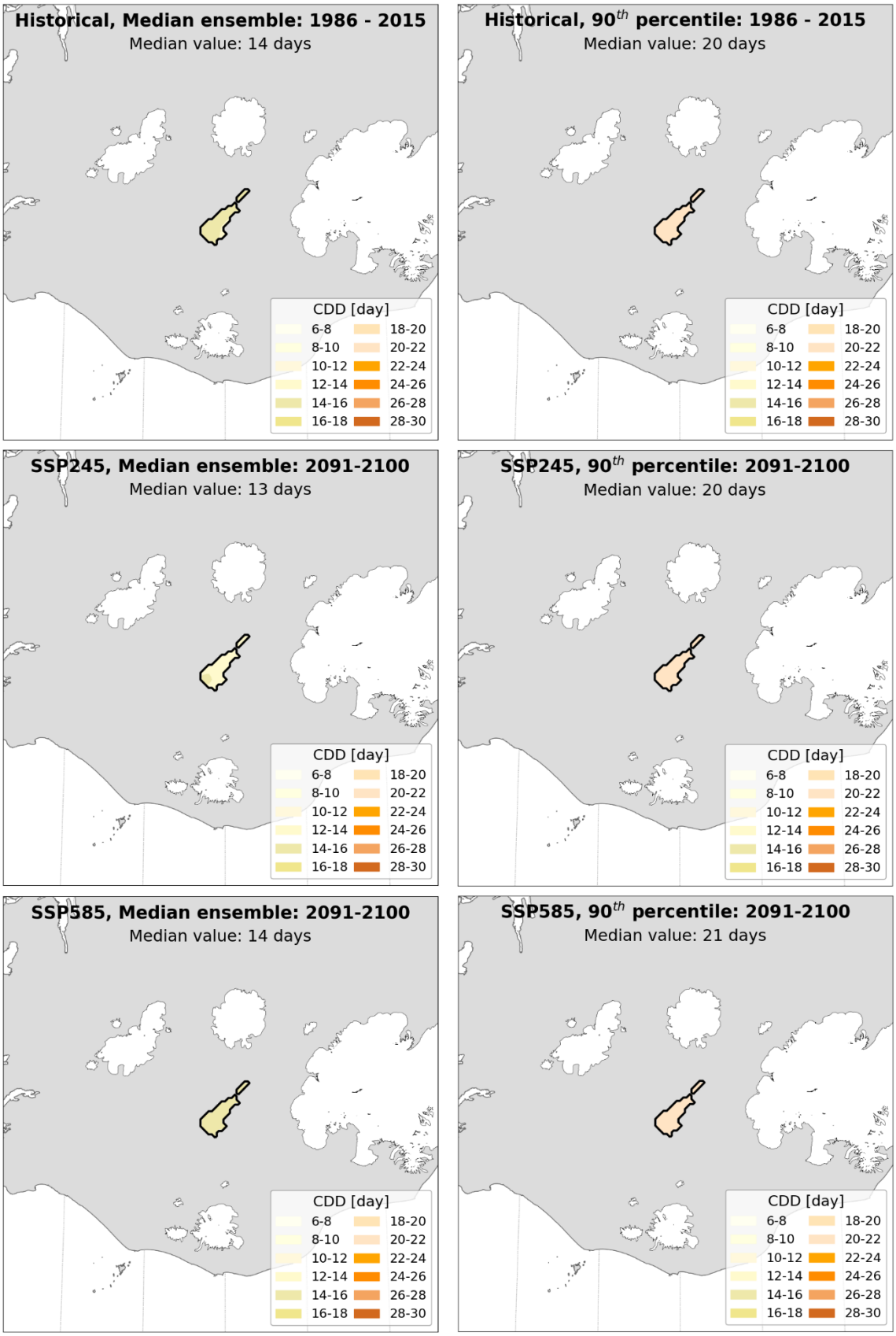

Figure VI.3 — CDD maps for catchment Búðarháls based on the downscaled CMIP6 dataset averaged over a historical period (1986–2015) and two projections (2091–2100) based on median and 90th percentile of the ensemble of climate models.

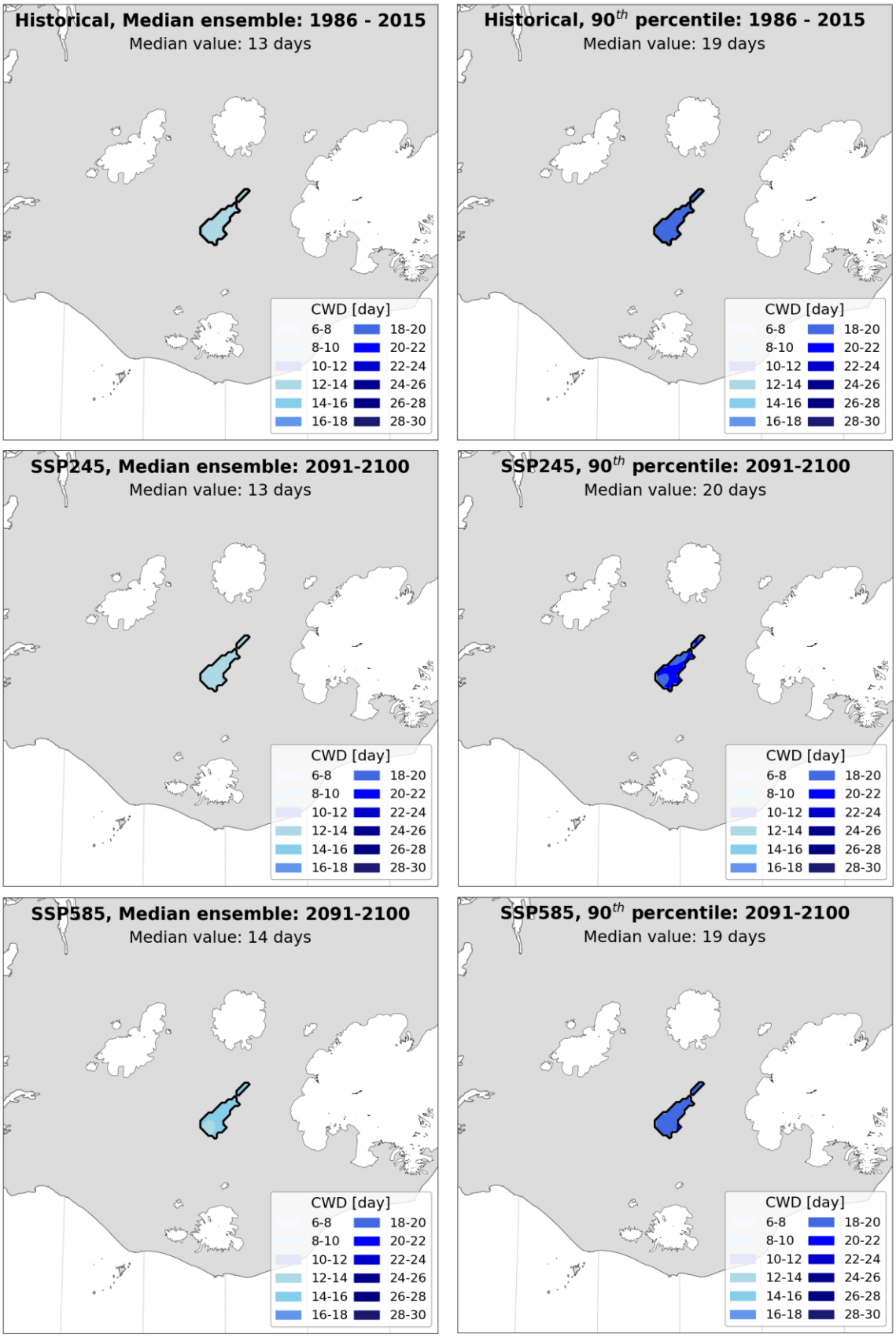

Figure VI.4 — CWD maps for catchment Búðarháls based on the downscaled CMIP6 dataset averaged over a historical period (1986–2015) and two projections (2091–2100) based on median and 90th percentile of the ensemble of climate models.

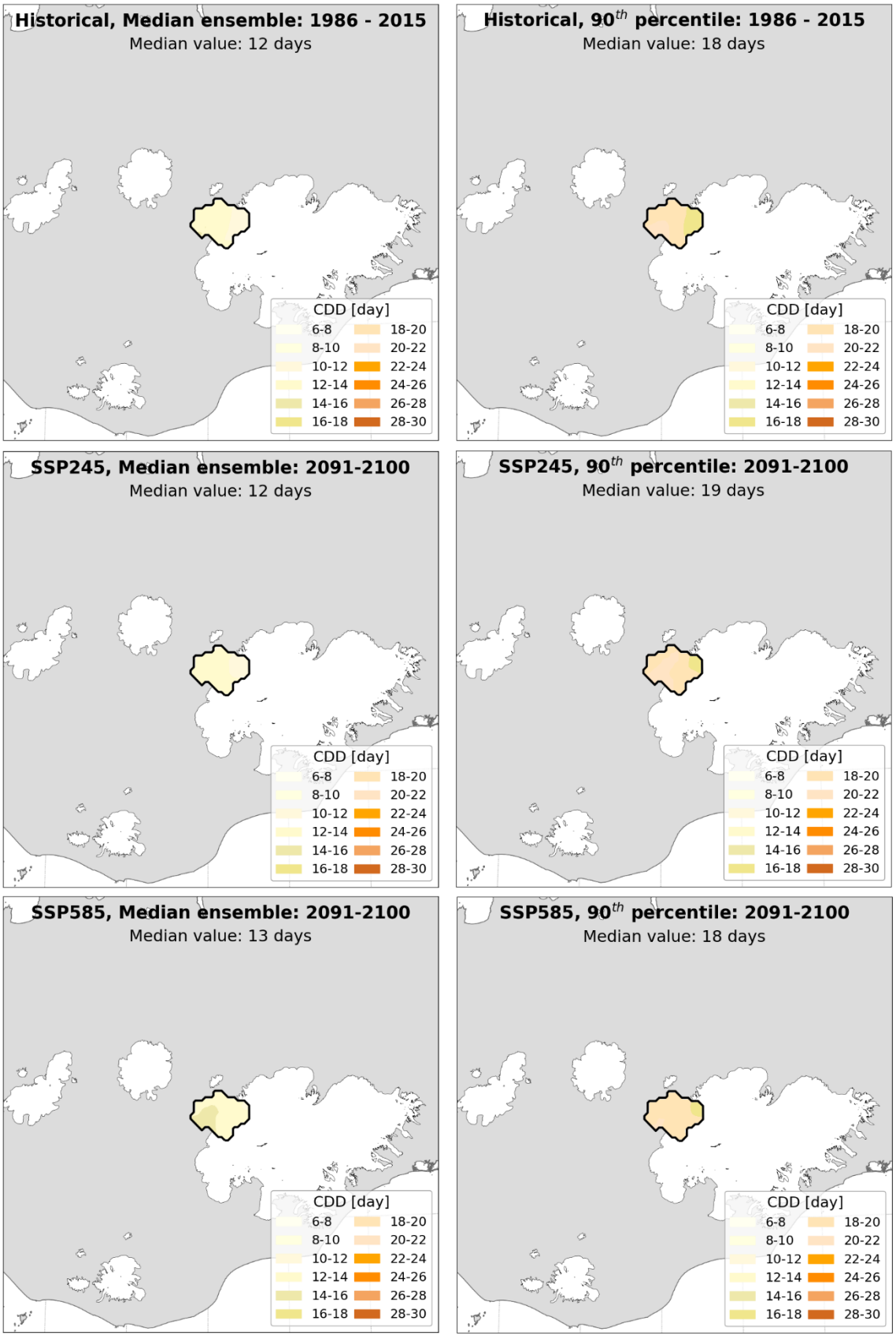

Figure VI.5 — CDD maps for catchment Hágöngulón based on the downscaled CMIP6 dataset averaged over a historical period (1986–2015) and two projections (2091–2100) based on median and 90th percentile of the ensemble of climate models.

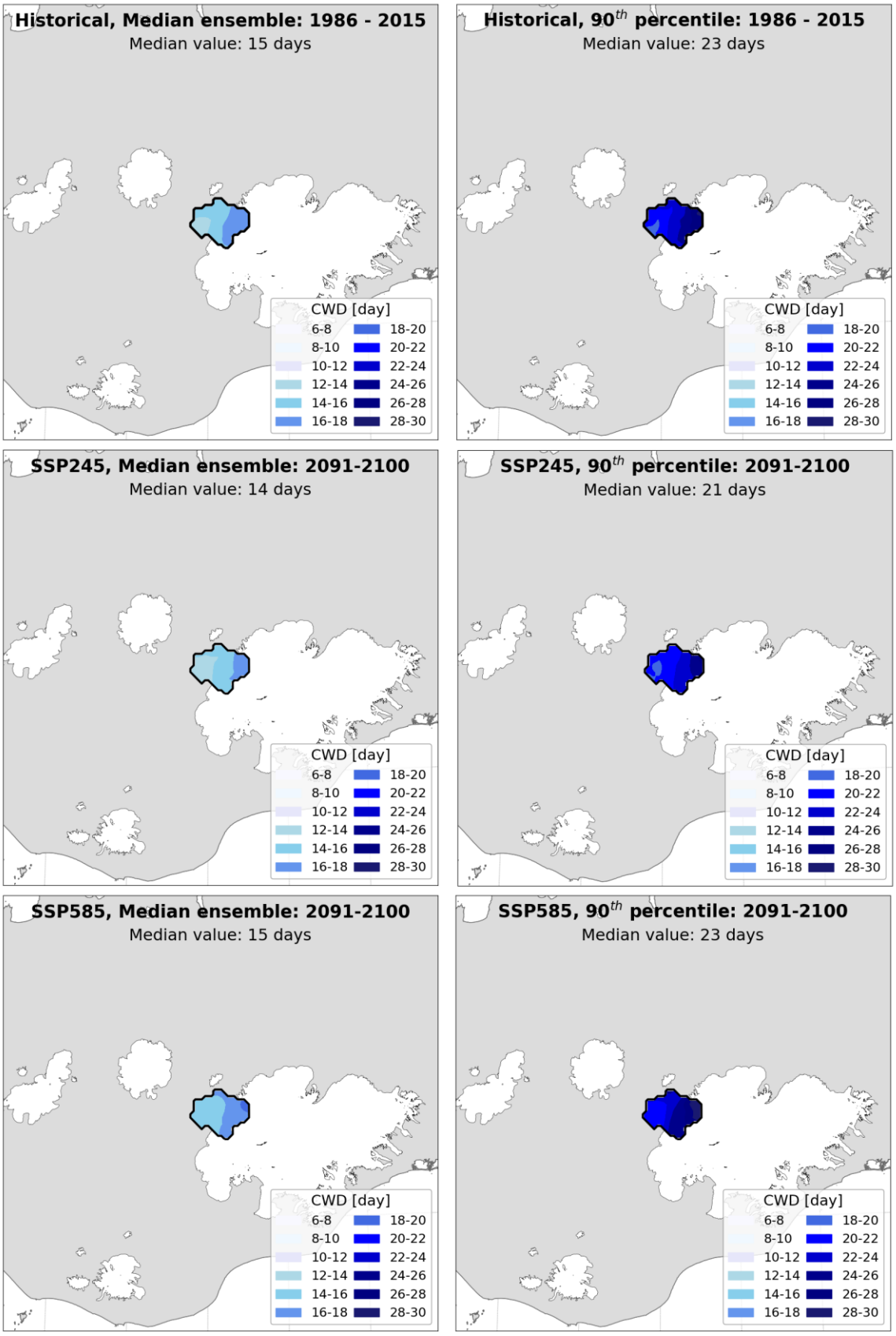

Figure VI.6 — CWD maps for catchment Hágöngulón based on the downscaled CMIP6 dataset averaged over a historical period (1986–2015) and two projections (2091–2100) based on median and 90th percentile of the ensemble of climate models.

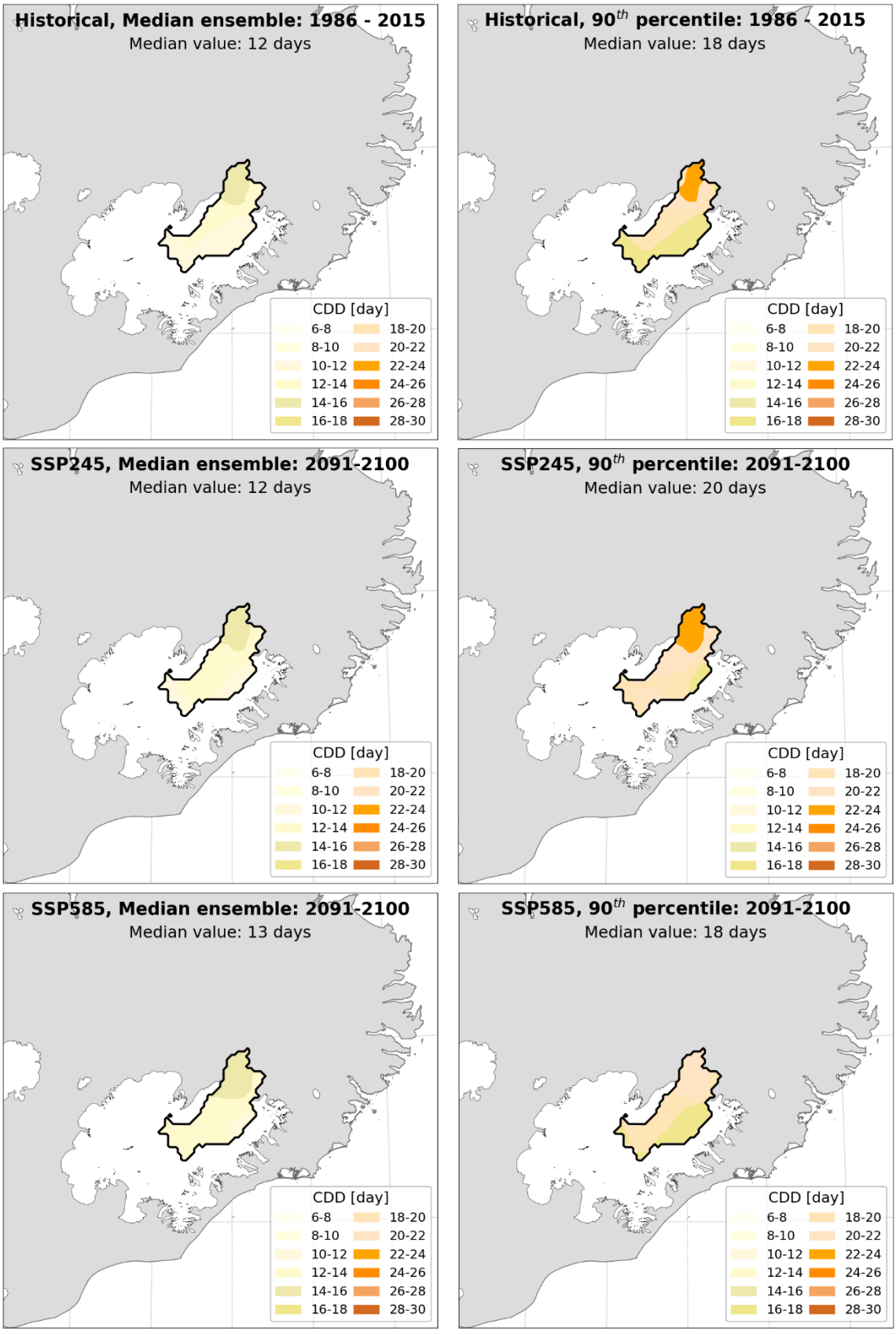

Figure VI.7 — CDD maps for catchment Hálslón based on the downscaled CMIP6 dataset averaged over a historical period (1986–2015) and two projections (2091–2100) based on median and 90th percentile of the ensemble of climate models.

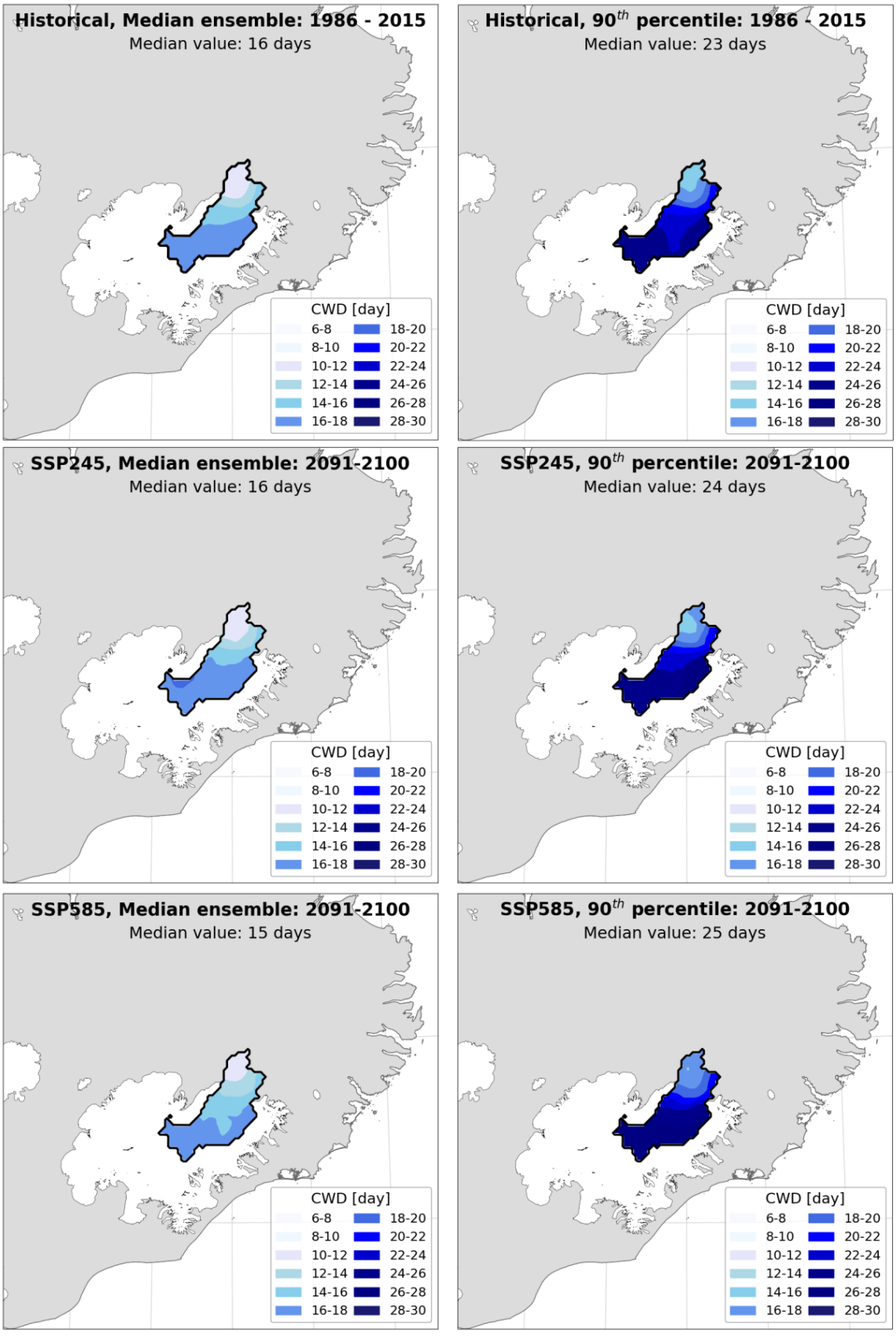

Figure VI.8 — CWD maps for catchment Hálslón based on the downscaled CMIP6 dataset averaged over a historical period (1986–2015) and two projections (2091–2100) based on median and 90th percentile of the ensemble of climate models.

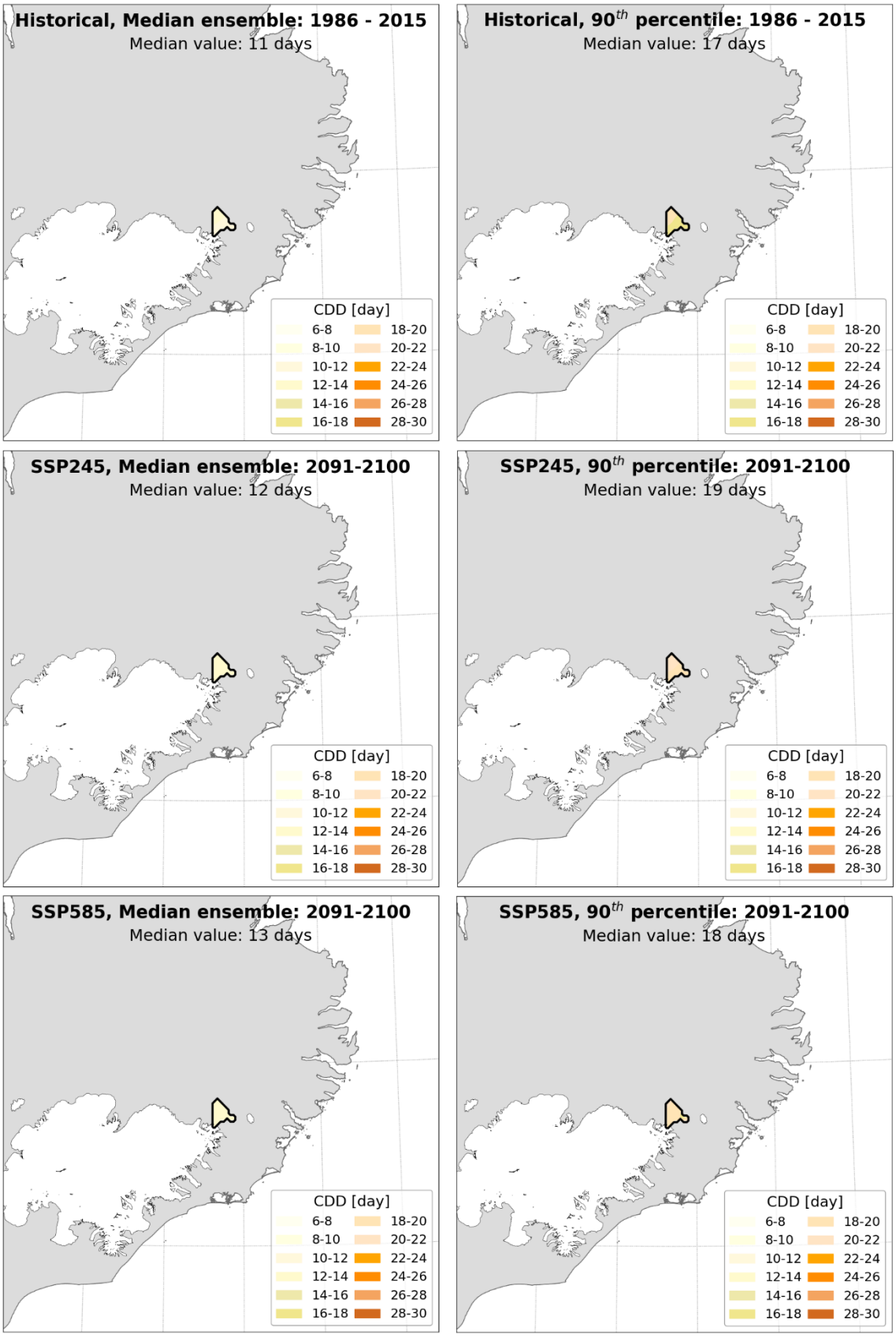

Figure VI.9 — CDD maps for catchment Hraunaveita based on the downscaled CMIP6 dataset averaged over a historical period (1986–2015) and two projections (2091–2100) based on median and 90th percentile of the ensemble of climate models.

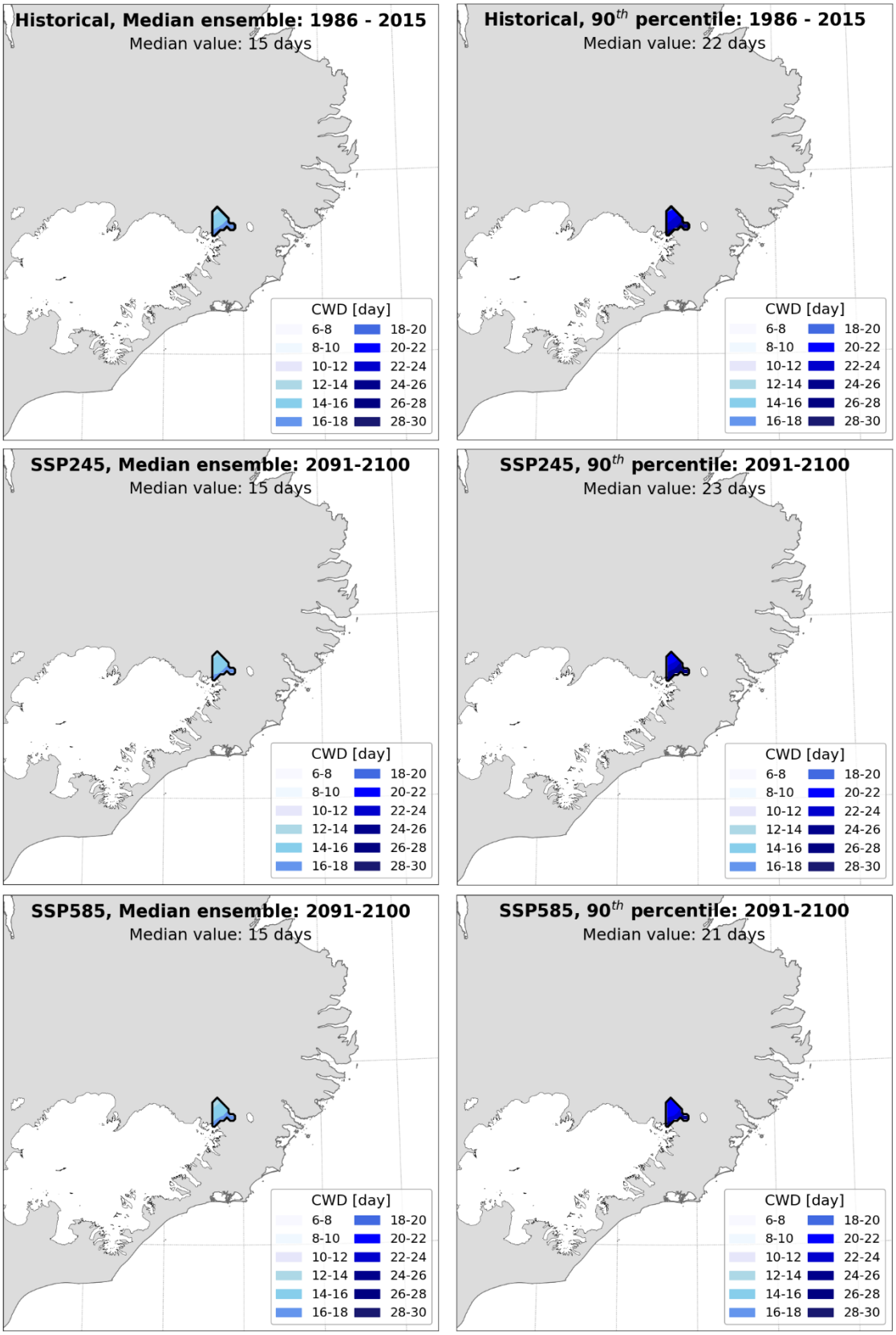

Figure VI.10 — CWD maps for catchment Hraunaveita based on the downscaled CMIP6 dataset averaged over a historical period (1986–2015) and two projections (2091–2100) based on median and 90th percentile of the ensemble of climate models.

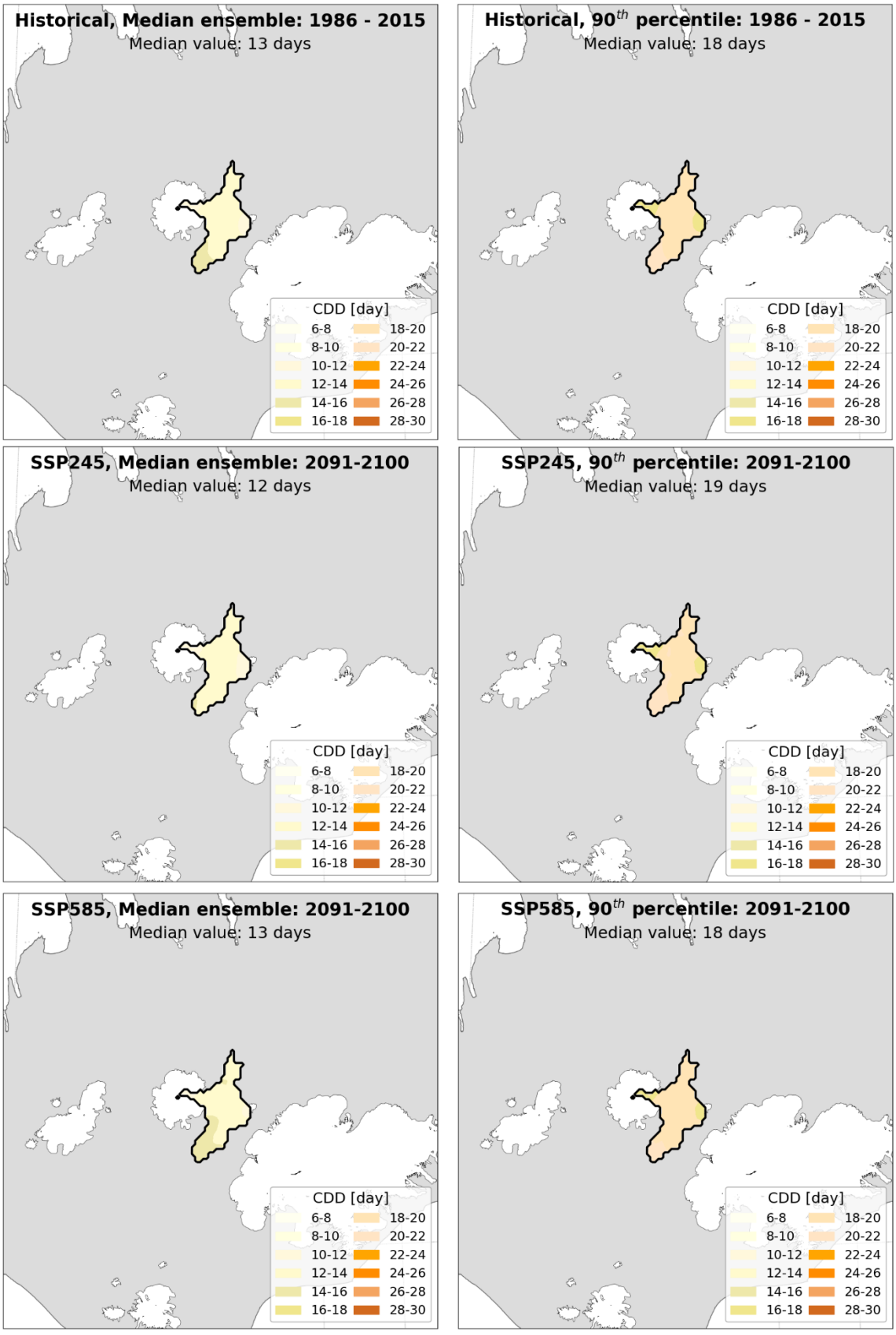

Figure VI.11 — CDD maps for catchment Kvíslaveita based on the downscaled CMIP6 dataset averaged over a historical period (1986–2015) and two projections (2091–2100) based on median and 90th percentile of the ensemble of climate models.

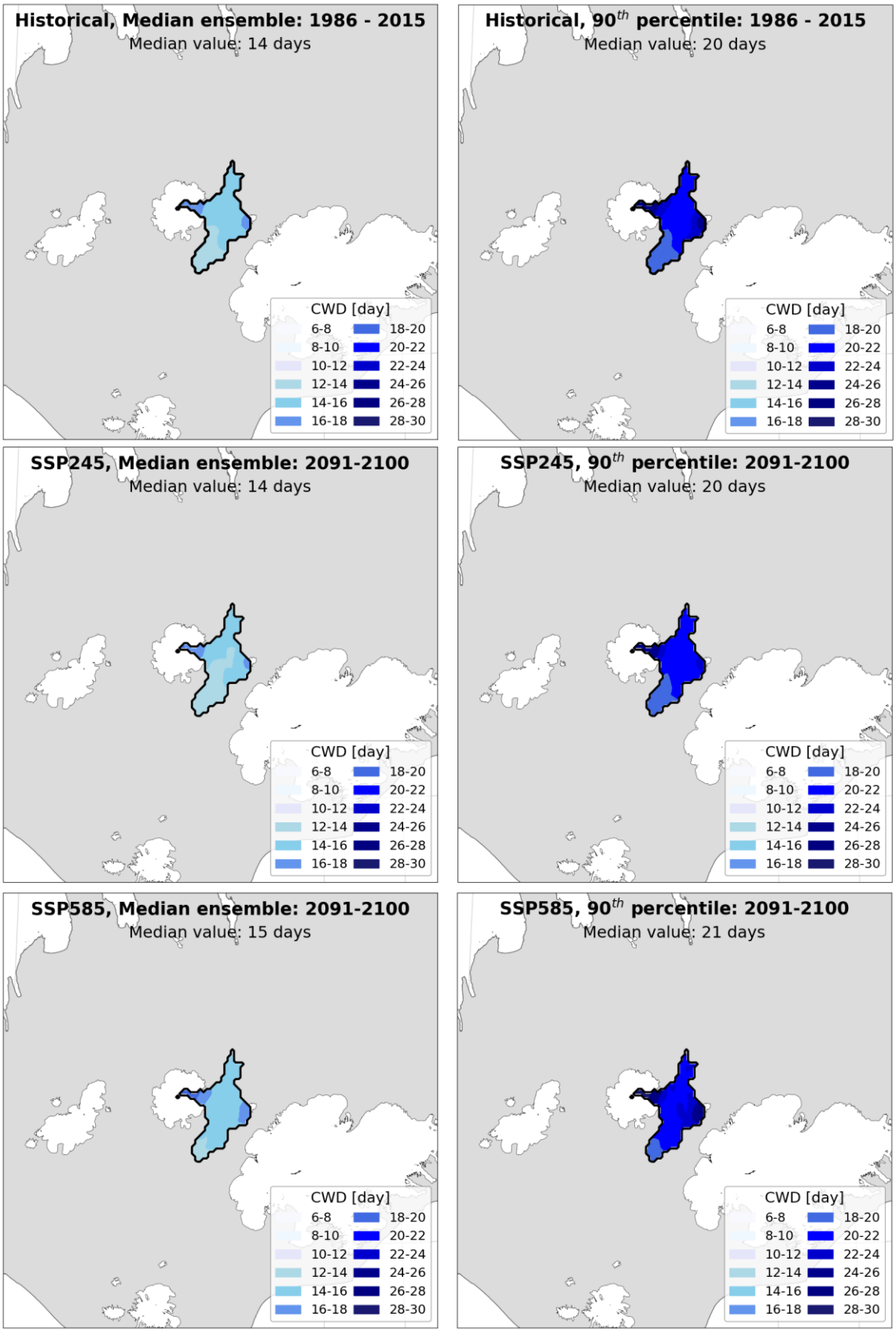

Figure VI.12 — CWD maps for catchment Kvíslaveita based on the downscaled CMIP6 dataset averaged over a historical period (1986–2015) and two projections (2091–2100) based on median and 90th percentile of the ensemble of climate models.

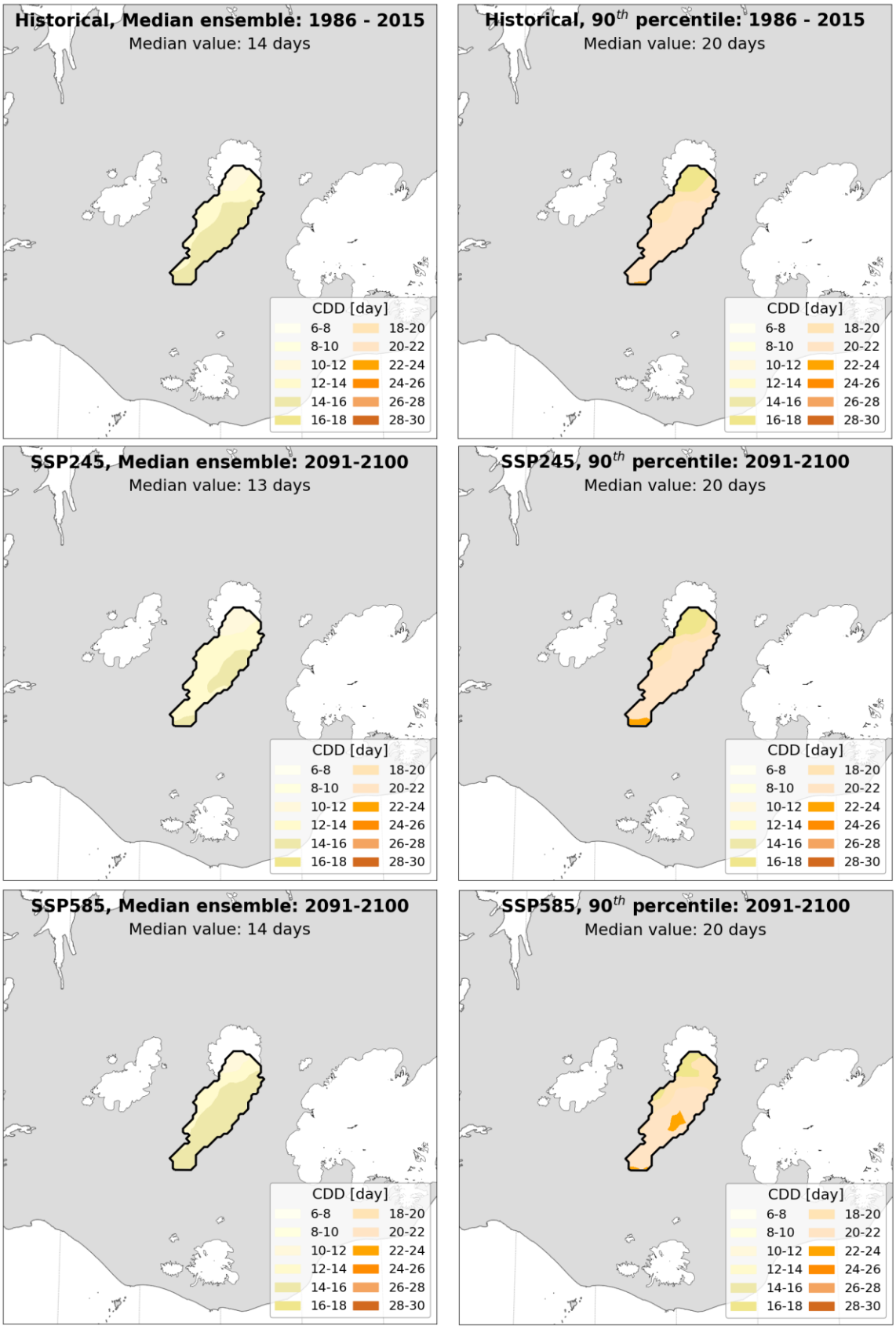

Figure VI.13 — CDD maps for catchment Sultartangi based on the downscaled CMIP6 dataset averaged over a historical period (1986–2015) and two projections (2091–2100) based on median and 90th percentile of the ensemble of climate models.

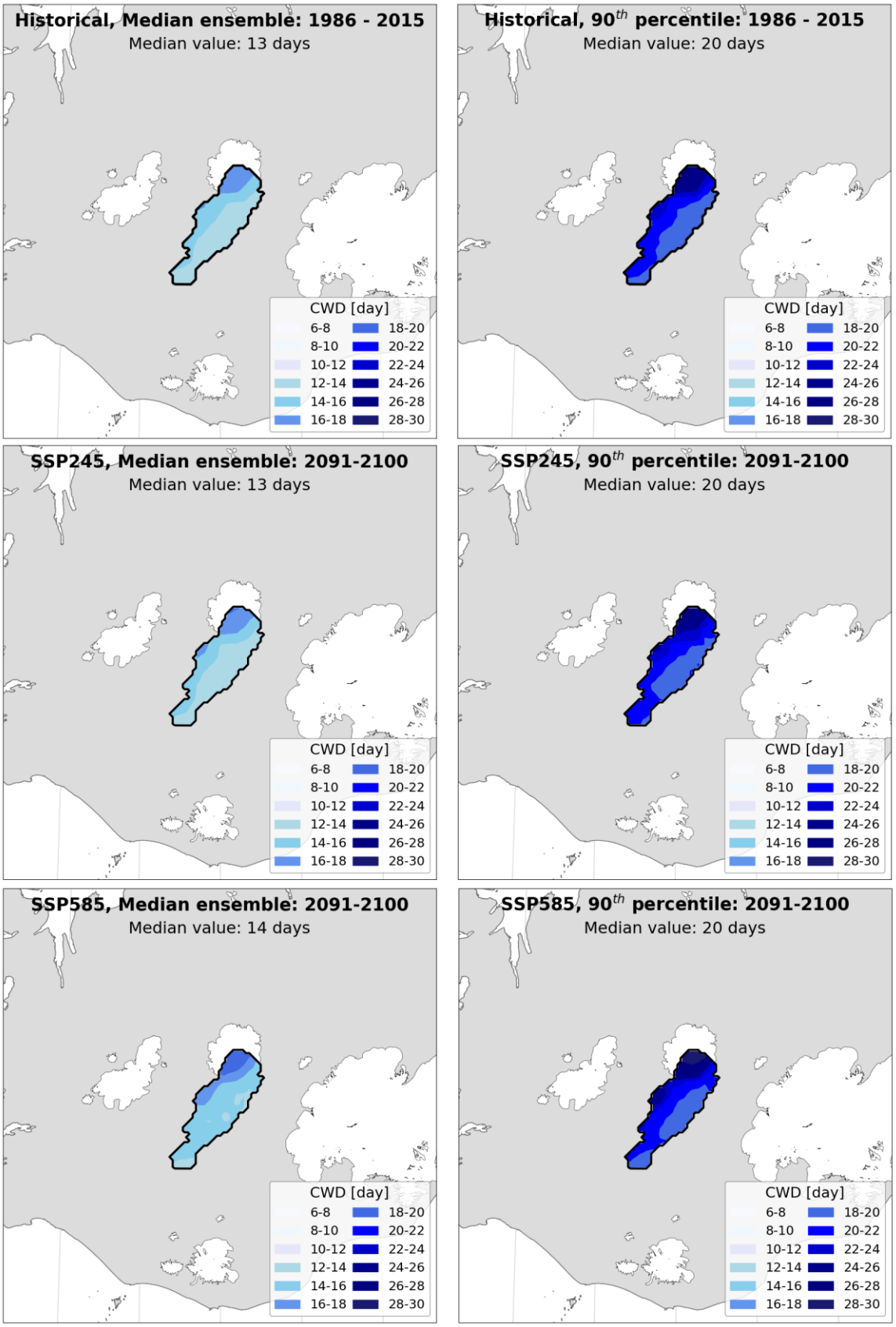

Figure VI.14 — CWD maps for catchment Sultartangi based on the downscaled CMIP6 dataset averaged over a historical period (1986–2015) and two projections (2091–2100) based on median and 90th percentile of the ensemble of climate models.

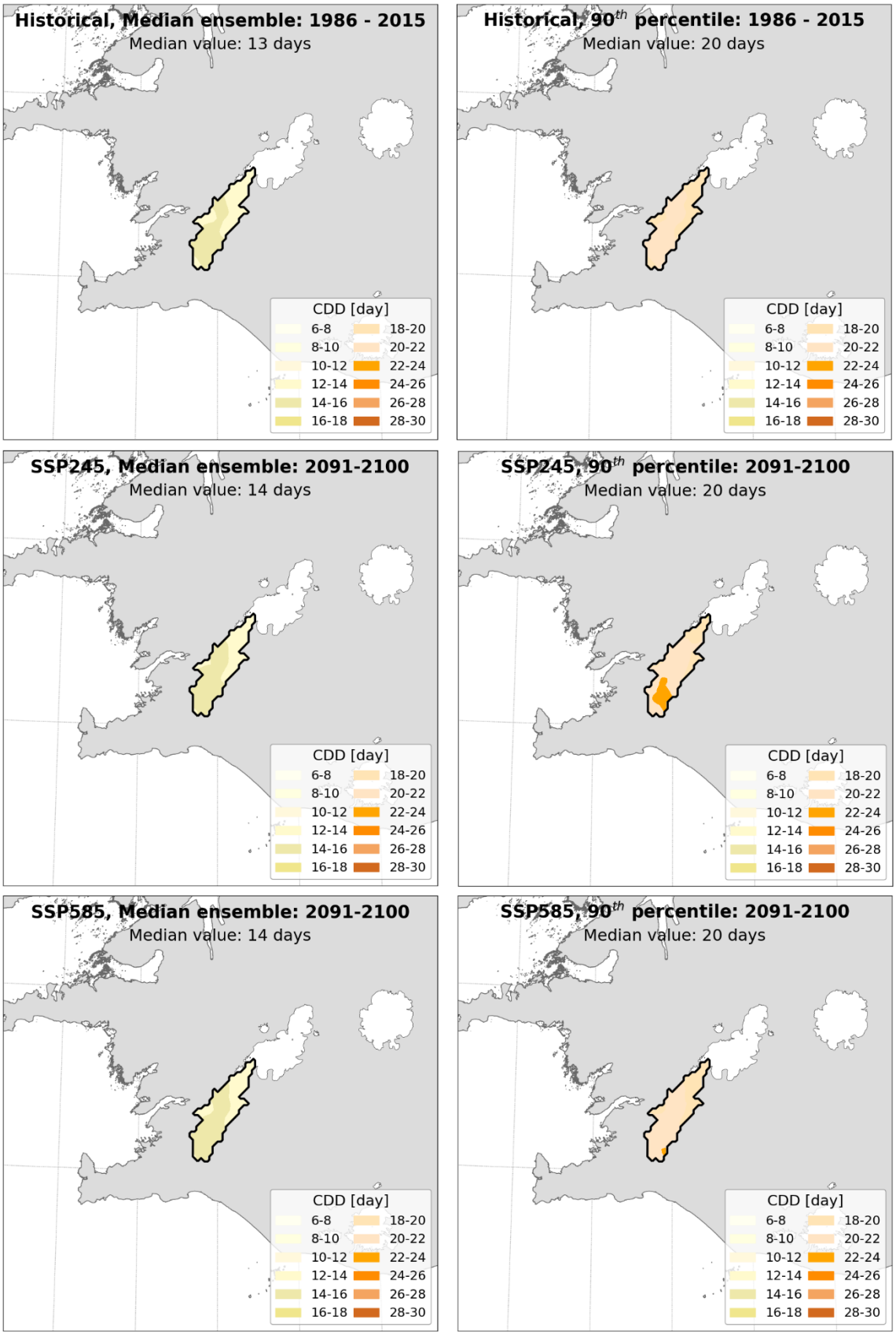

Figure VI.15 — CDD maps for catchment Þingvallavatn based on the downscaled CMIP6 dataset averaged over a historical period (1986–2015) and two projections (2091–2100) based on median and 90th percentile of the ensemble of climate models.

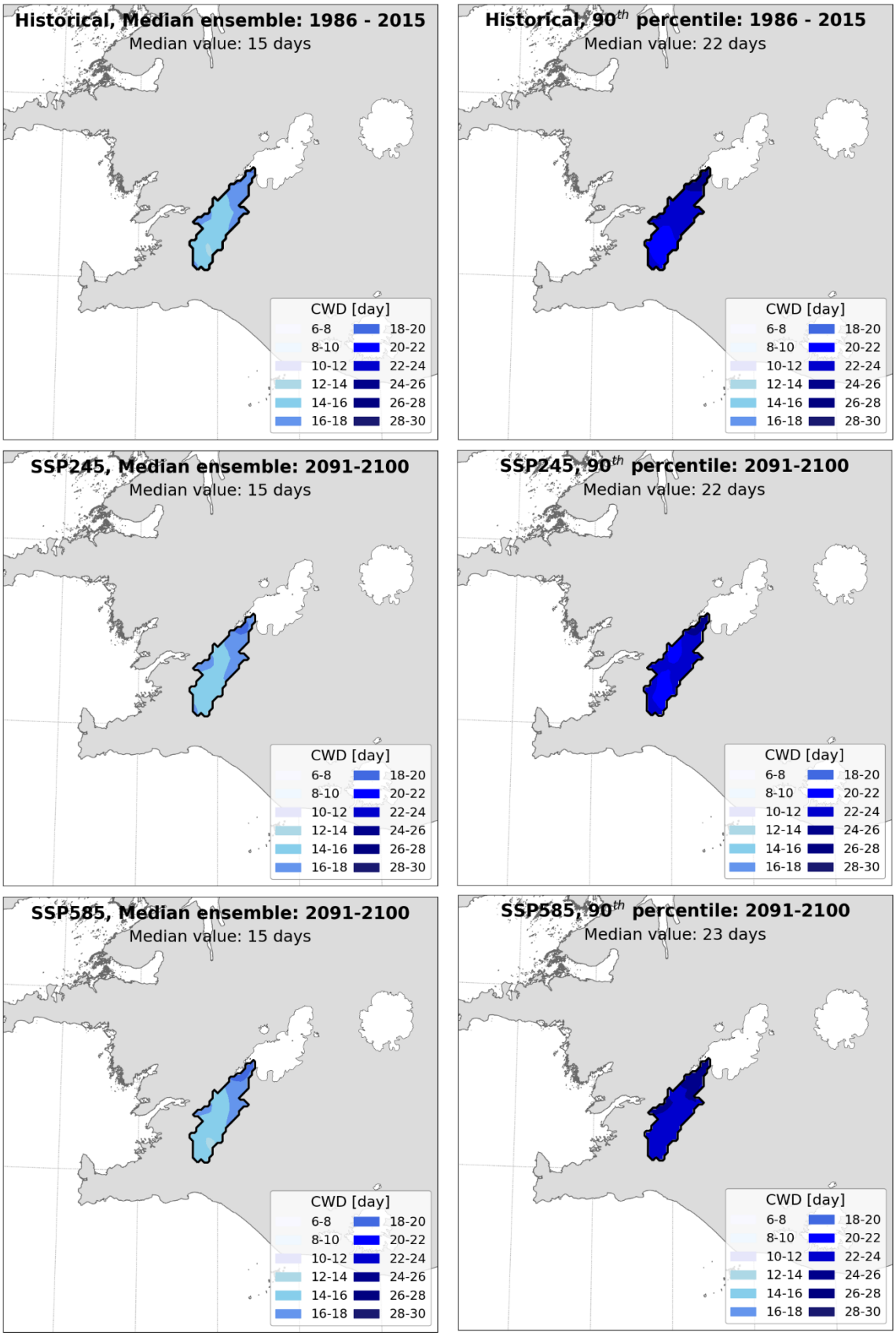

Figure VI.16 — CWD maps for catchment Þingvallavatn based on the downscaled CMIP6 dataset averaged over a historical period (1986–2015) and two projections (2091–2100) based on median and 90th percentile of the ensemble of climate models.

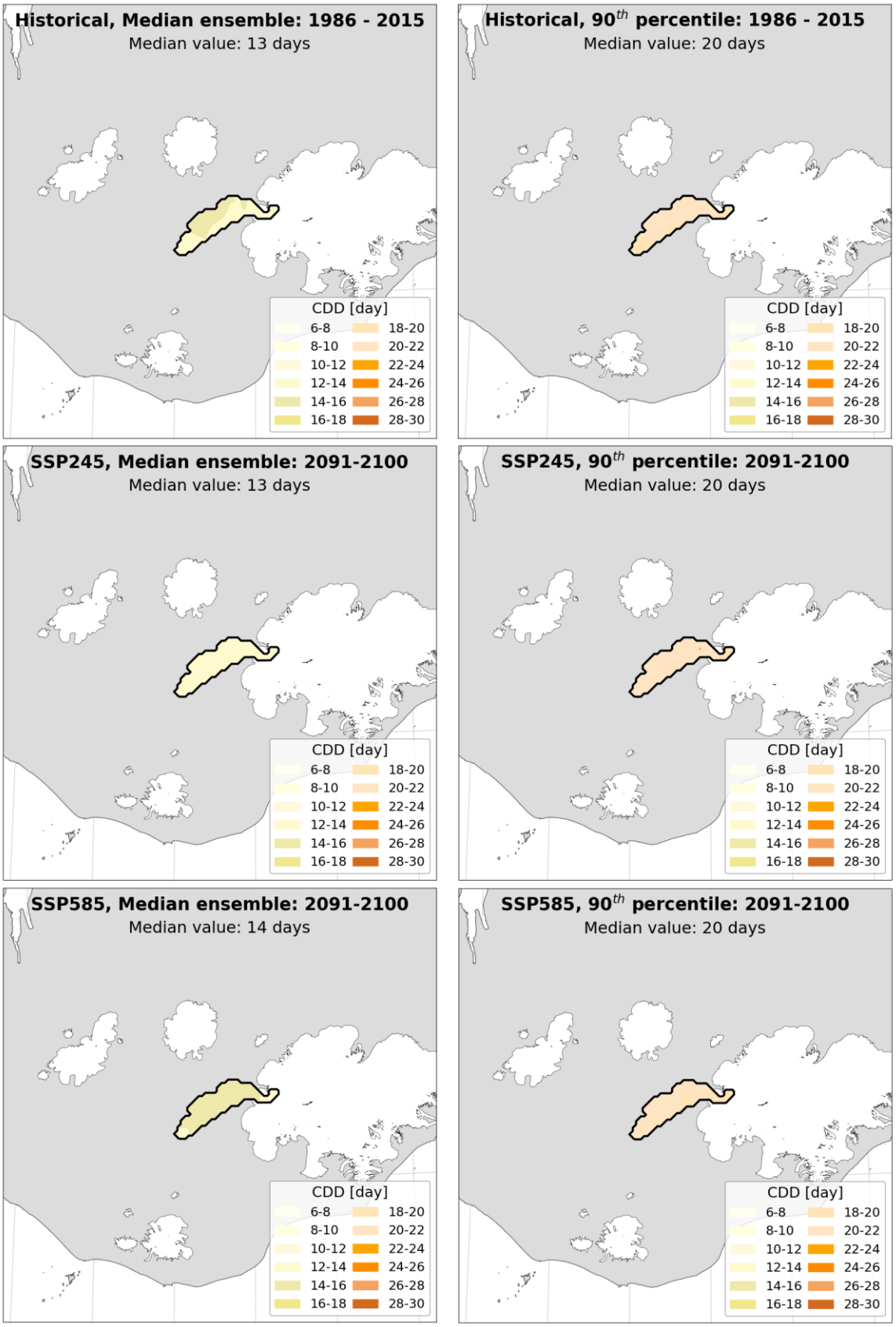

Figure VI.17 — CDD maps for catchment Þorisvatn based on the downscaled CMIP6 dataset averaged over a historical period (1986–2015) and two projections (2091–2100) based on median and 90th percentile of the ensemble of climate models.

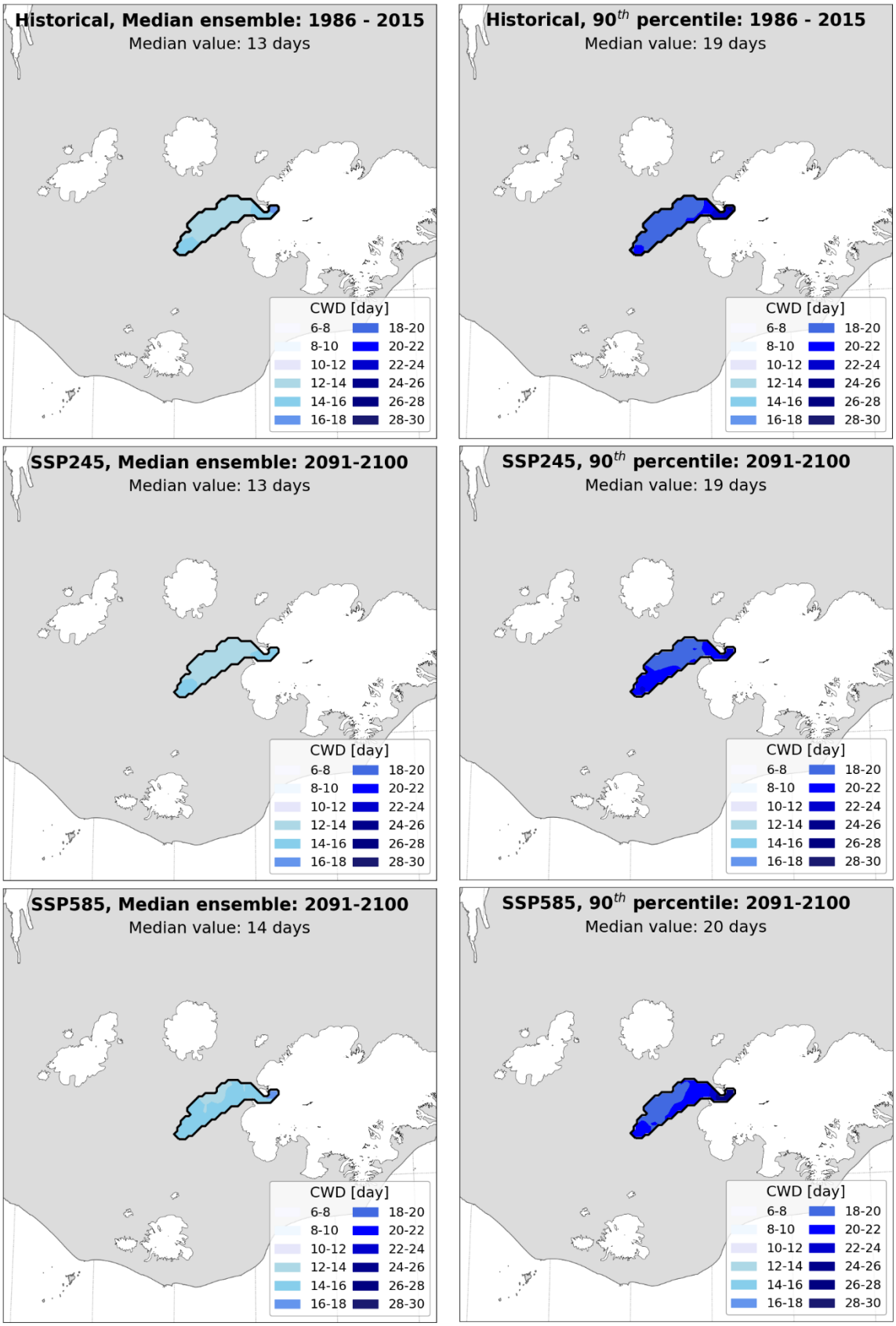

Figure VI.18 — CWD maps for catchment Þorisvatn based on the downscaled CMIP6 dataset averaged over a historical period (1986–2015) and two projections (2091–2100) based on median and 90th percentile of the ensemble of climate models.

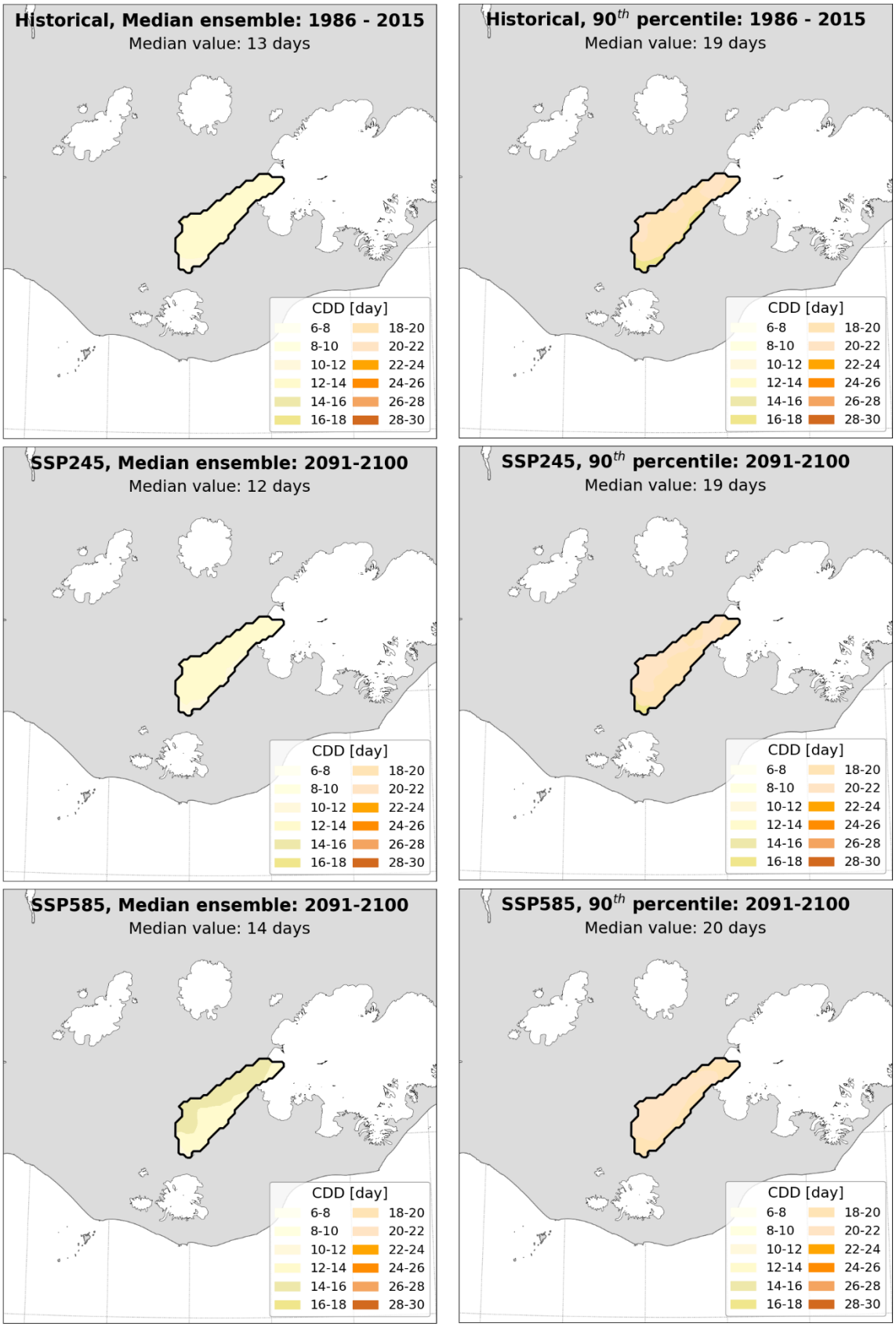

Figure VI.19 — CDD maps for catchment Tungnaá based on the downscaled CMIP6 dataset averaged over a historical period (1986–2015) and two projections (2091–2100) based on median and 90th percentile of the ensemble of climate models.

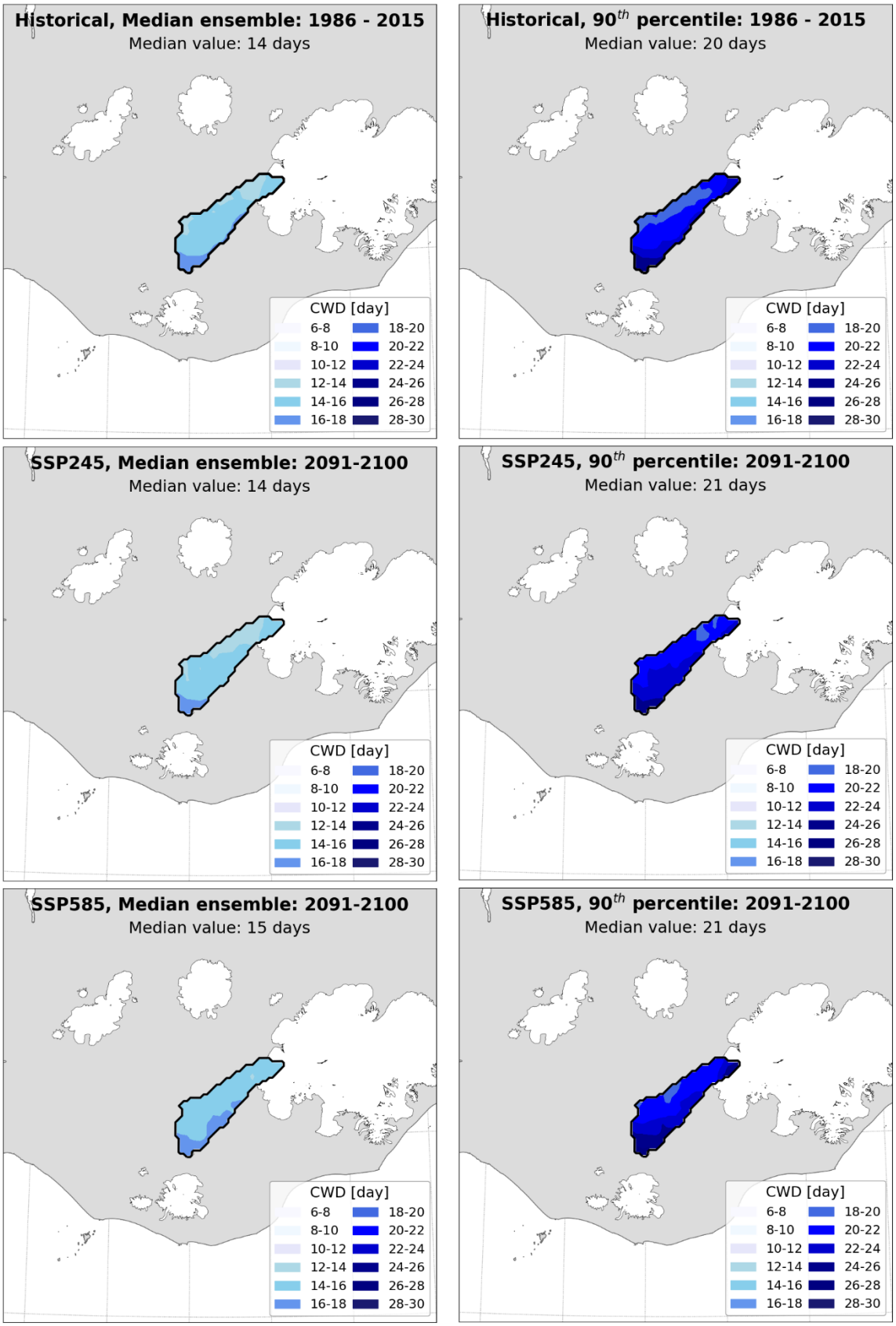

Figure VI.10 — CWD maps for catchment Tungnaá based on the downscaled CMIP6 dataset averaged over a historical period (1986–2015) and two projections (2091–2100) based on median and 90th percentile of the ensemble of climate models.

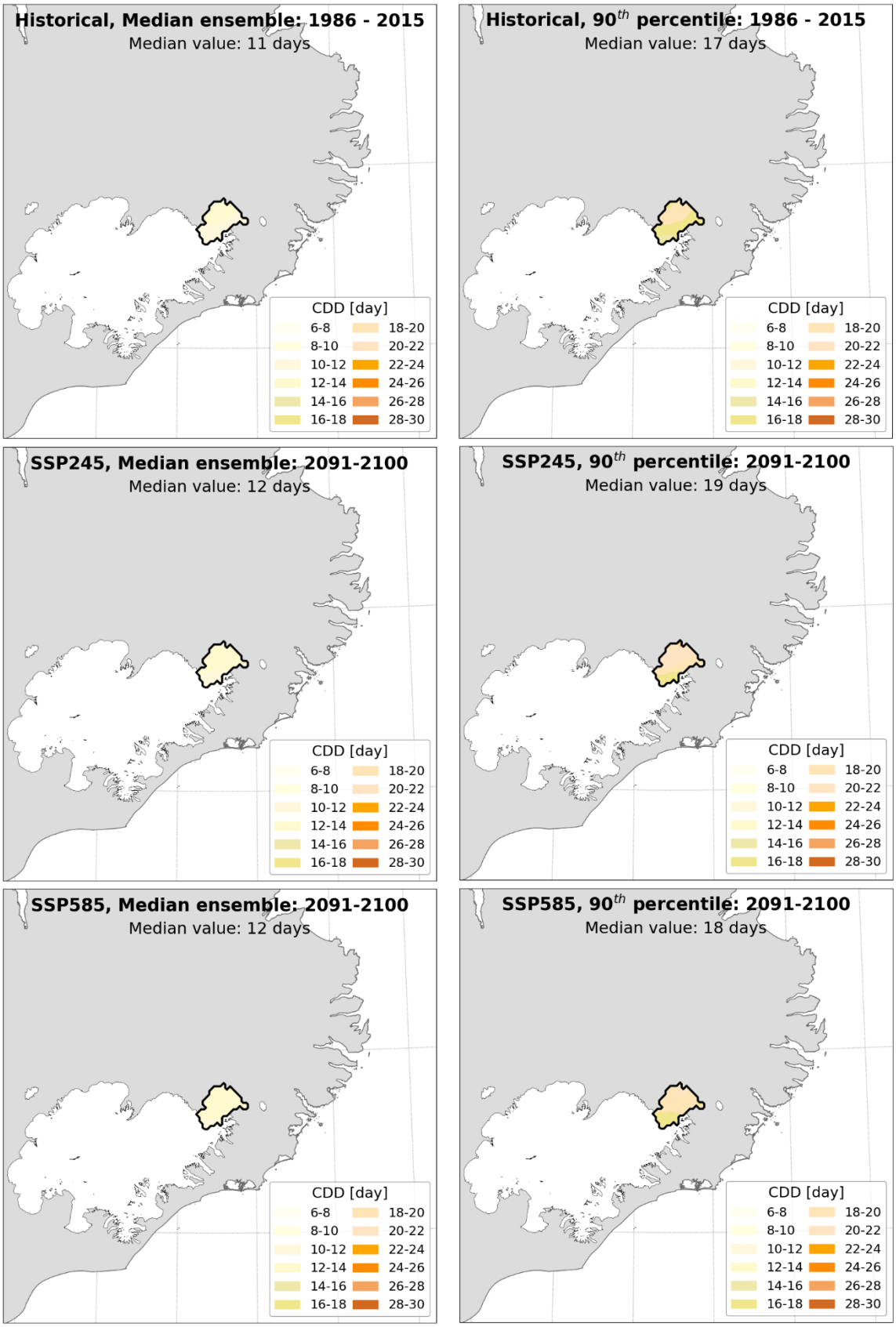

Figure VI.21 — CDD maps for catchment Ufsarlón based on the downscaled CMIP6 dataset averaged over a historical period (1986–2015) and two projections (2091–2100) based on median and 90th percentile of the ensemble of climate models.

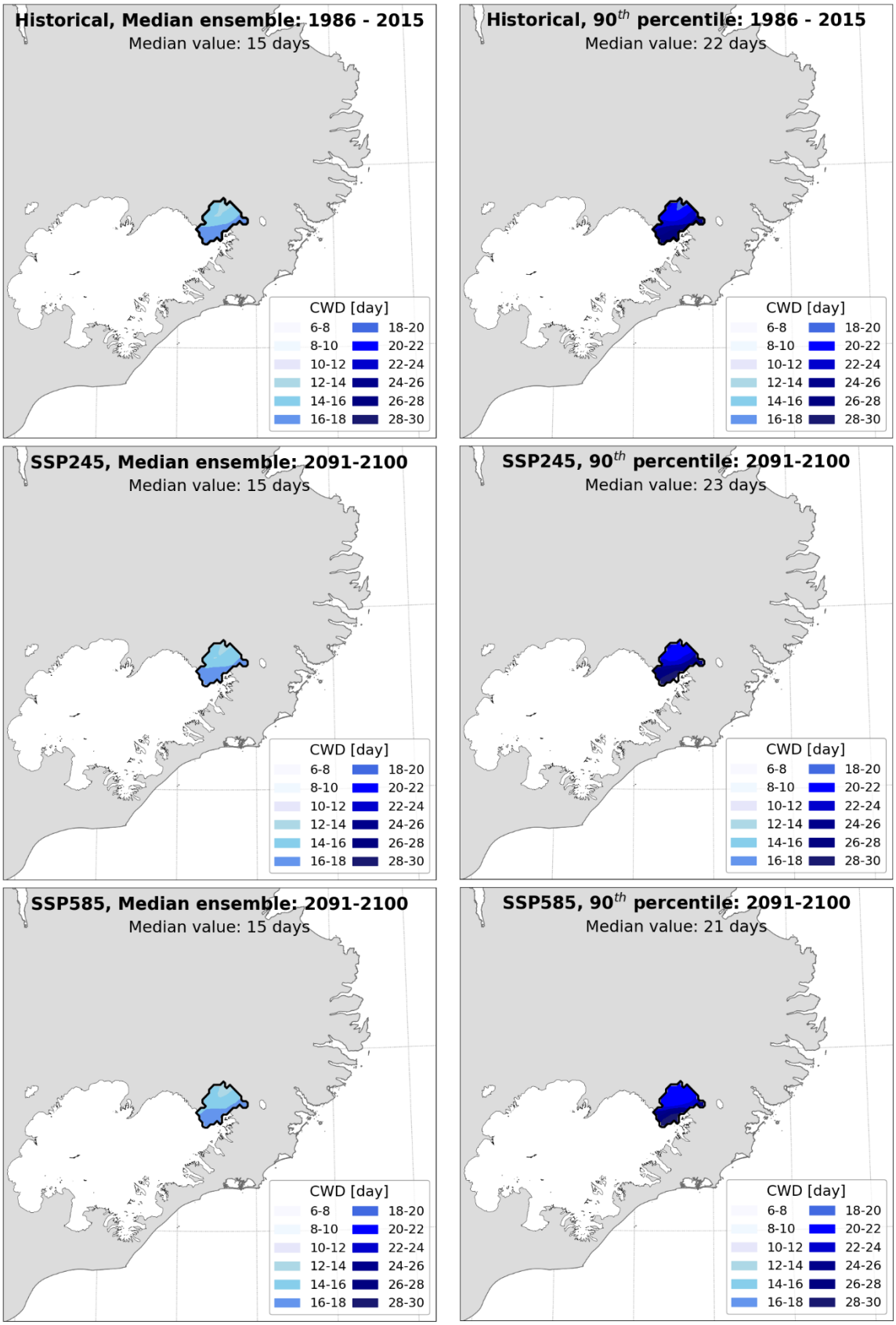

Figure VI.22 — CWD maps for catchment Ufsarlón based on the downscaled CMIP6 dataset averaged over a historical period (1986 — 2015) and two projections (2091 — 2100) based on median and 90th percentile of the ensemble of climate models.